# MODELLING SURFACE WATER FLOWS FOR UNGAUGED SITES WITHIN THE UPPER MARA RIVER CATCHMENT USING GEOMORPHOLOGIC CHARACTERISTICS

**SAMUEL MUHORO KINYANJUI**

**A Thesis Submitted to the Graduate School in Partial Fulfilment of the Requirements for the Master of Science Degree in Agricultural Engineering of Egerton University**

**EGERTON UNIVERSITY**

**NOVEMBER 2021**

## DECLARATION AND RECOMMEDATION

### Declaration

This thesis is my original work and has not been presented in this university or any other for the award of a degree

Signature: …… Date: ……..……

**Samuel Muhoro Kinyanjui**

**BM11/17512/17**

### Recommendation

This thesis has been submitted with our approval as University supervisors

Signature: …… Date: ……

**Prof. (Eng.) Japheth Ogalo Onyando**

Department of Agricultural Engineering

Egerton University

Signature: …… Date: ……

**Dr. Raphael Muli Wambua**

Department of Agricultural Engineering

Egerton University

## COPYRIGHT

## DEDICATION

This thesis is dedicated to my parent, Mr. Francis and Mrs. Josephine Kinyanjui for their encouragement, love and prayers during the study duration.

## ACKNOWLEDGEMENTS

At the completion of this thesis, I thank the Almighty God for his divine strength without which nothing could have been achieved. Thanks to the Department of Agricultural Engineering and the Faculty of Engineering and Technology staff of Egerton university for their concern and support during the development of this thesis. Thanks to Egerton university through the Centre of Excellence in Sustainable Agriculture and Agribusiness Management (CESAAM) for sponsoring this research work, the funds awarded enabled carry on with field work and data collection.

My heartfelt appreciation goes to my two supervisors and mentors; Prof. J. O. Onyando and Dr. R. M. Wambua, for their regular discussion, suggestions, continued guidance, trust and constructive criticism throughout the study period, which greatly contributed to the completion of this work.

My heart felt gratitude to my colleagues Mr. Jackson Mutinda and Mr. Edwine Amisi for their generous assistance on GIS and Remote Sensing techniques.

Thanks to my dear parent; Mr. Francis Kinyanjui Kibue and Mrs. Josephine Wanjiku Kinyanjui, and siblings, for their continued moral support, prayers and encouragement.

God bless you all.

## ABSTRACT

Remote sensing and GIS techniques allows the use of advanced catchment-scale hydrological models for addressing challenges of the scarce water resource. Scarcity of gauged data is a major constraint therefore, alternative techniques such as geomorphological characterization can provide insight on catchment hydrological characteristics. The objective of this study was to evaluate spatial distribution of surface water flows using geomorphological derived model parameters in the Upper Mara River Catchment. A semi-distributed ArcGIS based SWAT was calibrated and validated, based on gauged data, using Sequential Uncertainty Fitting Index algorithm on SWAT-Calibration and Uncertainty Program. The performance of the model was evaluated and reported. The catchment morphometry was derived from Digital Elevation Model in ArcMap using Spatial Analyst tool. The morphometry in nexus with mathematical map equations were used to derive geomorphological characteristics such as bifurcation ratio, rho coefficient, drainage density, infiltration number, form factor among others. Using formulated regressions SWAT model parameters were estimated from catchment geomorphology. A geomorphological-based SWAT model was setup, its performance compared to the generic model, and used to carried out for spatial surface water flow analysis over the Amala River catchment. The study found that, Amala River catchment was predominately covered by rainfed croplands (~64.7%) and Mollic Andosols soil (~73.6%). CN2 was the most sensitive parameter (t-stat=33.82 & P-value=0). SWAT model performed satisfactorily; NSE, $R^2$ and RSR values for calibration (validation) are 0.80 (0.51), 0.81 (0.73) and 0.45 (0.45), respectively. The catchment exhibits a dendritic drainage pattern with an average bifurcation ratio of 4.26 which is closer to the upper bound value of 5. The surface runoff yield efficiency was low and non-uniform with an average drainage density of 1.07 km/km$^2$. The geomorphological based model had NSE of 0.77 and $R^2$ of 0.78 which was a satisfactory performance. The study concluded that generic calibration using observed data gave a better model but where such data is unreliable geomorphological characteristics can be used to estimate model parameters and give a satisfactory model. The spatial flow analysis showed that surface water flows are the overall predominant component with an average of 372.3 mm annually and sub basins outlets derived are potential sites for water harvesting. Thus, the outcomes provide a baseline for informed siting of water pans, dams and other water harvesting structures.

## TABLE OF CONTENTS

## LIST OF FIGURES

## LIST OF TABLES

## LIST OF ABBREVIATIONS AND ACRONYMS

| | |
|---|---|
| a.m.s.l | above mean sea level |
| CHIRPS | Climate Hazards Group InfraRed Precipitation with Station |
| DEM | Digital Elevation Model |
| DOI | Digital Object Identifier |
| FAO | Food and Agricultural Organization |
| FORTRAN | Formula Translation |
| GC | Geomorphological Characteristics. |
| GIS | Geographical Information System |
| GLUE | Generalized Likelihood Uncertainty Estimation |
| GUI | Graphical User Interface |
| HBV | Hydrologiska Byrans Vattenbalansavdelning |
| HEC-HMS | Hydrologic Engineering Centre- Hydrologic Modelling System |
| HRU | Hydrologic Response Unit |
| HSPF | Hydrologic Simulation Program- Fortran |
| KENSOTER | Kenya Soil and Terrain Database |
| KMD | Kenya Meteorological Department |
| LCC | Land Cover Classification |
| LULC | Land Use Land Cover |
| MP | Model Parameters |
| NS | Nash-Sutcliffe |
| NYSKIP | Number of Years to SKIP |
| PBIAS | Percentage BIAS |
| ROTO | Routings Outputs to Outlets |
| SCS-CN | Soil Conservation Service- Curve Number |
| SRTM | Shuttle Radar Topography Mission |
| SRTM-DEM | Shuttle Radar Topography Mission- Digital Elevation Model |
| SUFI | Sequential Uncertainty Fitting Index |
| SWAT | Soil and Water Assessment Tools |
| SWAT-CUP | Soil and Water Assessment Tools- Calibration and Uncertainty Program |
| SWRRB | Simulator Water Resource in Rural Basins |

| | |
|---|---|
| USGS | United States Geological Survey |
| WRA | Water Resources Authority |

# CHAPTER ONE
# INTRODUCTION

## 1.1 Background Information

Water scarcity has become a major concern globally. Guppy and Anderson (2017) estimates more than 40% of the approximately 7.2 billion total world's population faces serious fresh water scarcity. This global challenge is rooted down to catchments degradation and climate variability. Climate changes and land degradation are considered as major contributors to variations in the hydrological response of a catchment (Krysanova & White, 2015). Knowledge on how the hydrological response and water resources is affected by these changes is crucial for creating reliable water Best Management Plans. Various modelling tools that generate surface water flow predictions in given ranges of space and time scales have been developed to aid in proper management of water and the environment under varying climate (Devia et al., 2015). However, most catchments globally are scarcely gauged (Nkonge, 2017; Sellami et al., 2014) and most of the hydrological models were developed in temperate climate. Thus, the main limitation in adopting these models in ungauged outlets is the determination of parameter values in local climate, which is traditionally done by calibration using gauged stream flow data.

Africa has vast freshwater resource: however, based on World bank classification of 2000, 8.3 % of the countries in the world are water-scarce. Kenya falls under this class with a current annual renewable freshwater of 450 $m^3$ per capita. A country is classified as water-scarce if its annual renewable freshwater per capita is less than 1,000 $m^3$ (World Bank 2000). Uganda and Tanzania have annual freshwater per capita of 2,940 and 2,696 $m^3$ per capita per annum respectively in comparison to Kenya (Mulwa et al., 2021). The is need to monitor this scarce resource and conserve it.

Given Africa's countries weak economy status, installation and operation of river gauging stations are inadequate to enable effective water resource planning. African communities are increasingly adopting rainfall-runoff models to study, prevent and manage natural disasters, and manage their water resources sustainably (Bingwa, 2013; Mwania, 2014; Nkonge, 2017). Adoption of these models involves the transfer of hydrologic information (model parameters or stream flow) from a gauged outlet to ungauged outlet of interest (Bao et al., 2012; Lee et al., 2016; Nkonge, 2017). Although various research with rainfall–runoff model parameter estimation methods for ungauged catchments has been done successfully, there is a need to

continually improve these and to test their applicability in different climatic and land use conditions (Zvolenský et al., 2007).

Catchments are the large reservoirs of fresh water accessible for utilization on land, where water is stored as river storage, soil moisture, bio water, aquifer storage and surface storage. Most development on water resources relies on the capacity of a catchment to store rainwater and release it. Land degradation leads to reduced infiltration and increased surface runoff. These result in low catchment water storage in terms of soil water and groundwater recharge. Furthermore, if the surface runoff is not harvested and stored within the catchment as surface storage it is yielded as flash floods. This implies less water is stored within the catchment and thus shortages during dry seasons. Most catchments in Kenya are faced by adverse climatic changes and increased land degradation (Kambombe, 2018). Among them is the Mara River catchment, which is of national and regional economic importance (Osoro et al., 2018). Recent studies have shown reduced river baseflow and change in flow regimes (Mwania, 2014). Increased human activities, land degradation and uncontrolled river and runoff harvesting are pointed out as major contributors (Kipampi et al., 2017). To understand and curb these impacts and effects on hydrologic systems thorough site-specific studies has to be done.

Accurate and reliable prediction of hydrologic responses is extremely important for planning and managing water resources (Bao et al., 2012). Thus, it is important to study the hydrologic response of a catchment and develop alternative ways of storing the surface runoff for use and as a relief to depleting groundwater resources and river baseflow. For such a study, recorded data gives the best results, however in most developing countries, Kenya included, majority of the catchments are ungauged or lacks proper instrumentation. Thus, other means such as use of remote sensed data and hydrological modelling are some of the best alternatives (Onyando & Sharma, 1995). In most cases, rainfall-runoff relationships are developed for gauged catchment where data was available for calibration. For ungauged catchments, model parameters can be obtained by relating them to catchment physical characteristics through suitable coefficients and regression analyses (Bao et al., 2012).

The runoff resulting from a catchment is a response function of rainfall received within the catchment (Nyadawa & Mwangi, 2010). According to Bansod and Ajabe (2018), the hydrological response of a catchment depends on various physiographic features. Such features are well understood by geomorphological analysis (Chethan & Vishnu, 2018) which characterize

the catchment based on geometrical properties, depicting the relationships among dimensional properties, and topological properties detailing the drainage network (Mark, 1975). A quantitative analysis of these characteristics provides insights on the configuration of the earth's surface, the shape and dimension of its landforms and quantitative description of the drainage network (Charizopoulos & Psilovikos, 2015; Pareta & Pareta, 2011). These characteristics influence the hydrologic properties of a catchment such as; drainage pattern, time of concentration, lag time and intensity of erosional processes (Altaf et al., 2013).

Detailed description of geomorphologic characteristics of many river catchments and their influence on hydrologic response in Kenya are limited (Nyadawa & Mwangi, 2010). Globally, a lot of geomorphological analysis have been done (Bansod & Ajabe, 2018; Gunal & Guven, 2014; Mark, 1975; Pareta & Pareta, 2011). However, geomorphologic characteristics and their relationship to hydrology are not transferrable (Nyadawa & Mwangi, 2010). These characteristics are catchment specific and therefore unique in nature. The geomorphologic characterization of a catchment provides an insight on its hydrologic response (Bansod & Ajabe, 2018).

Most studies have used topographic maps as the primary data for geomorphologic analysis. With advances in geographical information system (GIS) and wide availability of digital elevation model (DEM) data, it possible to derive geomorphologic parameters based on DEM analysis (Bansod & Ajabe, 2018). GIS techniques are crucial in assessing various terrain and morphometric parameters of the drainage basins and watersheds, as they provide a flexible environment and a powerful tool for the manipulation and analysis of spatial information (Pareta & Pareta, 2011).

## 1.2 Statement of the Problem

Recent studies have shown that degradation of forest cover in the upper Mara River catchment and high-water abstractions for industrial, domestic and agricultural purposes has decreased water quantity in the river (Kipampi et al., 2017; Osoro et al., 2018). This is coupled with failures of local, national and regional legislation and institutional structures (in charge of water resources) to ensure sustainable development within the catchment (Osoro et al., 2018). With increased construction of water pans and water retention structures as an alternative water source within the catchment, reliable surface water flow data is needed for sustainable design

and operation of water storage structures. Such data is only readily available for gauged catchment points. However, construction of hydrologic structures such as dams or water pans mostly require a prediction to be made of the surface water flow at an ungauged outlet within the catchment. Therefore, alternative tools that are capable of predicting the surface water flow at such ungauged outlets are needed for informed development (Nongthombam et al., 2011). Geomorphologic-based tool gives the best alternative (Bao et al., 2012).

## 1.3 Objectives

### 1.3.1 Broad objective

The broad objective of this study was to model and evaluate spatial distribution of surface water flows using geomorphologically derived model parameters in the Upper Mara River Catchment.

### 1.3.2 Specific objectives

The specific objectives were to;

(i) Calibrate and validate SWAT model for Upper Mara River catchment.

(ii) Derive regression models based on geomorphological characteristics of the catchment.

(iii) Simulate spatial surface water flows distribution within the catchment using geomorphologic-derived parameters on the SWAT model.

## 1.4 Research questions

The research questions for this study were;

(i) How reliable is SWAT model in Upper Mara River catchment at catchment and sub-catchments levels?

(ii) How does geomorphological characteristics relate to the catchment hydrologic parameters?

(iii) How does surface water flows vary spatially over the catchment as simulated using geomorphologic-based SWAT model?

## 1.5 Justification

The concept of safe water yield was introduced and defined by Sophocleous (1997), as the accomplishment and maintenance of a long-term balance between the annual groundwater abstraction and the annual volume of recharge. With changes in land use and advancing land degradation the groundwater recharge has been depleting and thus decreased river base flow. The need for more water for agricultural use, industrial use and the increasing population in the upper Mara River catchment has led to increased river abstractions. Thus, there is need to harvest surface water flows to augment ground water and river abstraction.

For proper management of large-scale development in surface runoff harvesting and storages such as dam reservoirs, water pans or direct river abstraction, siting and designing of these developments requires a deep knowledge of surface water flow spatial variability and amounts. With limited gauges in the catchment the only resort is remotely sensed data and catchment modelling to obtain such information. Rainfall-runoff modelling is limited by data scarcity in ungauged catchments since hydrological models are traditionally calibrated and validated using gauged stream flow data. Therefore, to apply hydrological models on ungauged catchments, regression equations was needed which easily related measured catchment characteristics to model parameters (Zelelew & Alfredsen, 2014). This study derived regression equations to estimate model parameters based on geomorphology of the catchment, established model parameters for ungauged sub-catchments and did a detailed spatial assessment of the surface water flows on the catchment. This facilitated hydrological modeling, water pan siting and improved management of water resource in the catchment.

## 1.6 Scope and Limitations

This study was carried out in the Upper Mara River catchment and was mainly focusing on surface water processes and storages in Amala sub-catchment. The following assumptions were made; effect of land use change within the calibration period was not accounted for, and that when SWAT model was calibrated at the gauging point the parameters for the sub-catchments were accurate and were to be used for regression analysis. There was limited weather gauging within the catchment.

# CHAPTER TWO
# LITERATURE REVIEW

## 2.1 Surface Hydrology

Hydrology is of key importance for ecosystems. The term hydrology refers to the study of earth's water; its occurrence, circulation and distribution, its physical and chemical properties and its relationship with the environment within each phase of the hydrologic cycle (Chow et al., 1988; Shaw, 1994). Hydrologic cycle as described by Chow et al. (1988) is a continuous maze of earth's water circulation paths and is the central focus of hydrology.

Most hydrologic studies are related to estimating the quantity and quality of earth's water in various stages of the hydrologic cycle, both in time and space. To effectively achieve this, the need for areal focus of research bore the concept of catchment hydrology (WMO, 2009). A catchment is the basic hydrologic system, where the heterogeneity and complexity of hydrologic processes and interactions between water resource, land surface, climatic factors and human activities can be studied (Fadil et al., 2011). Over the years hydrologic systems have been used effectively to model water flows. The output characteristics at the pour point of a catchment subjected to a given rainfall scenario is termed as hydrologic response of that catchment. Different variations have been observed in hydrologic systems and response due to changes in land use/cover, soil types, increased water abstraction and variation induced by climate change (Devia et al., 2015).

### 2.1.1 Rainfall-Runoff Generation

The surface hydrology describes the flow paths, dynamics, and storages of water on the earth's surface. Precipitation falls on crop/vegetation cover or on bare land. The portion of rain water stored on land surface is referred as depression storage. When depression storage has been exceeded, water flows downslope as surface water flow. The portion trapped by the vegetation canopies is termed as interception storage. The amount of interception storage depends on vegetation characteristics. When the storage capacity of vegetation has been exceeded, water drips off branches and leaves, as through-fall or stem-flow, to the ground, where it either enters the soil or joins surface water flow (Raude, 2006). The quantity retained and does not infiltrate into the soil nor does it flow down slope constitute the surface retention. The processes involved in surface water flow includes portion of the hydrologic cycle starting at surface retention of

rainfall at the land surface, flow down slope to the confined channel flows ending with flow in the streams at the pour point of the catchment. Surface hydrology also considers the interaction between the surface water and groundwater such as subsurface water flow and groundwater contribution to surface water flow. To conceptualized this interaction two ideologies have been developed; Horton overland flow and saturated overland flow detailed by Chow et al. (1988). The former occurs when the intensity of precipitation exceeds the infiltration capacity of the soil, while the latter occurs if the combination of precipitation intensity and duration saturates the soil and raises the water table to the surface. In Upper Mara River catchment both Horton overland flow and saturated overland flow are likely to occurs.

In the hydrologic cycle surface water flow connects precipitation to surface water reservoirs. In most circumstance, satellite-derived rainfall data is available, but for most catchment surface water flow or runoff data is not available or it is not sufficient for decision making and for research purposes. Recent researches have come up with alternative ways of deriving such information from the widely available remote sensed rainfall data and satellite imagery (Bao et al., 2012; Mwania, 2014).

### 2.1.2 Hydrologic Response

In hydrological research, surface runoff is as a result of rainfall-runoff relationship. Actually, land use land cover (LULC) on a catchment has been found to have major influence on hydrologic response (Kambombe, 2018). Hydrologic response is commonly expressed through runoff coefficient and it reflects a complex reaction of an interaction between rainfall and catchment physical characteristics (Nazir et al., 2015). According to Chow et al. (1988), runoff coefficient is the ratio of the peak rate of runoff to the intensity of rainfall for a given storm.

$$C = \frac{r_d}{\sum_{m=1}^{M} R_m} \quad (2.1)$$

Where;

C = runoff coefficient (dimensionless)

$r_d$ = runoff depth (mm)

$R_m$ = rainfall amount (mm)

m = rainfall events (1, 2, 3, ..., M)

For the purpose of design, engineers typically rely on tables of rational C values as a function of land cover. Such tables are found in most introductory engineering hydrology

textbook and are incorporated into design standards for local and state government agencies (Dhakal et al., 2011). However, this method provides only guidelines since the intensity-duration-frequency curves it requires are regionally based and not catchment specific (Onyando, 2004).

## 2.2 Review of Hydrologic Models

Hydrologic models can be categorized as deterministic or stochastic depending on how they treat randomness (Chow et al., 1988) and further classified based on spatial-temporal variations. Based on nature of input parameters, whether they are physical or conceptual, hydrologic models can also be classified as physically-based or conceptual models, respectively. Stochastic models partially account for randomness and their output is based on statistical predictions. Deterministic models do not account for randomness. Models in this category are suitable for forecasting since a given input always produces the same output (Dwarakish & Ganasri, 2015). These models can be further categorized as;

i. deterministic lumped model where parameters are averaged over spatial scale,
ii. deterministic semi-distributed model where parameters are lumped for Hydrologic Response Units (HRUs) (derived based on unique combination of land use and land cover, soil type, and slope) which are distributed over spatial scale, and
iii. deterministic distributed model where model parameters are grid-based and depends on spatial resolution of the inputs.

Use of hydrologic model is crucial in decision making for water resources management plan, formulation of policies and water regulations (Kambombe, 2018). A model is a physical or mathematical representation of a real-world system (Chow et al., 1988). A good model simulates the scenarios giving results close to reality with the use of minimal uncertainty, input parameter and model complexity. Hydrologic modelling is based on water balance concepts in conjunction with the continuity equation and the law of conservation of mass (Equation 2.2).

$$\left[\frac{\delta s_i}{\delta t} + e_i\right] + \left[\frac{\delta s_s}{\delta t} + e_s + q_s\right] + \left[\frac{\delta s_u}{\delta t} + e_t + e_u + q_f\right] + \left[\frac{\delta s_g}{\delta t} + q_g\right] = p \qquad (2.2)$$

Where;

s = storage (mm)

e = evaporation (mm)

q = fluxes (mm)

p = precipitation (mm)

t = time (s) and

i, s, u, f and g subscripts represent interception, surface storage, soil moisture, infiltration and groundwater recharge respectively.

δt= change in time(s)

δs= change in storage(s)

A hydrological model consists of various parameters and is mainly to describe and predict the characteristics of various hydrological processes (Devia et al., 2015). With advances in technology, science and computing capacities different models with unique characteristics and parameterization have been developed over the years. However, the limited availability of spatial and temporal data has been a major constraint to application of these models especially in developing countries (Fadil et al., 2011). Despite high adoption of modelling techniques, the quantification of water and its quality at any point in time and space is not yet precisely determined. The general concept of a hydrologic model system can be depicted by the example Figure 2.1. Examples of commonly used rainfall-runoff models are reviewed in sub-section 2.2.1 to 2.2.8.

### 2.2.1 Hydrologic Engineering Center- Hydrologic Modelling System (HEC-HMS)

This model was developed by US Army Corps of Engineers in 1998 (Ouedraogo et al., 2018). The HEC-HMS simulate hydrologic processes of dendritic catchment systems (Grillakis et al., 2011). The model contains hydrologic analysis techniques such as runoff generation equations, hydrologic routing, unit hydrographs and event infiltration (Ismael et al., 2017) and it is designed for both continuous and event-based hydrologic modelling. This model has been adopted successfully in local catchments and is a reliable model (Bingwa, 2013; Ismael et al., 2017; Ouedraogo et al., 2018). However, this tool is unable to model looping or branching networks and the model source code is not published for modification (Kambombe, 2018).

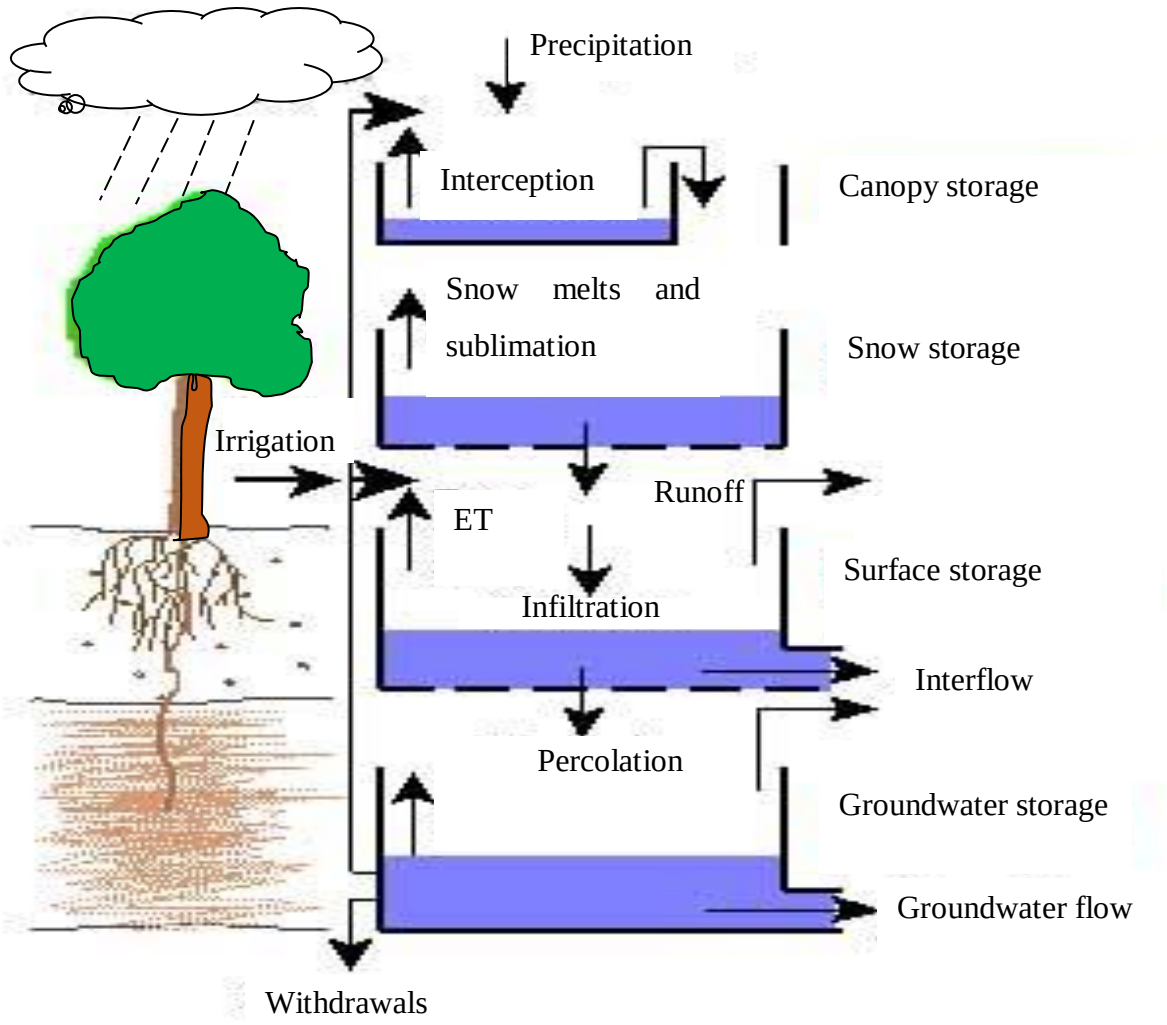


**Figure 2. 1: A pictorial depiction of a catchment hydrologic system (Source: Martz 2002)**

### 2.2.2 Hydrologic Simulation Program - Fortran (HSPF)

HSPF was developed in the 1960's as Stanford Catchment Model and since it is a widely used model it has seen continual development under support of USGS and EPA. It is a continuous, semi- distributed and conceptual model for water flow, sediment and chemical pollutants simulation both in the soil and in streams (Donigian, 2000). It combines spatially distributed physical parameters into hydrologic response units, simulates the output of these units and route the flows to the streams down slope. It takes hourly time step data and produces a time series of flow, sediments load and pollutant load at any segment in the catchment (Bicknell et al., 1996). HSPF package contains three catchment application components;

i. Pervious Land Segments (PERLND)

ii. Impervious Land Segments (IMPLND)

iii. Free-Flowing Reach Segments (RCHRES)

The model performance relies on the calibrated parameters and not on the specific information on physical dimensions and characteristics of the flow system (Liu & Tong, 2011) and thus a challenge where there is no enough data for calibration.

### 2.2.3 Hydrologiska Byrans Vattenbalansavdelning (HBV)

HBV is a semi- distributed conceptual model extensively used in operational hydrological forecasting and water balance studies that is characterized by attempts to cover the most important runoff generating processes using a simple and robust structure, and a small number of parameters (Abebe et al., 2010). It runs on daily or monthly rainfall, evaporation and air temperature data (Devia et al., 2015). The model partitions a catchment into sub-catchments, which are further divided into different elevation and land cover zones. The general water balance equation for the model is;

$$P - E - Q = \frac{\partial}{\partial t}[S_P + MC + S_{GW1} + S_{GW2} + S_R] \quad (2.3)$$

Where;

P = precipitation (mm)

E = evaporation (mm)

Q = runoff depth (mm)

$S_P$ = the snow component (mm)

MC = soil moisture (mm)

$S_{GW1}$ = upper groundwater zone storage (mm)

$S_{GW2}$ = lower groundwater zone storage (mm)

$S_R$ = volume of surface reservoir (mm)

$\delta/\delta t$ = the rate of change with time

The latest release, HBV-96, with full distribution into sub-catchments and statistical distribution of some properties within these sub-catchments, the HBV model is now a fully distributed hydrological model (Bergström et al., 2001). However, HBV is a commercial software and thus its use is limited by accessibility for a license.

### 2.2.4 Soil and Water Assessment Tool (SWAT)

SWAT is an eco-hydrological model for basin scale assessments (Arnold et al., 2012), developed by the United States Department of Agriculture. The model is a merger of two models, Simulator for Water Resources in Rural Basins (SWRRB) and Routing Outputs to Outlet (ROTO) models (Williams et al., 2008), with progressive development over the years on different GIS interfaces (Gasman et al., 2007). SWAT is a powerful continuous-time dynamic model. However, it is a semi-distributed model where the catchment is modelled at reasonably spatial disaggregation scheme into sub-catchments which are further divided into HRUs (Devia et al., 2015). This model was designed to evaluate and predict the water and sediment circulation and agricultural production with chemicals within a catchment. As a semi- distributed physically based model, SWAT combines processes and analyses spatially the above input data and it has to be coupled with a GIS software (Fadil et al., 2011). The model has been widely used in data scarce catchments and yielded reliable results (Kambombe, 2018). Simulation of the hydrological processes of a catchment is separated into a land phase and water or routing phase (Schmalz et al., 2015) as described in sections 2.2.5 and 2.2.6.

SWAT model operates by dividing the catchment into sub-catchments. Each sub-catchment is further discretized into a series of hydrologic response units (HRUs), which are unique soil-land use combinations. The simulation of the land phase is based on the water balance equation, which is calculated separately for each HRU (Equation 2.4).

$$SW_t = SW_0 + \sum_{i=1}^{t}\left(R_{day} - Q_{surf} - E_a - W_{seep} - Q_{gw}\right)_i \quad (2.4)$$

Where;

t = time (days)

$SW_t$ = final soil water content (mm)

$SW_0$ = initial soil water content (mm)

$R_{day}$ = precipitation depth on $i^{th}$ day (mm)

$Q_{surf}$ = amount of surface runoff on $i^{th}$ day (mm)

$E_a$ = evaporation depth on $i^{th}$ day (mm)

$W_{seep}$ = depth of water entering the vadose zone from the soil profile on $i^{th}$ day (mm)

$Q_{gw}$ = amount of return flow on $i^{th}$ day (mm)

The water in each HRU is stored in four storage volumes in the model; snow (not applicable in this study), soil profile, shallow aquifer and deep aquifer (Figure 2.2).

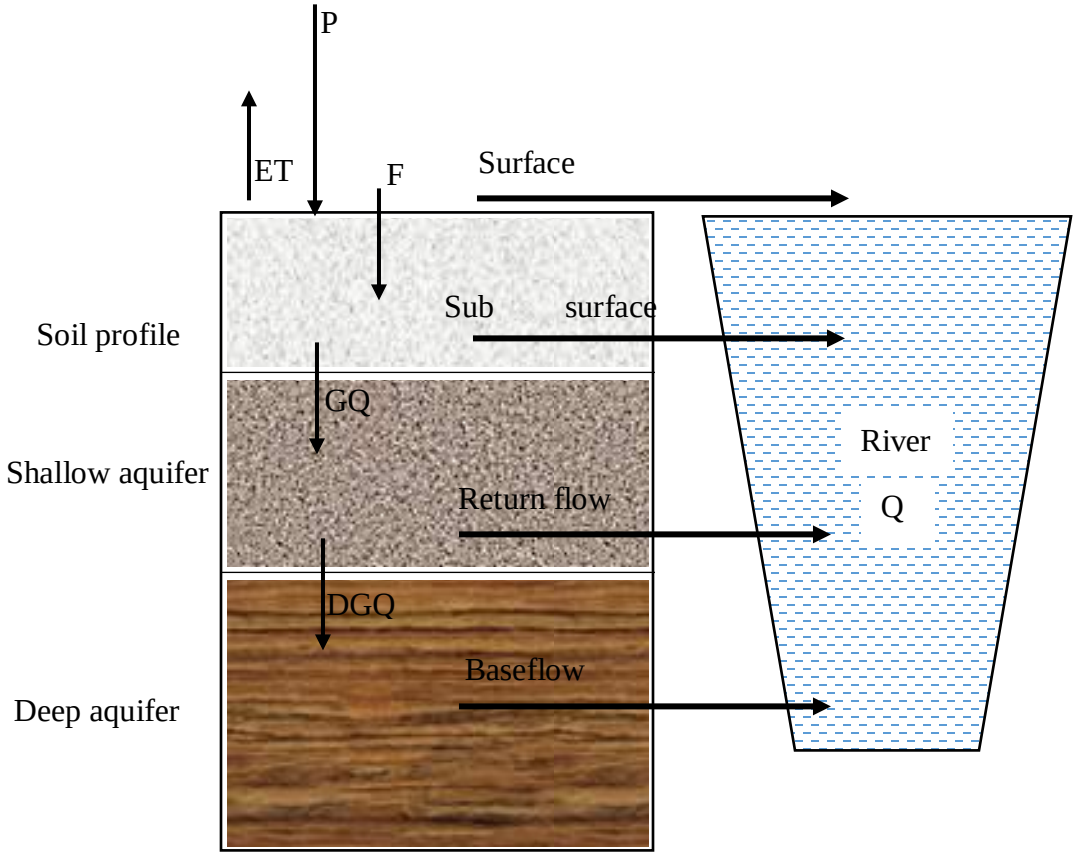


**Figure 2. 2: The flow components of SWAT (Adopted from; Neitsch et al., 2011)**

Surface water flow is that part of rainfall that runs downslope over the land surface either as overland flow or channel flow. For surface runoff component ($Q_{surf}$) estimation, at HRU level, SWAT model provides two abstraction methods namely; the SCS-CN method and the Green-Ampt infiltration method. SCS-CN method takes rainfall data in daily time step while the Green-Ampt method requires hourly time step.

Green-Ampt infiltration was developed in 1911. It is based on physical parameters of the soil including hydraulic conductivity and soil suction head. It assumes a saturated front moving uniformly downward through the vadose zone, which has specified initial moisture content. The Green-Ampt equations are given as;

$$f_{(t)} = K\left[1 + \frac{h_0 + h_s}{l}\right],\ f_{(t)} = \frac{\partial F_{(t)}}{\partial t} \quad (2.5)$$

$$F_{(t)} - (h_0 - h_s)\Delta\theta \ln\left[1 + \frac{F_{(t)}}{(h_0 - h_s)\Delta\theta}\right] = Kt \quad (2.6)$$

Where;

$f_{(t)}$ = infiltration rate (mm/h)

K = effective hydraulic conductivity

$h_o$ = depth of ponding water over the soil surface (mm)

$h_s$ = capillary suction head at the wetting front (mm)

L = depth of wetting front below the bottom of pond (mm)

$F_{(t)}$ = cumulative infiltration depth (mm)

$\Delta\theta$ = soil moisture deficit (= $f_e - \theta_i$)

$f_e$ = effective porosity (ratio)

$\theta_i$ = initial (antecedent) moisture content (%).

Soil Conservation Service -Curve Number (SCS-CN) method is a widely used conceptual model for estimating direct runoff amount following a given rainfall event. It was developed by Soil Conservation Service of USA in 1969. This method uses rainfall, infiltration/soil properties and antecedent moisture condition of the soil as data inputs. It relies on only one parameter- the Curve Number, CN. It is among the popular methods for computing the runoff volume from a rainstorm because it is simple, easy to understand, apply, stable and accounts for most of the runoff in a catchment. The SCS-CN method was originally developed for its use on small agricultural catchments and has since been extended and applied to rural, forest and urban catchments. This method is based on the water balance equation and two basic hypotheses. Using SCS-CN method the surface runoff is estimated as;

$$Q_{surf} = \frac{(R_{day} - I_a)^2}{R_{day} - I_a + S} \quad (2.7)$$

$$S = 25.4\left(\frac{1000}{CN}\right) - 10 \quad (2.8)$$

Where;

$I_a$= the initial abstractions (approx.=0.2 S)

S = retention parameter

CN = the curve number (dimensionless).

To operate CN in a continuous mode, runoff is estimated from a daily rainfall record of approximately 30 years (Williams et al., 2011). Among many, Nayak et al. (2012) successfully applied SCS-CN to quantify the likely changes in the surface runoff in a catchment as an impact of the planned or unplanned changes made in the land use. The weighted average Curve

Numbers (CN) for both the years calculated on the basis of land use/cover type and hydrologic soil class in the catchment area were used.

## 2.3 SWAT Application

The model runs in different GIS platforms commonly ArcGIS and QGIS software. QGIS is an open software with great improvements over the years but has a poor processing stability as compared to ArcGIS. On ArcGIS SWAT is installed as a plugin termed as ArcSWAT. The inputs for the model are; DEM, soil data, land use data and weather data. This data is first prepared on ArcGIS, clipped and projected before importing into the model. The model simulation outputs are; surface runoff, infiltration, evapotranspiration, lateral flow, percolation to shallow and deep aquifer and channel routing (Kambombe, 2018).

The SWAT parameters are physically based and have a significant relationship with geomorphological characteristics of a catchment (Lee et al., 2016). More to this, the model is available as an open-source tool and its source code are available for modification. This has seen the model improve with a lot of documentation, research papers and development of huge literature database (Gasman et al., 2007; Kambombe, 2018). It is a user-friendly tool backed with available free information and user groups, thus was selected for this study. Tabulated below are some of the model parameters that have influence on surface water flow simulation (Table 2.1).

### 2.3.1 Sensitivity Analysis

Parameter sensitivity analysis is the process of determining the rate of change in model output with respect to changes in model parameters (Nkonge, 2017). It is crucial to identify sensitive parameters to ease calibration process. There are two types of sensitivity analysis methods commonly used; local, by changing values one at a time, and global, by allowing all parameter values to change. The two analyses may give different results. Sensitivity of one parameter often depends on the value of other related parameters; hence, the problem with one-at-a-time analysis is that the correct values of other parameters that are fixed are never known. The disadvantage of the global sensitivity analysis is that it needs a large number of simulations (Arnold et al., 2012). The global analysis method will be used in this study under SWAT-CUP as detailed in section 2.3.2.

**Table 2. 1: SWAT model parameters that influences surface water flow simulation**

| Parameter | Description | Unit |
|---|---|---|
| CN2* | The initial SCS runoff curve number for moisture condition and that determines the volume of surface runoff contributing to the total stream flow. It depends on several factors, including soil types, soil textures, soil permeability, land use properties and soil depth. | None |
| SURLAG | Surface runoff lag time; controls the fraction of the total water that is allowed to enter the stream on any specific day. | Days |
| SLOPE* | Average slope steepness | m/m |
| SLSUBBSN | Average slope length | M |
| CH_N | Manning's n value for tributary channel | None |
| CH_K2 | Channel effective hydraulic conductivity | mm/h |
| SOL_AWC | Available water capacity | mm/mm |
| SOL_ALB | Moist soil albedo | None |
| SOL_K | Soil hydraulic conductivity | mm/h |
| SOL_Z | Soil depth | Mm |
| ESCO | Soil evaporation compensation factor; directly influences the evapotranspiration losses from the catchment. | None |
| EPCO | Plant uptake compensation factor; expresses the amount of water needed to meet the plant uptake demand. | None |
| ALPHA_BF | Base-flow alpha factor; a factor that expresses the rate at which groundwater is returned to the surface water flow. | Days |
| GW_DELAY | Groundwater delay; the time required for water leaving the bottom of the root zone to reach the shallow aquifer where it can contribute to lateral groundwater flow. | Days |
| GW_REVAP | Groundwater "revap" coefficient; dimensionless coefficient controlling the rate of water movement between the root zone and the shallow aquifer. | None |
| REVAPMN | Threshold depth of water in the shallow aquifer for "revap" to occur | Mm |
| GWQMN | Threshold water depth in the shallow aquifer for return flow to occur | Mm |
| CANMX | Maximum canopy storage. | Mm |

### 2.3.2 Model Calibration Under SWAT-CUP

Initially, SWAT model was calibrated manually by changing model parameters and comparing/assessing the observed and simulated values. In recent past, semi-automatic calibration techniques and uncertainty analysis tools have been developed and widely used due to their capability of quantifying the degree of uncertainty in parameter estimation leading to more reliable models (Malagò et al., 2015). Most commonly used tools include; the optimization and uncertainty analysis methods, including parameter solution (ParaSol), sequential uncertainty fitting (SUFI-II) and generalized likelihood uncertainty estimation (GLUE). However, ParaSol underestimates the prediction uncertainty, while SUFI-II and GLUE provide larger uncertainty intervals, underlying the differences in their fundamental conceptualizations (Malagò et al., 2015).

The SUFI-II algorithm has been widely used in the calibration of the SWAT model at the large scale due to its easy implementation and the reduced number of models runs needed to achieve good prediction (Yang et al., 2008). With respect to other methods, SUFI-II is characterized by a high flexibility in the choice of various factors such as parameters and ranges, the time scale and the selection of gauged sub-catchments to be calibrated. Model calibration process entails adjusting model parameters so that its output agrees with the observed ground data. Calibration can be done using auto-calibration tools in SWAT-CUP or manually (Arnold et al., 2012). SWAT calibration and uncertainty program (SWAT-CUP) is software tool for SWAT model sensitivity analysis, auto calibration and validation. A set of observed data is imported some for calibration and other for validation into the tool and runs calibration algorithms such as the Generalized Likelihood Uncertainty Estimation (GLUE) or Sequential Uncertainty Fitting Index (SUFI) (Kambombe, 2018). The latter in commonly used for rainfall- runoff modelling and thus selected for this study. SUFI-II algorithm is defined as the difference between simulated and observed variables (Arnold et al., 2012). Model validation measures the performance of the model.

### 2.3.3 Model Validation

Given that; the observed ground stream flow is $Q_{obs}$, the model simulated stream flow is $Q_{sim}$, number of daily discharge values is n and the average observed discharge is $\overline{Q}_{obs}$, SWAT-CUP has the following algorithms available for model validation;

i. Nash-Sutcliffe (NS) model efficiency

This indicates how good a plot of observed versus simulated data fits the 1:1 line and is computed as a ratio of residual variance to measured data variances (Equation 2.9).

$$NS = 1 - \frac{\sum_{i=1}^{n}(Q_{obs} - Q_{sim})^2}{\sum_{i=1}^{n}(Q_{obs} - \overline{Q}_{obs})^2} \quad (2.9)$$

Where;

NS= Nash-Sutcliffe model efficiency (dimensionless)

$Q_{Obs}$= Observed ground stream flow ($m^3/s$)

$Q_{sim}$= Model simulated stream flow ($m^3/s$)

$\overline{Q}_{obs}$= Average observed discharge ($m^3/s$).

NS values range between $-\infty$ and 1, if the values approach one, the model performance is acceptable (Nash & Sutcliffe, 1970).

ii. Percent bias (PBIAS)

This measures the average tendency of the simulated data to be large or smaller than the observed. The PBIAS is computed as (Equation 2.10);

$$PBIAS = \frac{\sum_{i=1}^{n}(Q_{obs} - Q_{sim})^2}{\sum_{i=1}^{n} Q_{obs}} \quad (2.10)$$

Where;

PBIAS= Percent bias (dimensionless)

$Q_{Obs}$= Observed ground stream flow ($m^3/s$)

$Q_{sim}$= Model simulated stream flow ($m^3/s$)

The optimal value of PBIAS is zero, values close to this indicates accurate model simulation. Positive values indicate model underestimation bias, and negative values indicate model overestimation bias (Mwania, 2014).

iii. Root mean square error-observations deviation ratio (RSR)

Computed as (Equation 2.11);

$$RSR = \frac{RMSE}{STDEV_{obs}} = \frac{\sqrt{\sum_{i=1}^{n}(Q_{obs} - Q_{sim})^2}}{\sqrt{\sum_{i=1}^{n}(Q_{obs} - \overline{Q}_{obs})^2}} \quad (2.11)$$

Where;

RSR= Root mean square error-observations deviation ratio (dimensionless)

RMSE= Root mean square error-observations ratio (dimensionless)

$STDEV_{obs}$= standard deviation of error (dimensionless)

$Q_{Obs}$= Observed ground stream flow ($m^3/s$)

$Q_{sim}$= Model simulated stream flow ($m^3/s$)

$\overline{Q}_{obs}$= Average observed discharge ($m^3/s$)

Model simulation is judged as satisfactory if NSE > 0.5, RSR ≤ 0.70 and PBIAS ±25% (Mbungu & Kashaigili, 2017).

## 2.4 Catchment Geomorphologic Characteristics

Variability in land surface properties due to topography, geometry of the land and soil characteristics creates significant heterogeneities that affect large-scale soil moisture dynamics, runoff production, and surface water flows (Bertoldi et al., 2006). Geomorphologic characteristic (GC) is the geometric depiction and stream channels network arrangement of a catchment. They are derived based on Strahler model; where the smallest recognizable streams are assigned order 1, where two streams of order 1 join the resulting stream is assigned order 2, and generally, where two streams of order i join, a stream of order i+ 1 results. If a stream of lower order joins another of higher order, the resulting stream retains the higher of the two orders. Finally, the order of the catchment is designated as the order of the stream reaching its pourpoint (Chow et al., 1988). Geomorphologic characteristics entails; linear properties, areal properties and relief aspect of channel network and of the catchment area (Lee et al., 2016).

### 2.4.1 Bifurcation Ratio

This is a characteristic that gives the relationship between the number of streams of a given order and the number of streams of the next higher order. As given in the following equation:

$$R_b = \frac{N_n}{N_{n+1}} \quad (2.12)$$

Where;

$R_b$ = bifurcation ratio(dimensionless)

$N_n$ = number of streams of the order n

$N_{n+1}$= number of streams of the order n+1

Very high values of this ratio indicate steep slopes, easily eroded soils and such catchment properties present a wide hydrographic network with many tributary streams with rapid response to precipitations (Aparicio, 1996).

### 2.4.2 Drainage Density

The drainage density of a catchment represents the closeness of spacing of channels (Chow et al., 1988). It expresses the capacity to drain a given volume of water from a catchment and it is given as follows;

$$D_d = \frac{\sum L_i}{A} \quad (2.13)$$

Where;

$D_d$= drainage density($m^{-1}$)

A= total catchment area($m^2$)

$L_i$= total stream channel length in the catchment(m).

Various variables aggregately impact the drainage density, such as climate, geography, infiltration capacity, vegetation, and topography of the catchment. The lower values of drainage density impact more prominent infiltration. In the regions of higher drainage density, the infiltration is less and surface overflow is more (Bertoldi et al., 2006).

### 2.4.3 Mean Length of Overland Flow

The mean length of overland flow is defined as the average distance that water from precipitation will have to cover to reach a nearby stream. It is equivalent to one half the reciprocal of the drainage density.

$$\overline{L} = \frac{1}{2D_d} \quad (2.14)$$

Where;

$\overline{L}$= mean length of overland flow(m)

$D_d$= drainage density(m).

Horton noticed that length of overland flow is a standout amongst the most important factors influencing both the hydrologic and physiographic development of drainage basins (Chow et al., 1988).

### 2.4.4 Form Factor

The form factor is defined as the ratio of catchment area to the square of its length as;

$$F = \frac{A}{L^2} \quad (2.15)$$

Where;

F= form factor(dimensionless)

A= catchment area ($m^2$)

L= catchment length (m)

A catchment with higher form factor is normally circular and has higher peak flows for shorter length storms, though elongated catchment with lower values of form factor has low peak flows for longer span storms. The value of form factor for a circular catchment would always be less than 0.785 (Bertoldi et al., 2006).

### 2.4.5 Gravelius Compactness Coefficient

Compactness coefficient is defined as the ratio of the perimeter of the catchment to the perimeter of a circumference whose area is equivalent to the surface of the corresponding catchment. This index represents the shape of the surface of the basin, according to its delimitation, and its influence on runoff and the hydrograph resulting from a precipitation. It is expressed as:

$$K_c = \frac{0.28P}{\sqrt{A}} \quad (2.16)$$

Where;

Kc= gravelius compactness coefficient(dimensionless)

P= perimeter of the catchment (m)

A= area of the catchment($m^2$)

### 2.4.6 Correlation Between GCs and SWAT Parameters

The GCs derived above have a significant relationship with SWAT model parameter (Lee et al., 2016) and thus can be used to estimate model parameters. The parameters of the SWAT model, which is highly correlated with the GCs of a catchment are summarized in Table 2.2. However, Lee et al. (2016) didn't test and validate the use of geomorphologic derived model parameter on surface water flow modelling.

**Table 2.2: Geomorphic characteristics of a catchment versus SWAT parameter**

| Geomorphic characteristic | Equation | Description | Correlated SWAT parameter (Lee et al., 2016). |
|---|---|---|---|
| Linear properties | | | |
| Catchment length | L (km) | Distance in a straight line between pour point and the furthest point along the perimeter | |
| Total streams Length | $L_i$ (km) | Total stream channel length in the catchment | |
| Stream order | Strahler classification model | | |
| Relief properties | | | |
| Mean slope | S (%) | The average angle of inclination of the local surface relative to the horizontal plane. | SURLAG, SLOPE*, SOL_AWC, GW_REVAP, ESCO |
| Mean elevation | E (m) | Elevation difference between the highest and lowest points along the basin | SURLAG, SLOPE*, SOL_K, GWQMN |
| Areal properties | | | |
| Catchment perimeter | P (km) | The length of a catchment divide. | |
| Drainage area | A ($km^2$) | Total catchment area drained by a given stream length. | |
| Drainage density | (Eq. 2.13) | Higher values indicate the infiltration is less and surface overflow is more (Bertoldi et al., 2006). | CH_K2, SOL_ALB, SOL_K, SLSUBBSN, CANMX, EPCO, ALPHA_BF. |
| Bifurcation ratio | (Eq. 2.12) | High values indicate steep slopes and easily eroded soils. (Aparicio, 1996). | CANMX, SOL_K, SLSUBBSN, CN2*, EPCO, GWQMN, ESCO |
| Mean length of flow | (Eq. 2.14) | It affects time of concentration (Chow et al., 1988). | SOL_K, CH_N, CH_K2, SLSUBBSN, EPCO, GWQMN, SFTMP |
| Coefficient of compaction | (Eq. 2.16) | Relationship between the perimeter of the catchment and circumference of a circle of area equal to that of the catchment. | CH_K2, SOL_ALB, SOL_K, GW_REVAP, SLSUBBSN, REVAPMN, ALPAH_BF, GWQMN |
| Form factor | (Eq. 2.15) | Higher values indicate circular catchment with high peak flows for shorter length storms (Bertoldi et al., 2006). | SOL_K, GWQMN, CH_K2, REVAPMN, SLSUBBSN, EPCO and ALPAH_BF |

Mara River catchment is faced with several challenges; increased agricultural activities, deforestation, human settlement, flash floods, low flows, sedimentation and soil erosion (Kipampi et al., 2017; Osoro et al., 2018). Attempts to study the impacts of this challenges to its hydrology has been made, however, lack of reliable gauged data has been reported as the major limitation (Mwangi et al., 2016; Mwangi et al., 2017). SWAT model has been assessed for its applicability on the entire Mara River catchment, where a satisfactory performance was reported, but the model showed poor performance at Amala sub-catchment (Dessu & Melesse, 2012). Therefore, a focus study on SWAT applicability on Amala River catchment is necessary. To overcome the challenges of gauged data unreliability and inconsistency, use of geomorphological parameter in model calibration need to be assessed as a viable alternative.

# CHAPTER THREE

# MATERIALS AND METHODS

## 3.1 The Study Area

The study area was Amala River catchment which forms part of the upper section of the larger Mara River catchment. It is located between longitudes $35^0$ 22'' 30' and $35^0$ 52'' 30' East and latitudes $0^0$ 20'' 0' and $1^0$ 00'' 0' South as per Figure 3.1. The catchment is shared between three counties namely: Nakuru, Narok and Bomet counties.

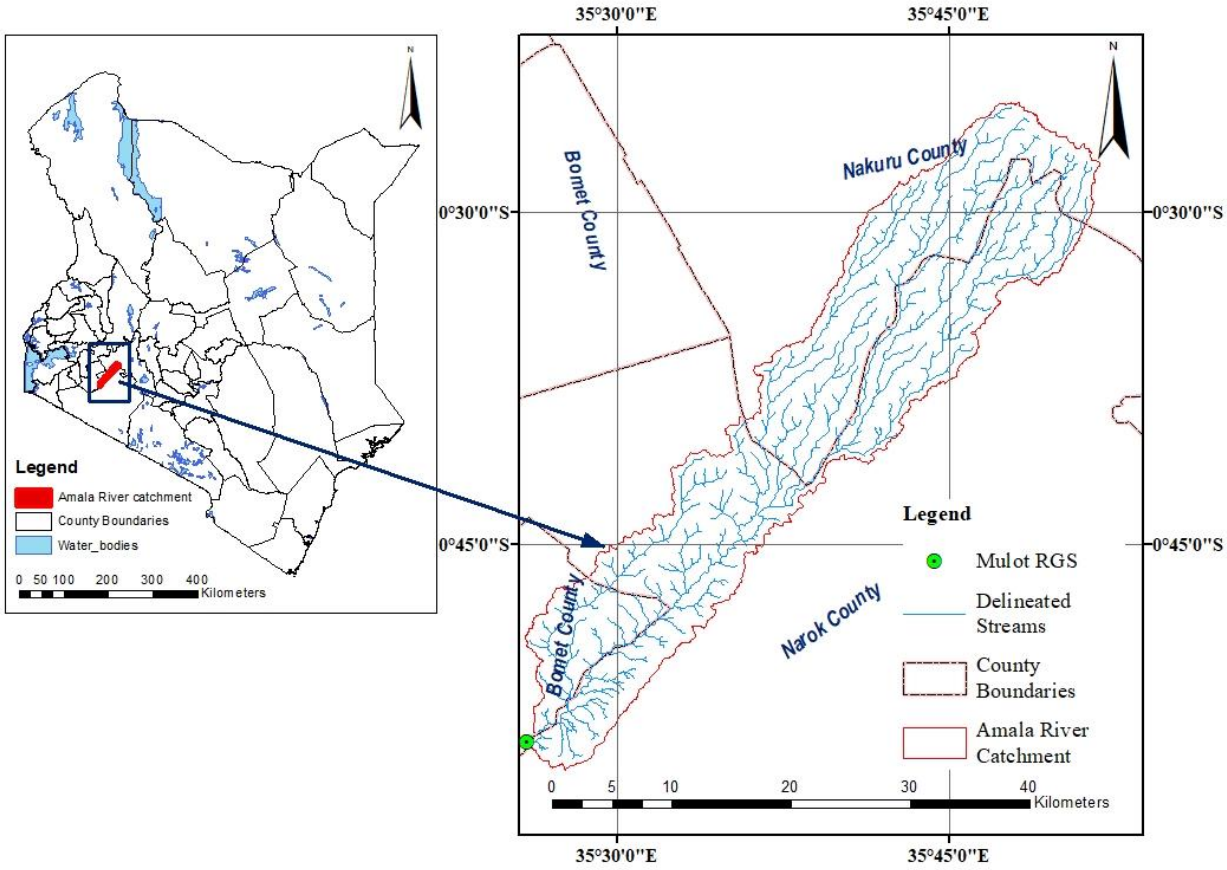


**Figure 3. 1: A study area map showing the location of Amala River Catchment**

Amala River is one of the two permanent tributaries of Mara River and its catchment is among the remnant of the largest indigenous montane forest in Kenya. The total catchment area is about 697.8 $km^2$. The river source from the South Western Mau Forest of Kenya at an elevation of 3065 m above mean sea level (a.m.s.l.) and its outlet is at 1845 m a.m.s.l in Mulot bridge gauging station. The catchment receives approximately an annual rainfall of 1400 mm (Dutton et al., 2018).

Mara River catchment is a trans-boundary land resource covering approximately 13750 $km^2$ partly in South Western Kenya and partly in North Western Tanzania (Kipampi et al., 2017). Mara River source from the South Western Mau Forest of Kenya at 3065m a.m.s.l. and drains into Lake Victoria at Musoma in Tanzania at 1130 m a.m.s.l. This great economic important regional river runs a stretch of 395 km (Mango et al., 2011). Masai Mara National Reserve and Serengeti National Park (a World Heritage Site and a Biosphere Reserve) are part of the catchment and depend on the upper side of the catchment for freshwater supply (Mutie et al., 2006). Thus, the catchment is of global conservation significance. Major tributaries are the Nyangores, Amala, Talek, Sand and Engare Engito on the Kenyan side. The Nyangores and Amala sub-catchments forms the Upper Mara River catchment. Amala River catchment is the focus of this study as detailed in the former paragraph.

## 3.2 SWAT Model Set-up, Calibration and Validation

The hydrologic behavior of the catchment was evaluated on SWAT model. The model was set up on ArcSWAT interface where ArcMap version 10.3 was used to prepare GIS model input. The model was calibrated and validated using gauged data for Amala River catchment on SWAT CUP version 5.1.6. using SUFI-II algorithm.

### 3.2.1 Data Acquisition and Processing

SWAT model has specific data input formats thus all data was processed into these formats and requirements as documented in the user manual (Winchell et al., 2013). Secondary climatic data from Kericho and Kaptunga weather stations were collected and preprocessed as inputs to SWAT model. Remote sensing datasets were obtained; source terrain, land cover data and CHIRPs rainfall product. The major input data for SWAT model include, digital elevation model, soil data, land cover and land use, climatic data (rainfall, temperature, relative humidity, radiation and wind speed) and weather generator statistics. Stream flow dataset, required for calibration and validation of the model, was obtained for Amala gauging station near Mulot bridge. The collected data sets and source are discussed in later paragraphs.

The meteorological data inputs used in this study, in daily time step, were; rainfall, wind speed, solar radiation, relative humidity and temperature. Rainfall data was obtained from Kaptunga forest station and used in nexus with CHIRPs rainfall product averaged over the

catchment. Daily maximum and minimum temperature, solar radiation, humidity and wind speed were obtained from Kericho KMD station which is near but outside the catchment. These datasets from Kericho were only used to calculate Weather generator statistics for the region. Microsoft Excel tool was used to prepare meteorological inputs text files as defined for the SWAT model (Winchell et al., 2013) on a daily time step. Weather statistical parameters were generated from these daily weather data in P-stat program (Appendix A.1). The statistics were used to customize weather generator database to local climatic condition. The customized weather generator database serves as a tool in SWAT to simulate the missing input data.

Landsat TM imageries were chosen as the primary data for land use classification. Product details of the imageries are given in Appendix A. 6. The date of acquisition of the imageries was 4$^{th}$ Feb, 2003. Using image analysis tool in ArcGIS the imageries were stacked and mosaic to full cover the study area. The mosaic raster was clipped to study area and classified. A supervised classification of the image using maximum likelihood was used. Google Earth Pro was used as a background map for creating the training samples. The resulting land use map (Figure 3.2) was then used in SWAT as input.

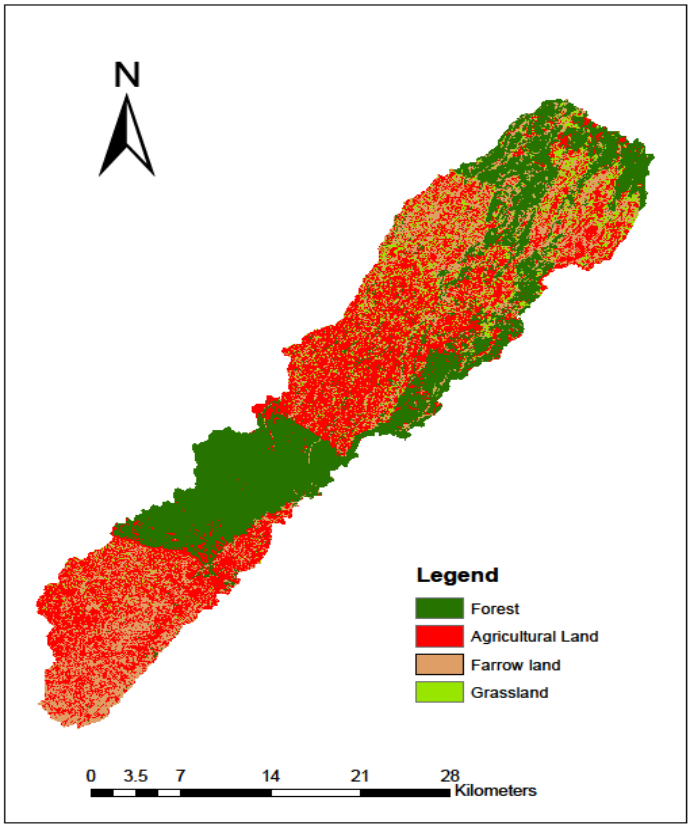


**Figure 3. 2: Land cover classification map for Amala River catchment**

In this study, the soil data classification model based on Food and Agriculture Organization of the United Nations version 3.6 was adopted. A soil map sourced from Kenya Soil and Terrain database (KENSOTER) at Soil Survey Department of Kenya was clipped to area of interest and reclassified into FAO soil classes (Figure 3.3). The soil data was required in SWAT model to derive soil hydraulic properties for stream flow prediction.

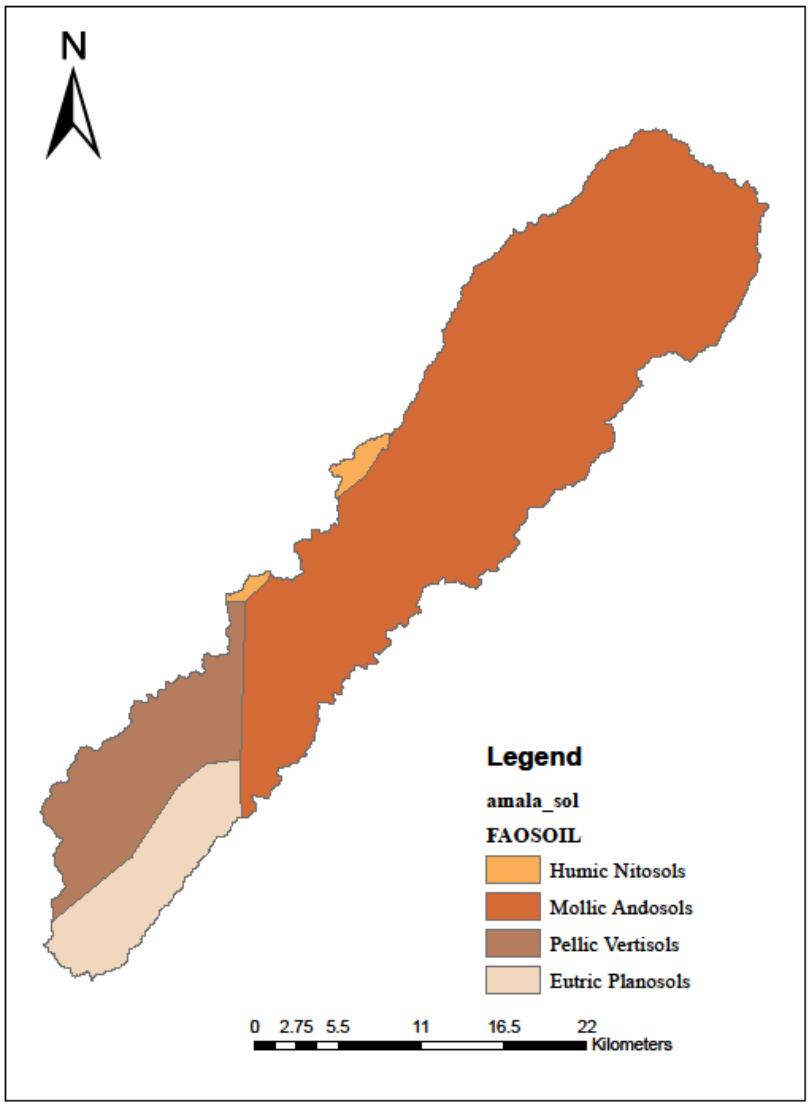


**Figure 3. 3: A map depicting characteristics and distribution of soils in Amala River catchment**

Elevation and terrain data were obtained from the Shuttle Radar Topography Mission-Digital Elevation Model (SRTM-DEM) product available in the United States Geological Surveys (USGS) portal (http: https://earthexplorer.usgs.gov/) (Figure 3.4).

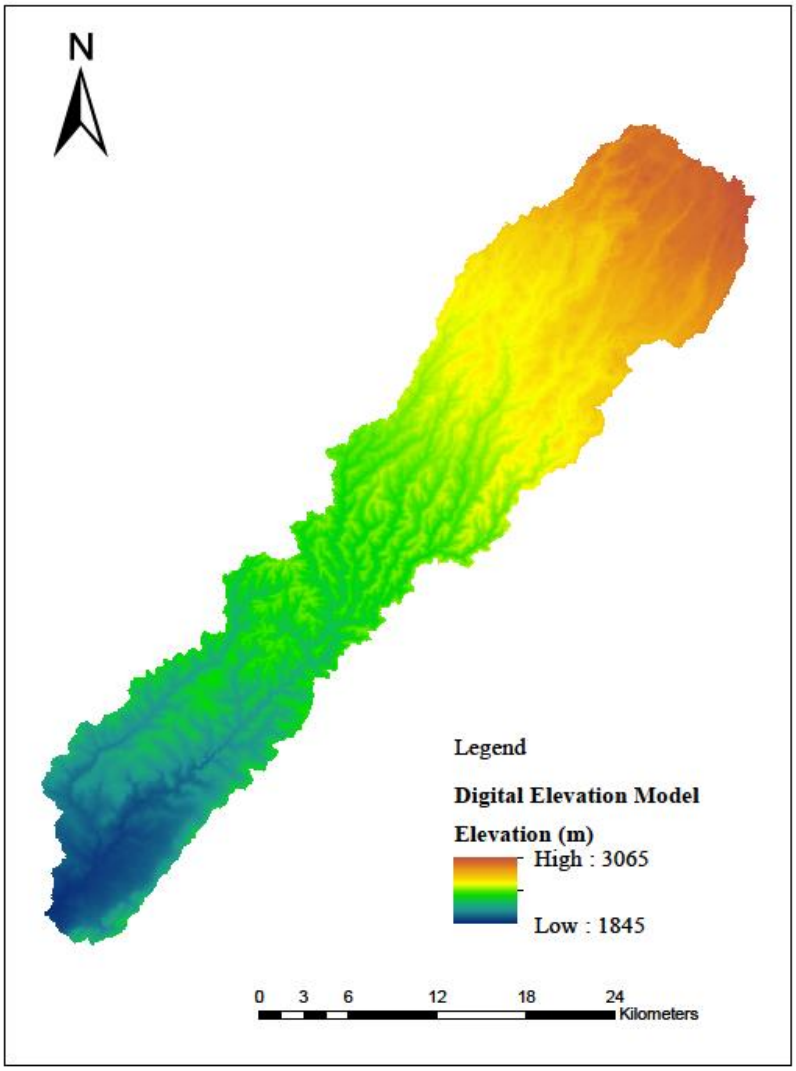


**Figure 3. 4: A digital elevation model map for the study area**

SRTM-DEM Global of Digital Object Identifier (DOI) number: 10.5066/F7PR7TFT, offer worldwide coverage of void filled elevation data at a resolution of 1 arc-second (30 meters). These DEM data were used to delineate the watershed and to analyze the drainage pattern of the land surface. The metadata of the source file is summarized in Table 3.1 below.

**Table 3.1: SRTM 1 arc-second global product details**

| | |
|---|---|
| Projection | Geographic |
| Horizontal Datum | WGS84 |
| Vertical Datum | EGM96 (Earth Gravitational Model 1996) |
| Vertical Units | Meters |
| Spatial Resolution | 1 arc-second (~30m) |
| Raster Size | 1-degree tiles |
| C- band Wavelength | 5.6 cm |

All the input map data, discussed above, were projected to WGS_1984_UTM_Zone_36S, the projection details were as in Table 3.2. This was necessary to ensure the maps are correctly overlaid during model set up.

**Table 3.2: A summary of the UTM projection used for the model set up**

| | |
|---|---|
| Datum | D_WGS_1984 |
| Units | Meters |
| Longitude of central meridian | 33 |
| Latitude of projection's origin | 0 |
| False easting | 500000 |
| False northing | 0 |

Hydrologic/stream flow data was obtained from the Water Resource Authority (WRA) for Amala River gauging station at Mulot bridge (1LB02). Amala gauging station whose code is 1LB02 was started in 1955 and is located at longitude 35.430E, latitude -0.890S and at an altitude of 1860m a.s.l. The dataset accessed were between 1955-2008 and 2011-2019 with some missing months in between. The was no need for filling small data gaps as the SWAT-CUP model used for calibration allowed use of data with gaps, where the user skipped the dates with missing values. The program recognized the skipped dates as missing data and excludes them in the process. However, calibration and validation data sets were picked for years with least gaps that is, 2000-2004 and 2005-2008 respectively.

### 3.2.2 SWAT Model Setup

The SWAT model was setup on ArcSWAT interface for the study area. The setup process for the model was in four stages; catchment delineation, HRU definition, weather data input and writing input tables (Duru, 2015). In catchment delineation, the pre-processed SRTM-DEM (clipped to a size slightly larger than the study area) was loaded into the interface**.** Predefined stream network option was used in this case where stream network and sub-catchment shapefiles generated in section 3.3 was imported to the interface. Finally, the catchment and sub-catchments parameterization was done by overlaying the elevation data, catchment boundary, sub-catchments, outlets and the stream network. A total of 25 sub-catchments were parameterized, the pour point near Mulot bridge was defined as the main outlet for the study area (Figure 3.5).

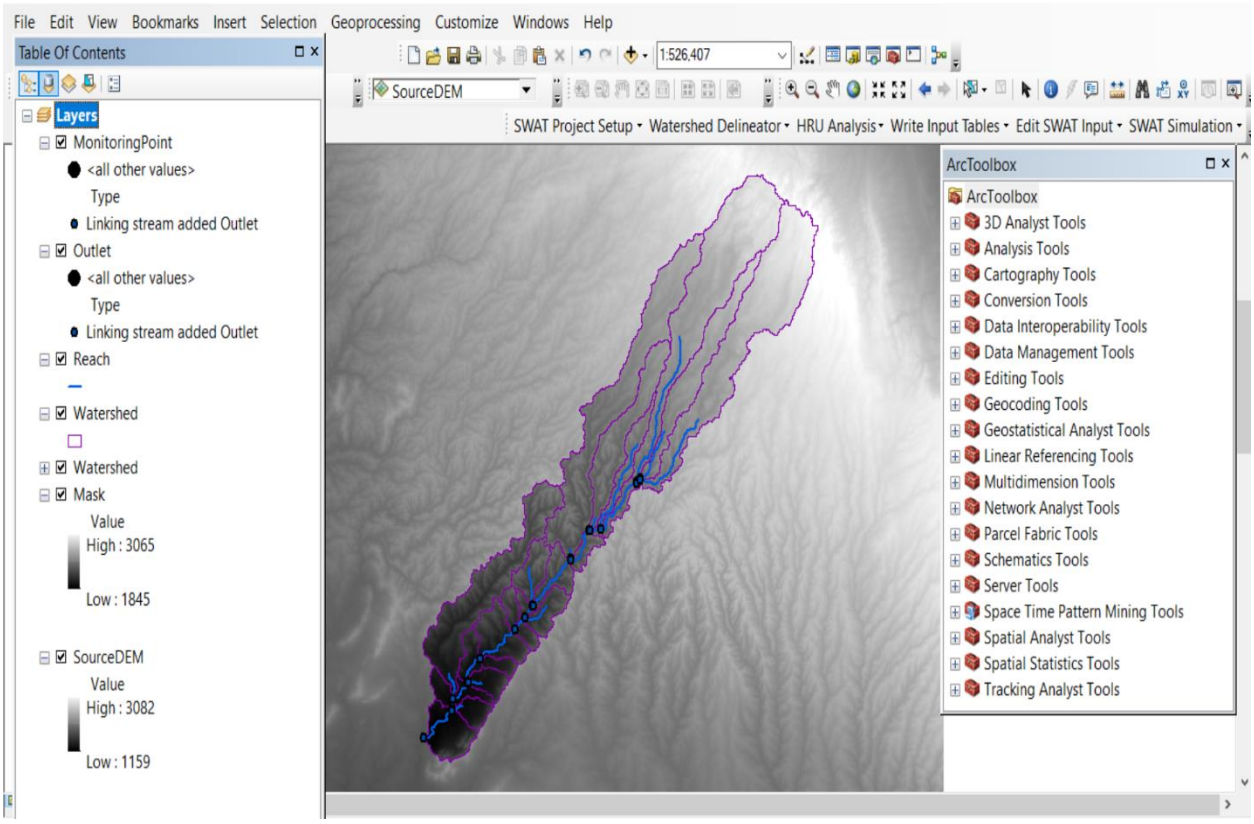


**Figure 3.5: Catchment delineation using predefined sub-catchment and stream network in ArcSWAT**

The model was now ready for HRU definition. The SWAT model being a semi distributed model, it lumped parameter at distributed units called hydrologic response units (HRUs) based on a unique combination of land cover, soil characteristics and slope. Prepared

land cover map was imported into the model and resampled from 14 classes into 5 classes. This was necessary to meet the SWAT land use land cover input requirement. A user defined look up table was provided as a link between the land use land cover map classes and the model defined classes. A soil map (prepared in former section) was imported into the model and a look up table provided to link it to the model soil database. The model clipped the two maps, to fit the delineated catchment area, during importation. A slope map was generated from DEM by defining five slope classes and class limits as shown in Table 3.3 below:

**Table 3. 3: User tables for definition of slope classes**

| Slope class | Lower limit (>=) | Upper limit (<) |
|---|---|---|
| 1 | 0 | 5 |
| 2 | 5 | 7.5 |
| 3 | 7.5 | 10 |
| 4 | 10 | 20 |
| 5 | 20 | 9999 |

The three maps were each reclassified, resampled to same resolution and then overlaid to create HRUs as shown in the Figure 3.6. In HRUs definition of the model availed two options; to create multiple or single HRUs per sub-catchment. The former option was picked for this study, where multiple HRUs in a sub-catchment were created. This ensured high spatial distribution of parameters in the model, the following default thresholds values were used;

- land use percentage (%) over sub-catchment area = 5%
- soil class percentage (%) over land use area = 5%
- slope class percentage (%) over soil area = 5%

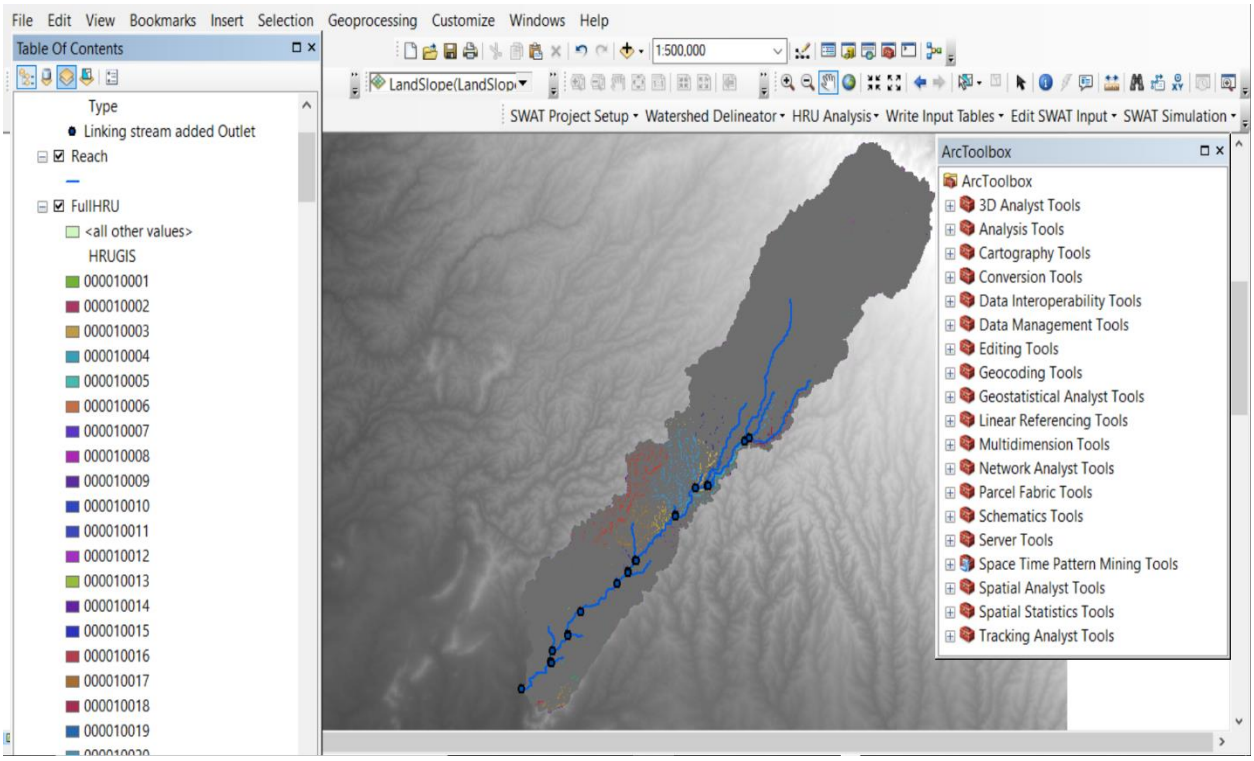


**Figure 3. 6: Hydrologic Response Units (HRU) distribution screen capture**

Five elevation bands were created over the catchment to distribute spatially the temperature and precipitation lapses. A final HRUs report was generated characterizing a total of the 253 HRUs and 25 sub-catchments successfully created over the catchment. Weather data definition in the model was done by providing the required weather data; precipitation, maximum and minimum temperature, relative humidity, solar radiation and wind speed, in text file formats (Appendix A.2). The model has a built-in weather database for USA which help simulate missing data in that region, to customize the weather generator for the study region climatic condition, derived weather statistics are written in the database manually. Thus, missing records were simulated using a regionalized statistical weather generator database. The statistics required by the weather generator were as in Table 4.2 (in chapter 4) derived from KMD Kericho station weather data for 10 years (2001-2010) to represent the regional parameter. The equations used are documented in SWAT user manual (Winchell et al., 2013).

SWAT model writes input tables into its database by converting all the user defined input files (the watershed delineation, land use, soil data, HRUs created and weather files) into FORTRAN format. Therefore, after all input files were successfully imported into the model the

input tables were written by selecting the 'write all files' option. After which the model was now fully set up for the catchment.

### 3.2.3 SWAT Model Simulation

After a successful model set up the "Run SWAT" icon becomes available under the SWAT simulation tools. Using this GUI, the simulation period was set as 01/01/1998 to 12/31/2004, a monthly flow printout option was selected and a warm up period for the model (NYSKIP) of 2 years was also set. This means that the year 1998 and 1999 were simulated to initialize the model and no output was given for these 2 years, the simulation output only included 5 years from 2000-2004. The other setting made were as depicted in the Figure 3.7 below, by selecting the SWAT run option a simulation was made.

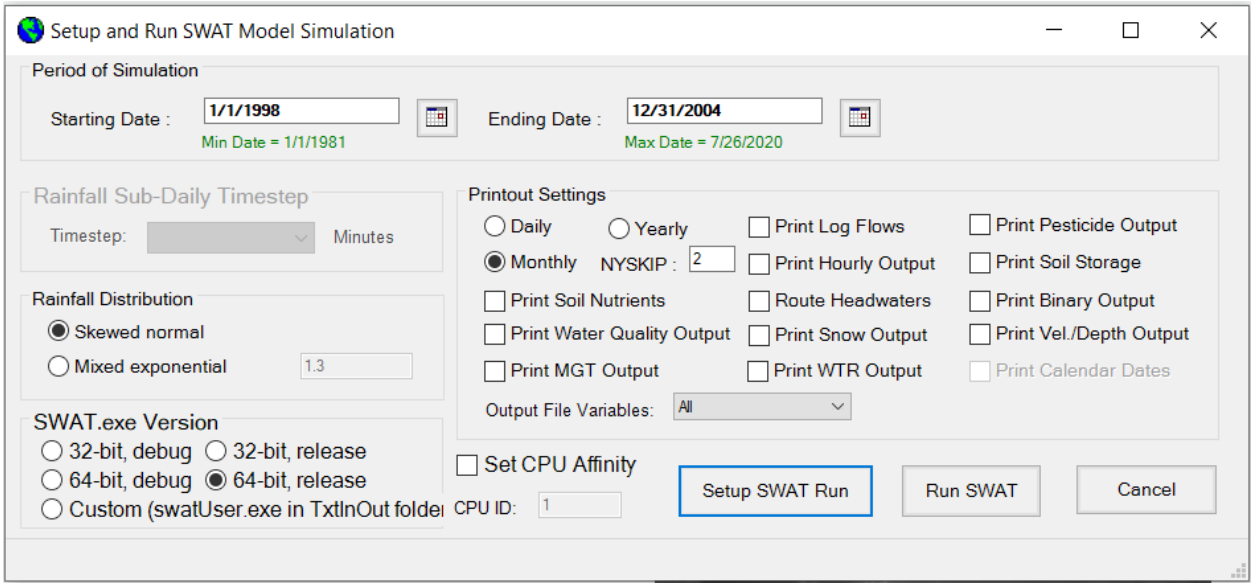


**Figure 3. 7: SWAT model simulation graphical user interface (GUI)**

Simulation results were printed out by the model in a text file which can be import in other software for analysis or visualization. A visualization of the model output using "read SWAT output" option is depicted in Figure 3.8 below. The figures show a summary of the initial model run, hydrological output. The model was now ready for sensitivity analysis, calibration and validation.

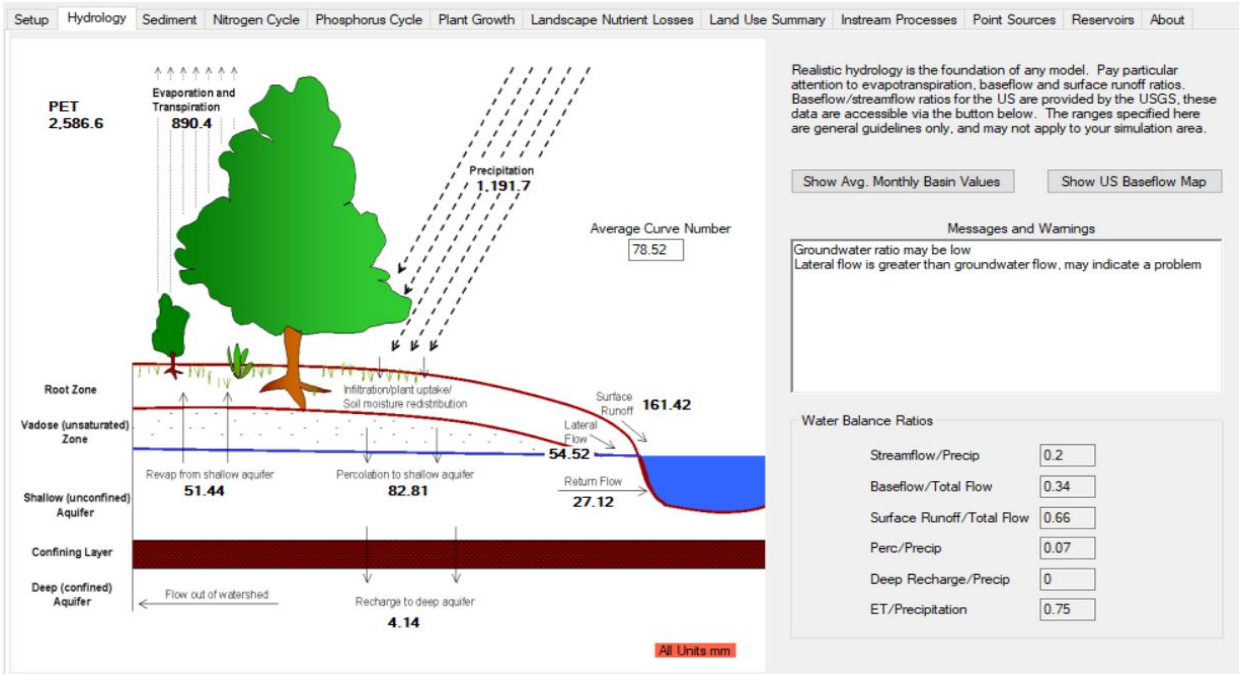


**Figure 3. 8: Hydrologic simulation output of the initial model before calibration**

### 3.2.4 SWAT Model Parameterization for Sensitivity Analysis, Calibration and Validation

A new project was created and the established SWAT model package contained in "TxtInOut" directory was imported on SWAT-CUP for sensitivity analysis, calibration and validation. All applied parameter identifiers were based on literature review and physical meaning reflecting the physical characteristics of the modelled catchment. The parameterization scheme defined by Abbaspour in 2015 was used as follows;

x_<parname>.<ext>_<hydrogrp>_<soltext>_<landuse>_<sub-catchment>_<slope>

Where;

x_= the type of change to be applied to the parameter, three choices are available;

v_= replace; the existing parameter value is to be replaced by the given value

a_= absolute; the given value is added to the existing parameter value

r_= relative; the existing parameter value is multiplied by (1+ a given value)

<parname> = SWAT parameter name

<ext> = SWAT file extension code for the file containing the parameter

<hydrogrp> = (optional) soil hydrological group

<soltext> = (optional) soil texture

<landuse> = (optional) name of the land use category

<subbsn> = (optional) sub-catchment number(s)

<slope> = (optional) slope

Different combinations of the above options were used to describe parameter identifiers during modification of model files in sensitivity analysis, calibration and validation processes. Global assigning of parameters was done by omitting the optional identifiers defined above. Table 3.4 in the later section shows the parameterization used in this study.

### 3.2.5 Sensitivity Analysis

In sensitivity analysis, an algorithm was used to determine and rank the influence a set of parameters have on simulated discharge. Before calibration of the model, identification of both physical and conceptual parameters that have greater influence on model performance was done. Sensitivity analysis process involved establishing the rate of change in model output with respect to changes in model parameters. SWAT- Calibration and Uncertainty Program (SWAT-CUP) was used to do a global sensitivity on 13 parameters. These parameters were chosen based on previous studies in the region (Dessu & Melesse, 2012; Mwangi et al., 2016).

**Table 3.4: Parameter selected for global sensitivity analysis and their parameterization**

| No. | Parameter selected | Parameterization | Initial range for sensitivity analysis |
|---|---|---|---|
| 1 | CN2 | r__CN2.mgt | -0.2 to 0.2 |
| 2 | SOL_AWC | a__SOL_AWC(..).sol | -0.1 to 0.1 |
| 3 | ESCO | v__ESCO.bsn | 0 to 1 |
| 4 | GWQMN | r__GWQMN.gw | -0.2 to 0.2 |
| 5 | GW_REVAP | v__GW_REVAP.gw | 0 to 200 |
| 6 | REVAPMN | r__REVAPMN.gw | 0 to 152 |
| 7 | ALPHA_BF | v__ALPHA_BF.gw | 0.89 to1.0 |
| 8 | SOL_K | r__SOL_K(..).sol | -0.1 to 0.1 |
| 9 | RCHRG_DP | r__RCHRG_DP.gw | -0.1 to 0.1 |
| 10 | SLSUBBSN | r__SLSUBBSN.hru | -0.1 to 0.1 |
| 11 | HRU_SLP | r__HRU_SLP.hru | -0.1 to 0.1 |
| 12 | OV_N | r__OV_N.hru | -0.1 to 0.1 |
| 13 | CANMX | a__CANMX.hru | 0.01 to 0.1 |

In SWAT-CUP, parameter sensitivities are determined by calculating the following multiple regression system, which regresses the Latin hypercube generated parameters against the objective function values.

$$f = a + \sum_{i=1}^{n} B_i b_i \quad (3.1)$$

Where;

f = the output value of the objective function

a = the regression constant

B = the model parameter

b = the coefficient of parameters.

A t-test is then used to identify the relative significance of each parameter $b_i$. In the analysis, the larger, in absolute value, the value of t-stat, and the smaller the p-value, the more sensitive a parameter is (Abbaspour et al., 2017). In the global sensitivity analysis, a period of 5 years (2000-2004) was used and 1000 simulations were made.

### 3.2.6 SWAT Model Calibration

This methodology aimed to minimize the difference between model simulated discharge and the observed corresponding discharge. Ideally, the calibration methodology used was an optimization algorithm;

$$\min: f(\theta) = \sum_{j=1}^{v}\left[w_j \sum_{i=1}^{n_j}(Q_0 - Q_s)_i^{\,2}\right] \quad (3.2)$$

Or

$$\max: f(\theta) = \sum_{j=1}^{v}\left[w_j\left(1 - \frac{\sum_{i=1}^{n_j}(Q_0 - Q_s)_i^{\,2}}{\sum_{i=1}^{n_j}(Q_0 - \overline{Q_s})_i^{\,2}}\right)\right] \quad (3.3)$$

Where;

$f(\Theta)$ = the objective function

$Q_0$= Observed ground stream flow ($m^3/s$)

$Q_s$= Model simulated stream flow ($m^3/s$)

$\overline{Q_s}$ = Average observed discharge ($m^3/s$)

v = the number of measured variables to be used to calibrate the model

$w_j$ = weight of the jth variable

$n_j$ = the number of measured observations in the jth variable.

The standalone SWAT Calibration and Uncertainty Program (SWAT-CUP) was used to calibrate the model (Figure 3.9). The model calibration was done by changing the most sensitive parameters and comparing the simulated to the observed stream flow while optimizing the objective function based on NSE and $R^2$ as given in Equation 3.2 and 3.3.

To achieve this on SWAT-CUP, SUFI-II algorithm was selected as the optimization procedure for the calibration process. All SWAT model files were written into SWAT-CUP directory under the SUFI-II, where the algorithm can access them for modification during calibration simulations. The following input files were prepared as user control on the process; Par_inf.txt, SUFI2_swEdit.def, Observed_rch.txt, var_file_rch.txt, SUFI2_extract_rch.def, Observed.txt and Var_file_name.txt.

In Par_inf.txt, 13 model parameters to be optimized, their ranges of sampling and the parameterization used were defined and number of simulations to make in the current iteration was specified. SUFI2 is iterative and therefore 4 iterations were taken- each iteration consisted of 1000 simulation. The parameter defined and their ranges were as depicted in Table 3.4 in former section. In SWAT_swEdit.def file, the start and end simulation were set as 1 and 1000 respectively. For observation data input file (observed_rch.txt), gauged discharge data for the calibration period was provided to the process through this file. Other information was defined under this file such as total count of observed data (=60), number of variables (=1), name of the variable (= stream flow) and sub-catchment identification number to be included in the objective function (= '25'). To enable extraction of SWAT model files for modification commands/instructions were coded in two text files (Var_file_rch.txt and SUFI2_extract_rch.def). Finally, the objective function was defined based on NSE, as discussed in former paragraphs, using Var_file_name.txt. In Var_file_name.txt file, all the variables included in the objective function were defined. An observed.txt containing the same information as in "Observation_rch.txt" plus goal threshold for the objective function was prepared as input to the objective function.

Simulation on SWAT-CUP was repeated until the model reaches stability (4 iterations each 1000 simulations were made). Observed monthly stream flow data for five year (2000-2004) were used in the calibration process. This involved carrying out parameters adjustment and producing simulated stream flow which is then compared to the observed stream flow. The best simulation parameters and indices was reported as the calibration results.

During the calibration process, the model uncertainty was evaluated. An identification of all possible model solutions in the acceptable range, given input uncertainties, was made and expressed as 95% prediction uncertainty (95PPU). Two statistical parameters were used to compare the 95PPU band with the observed discharge hydrograph. These statistics were defined as p-factor and r-factor. Where p-factor is the percentage of observed hydrograph covered by the 95PPU band and r-factor is a measure of the thickness of the 95PPU band and is calculated as the average 95PPU thickness divided by the standard deviation of the corresponding observed variable (Abbaspour et al., 2017);

$$\text{r factor}_j = \frac{\frac{1}{n_j}\sum_{t_{i=1}}^{n_j}\left(x_s^{t_i,97.5\%} - x_s^{t_i,2.5\%}\right)}{\delta_{oj}} \quad (3.4)$$

Where;

$x_s^{ti,97.5\%}$ and $x_s^{ti,2.5\%}$ = the upper and lower boundary of the 95PPU at time-step t and simulation i

$n_j$ = the number of data points

$\delta_{oj}$ = the standard deviation of the jth observed variable.

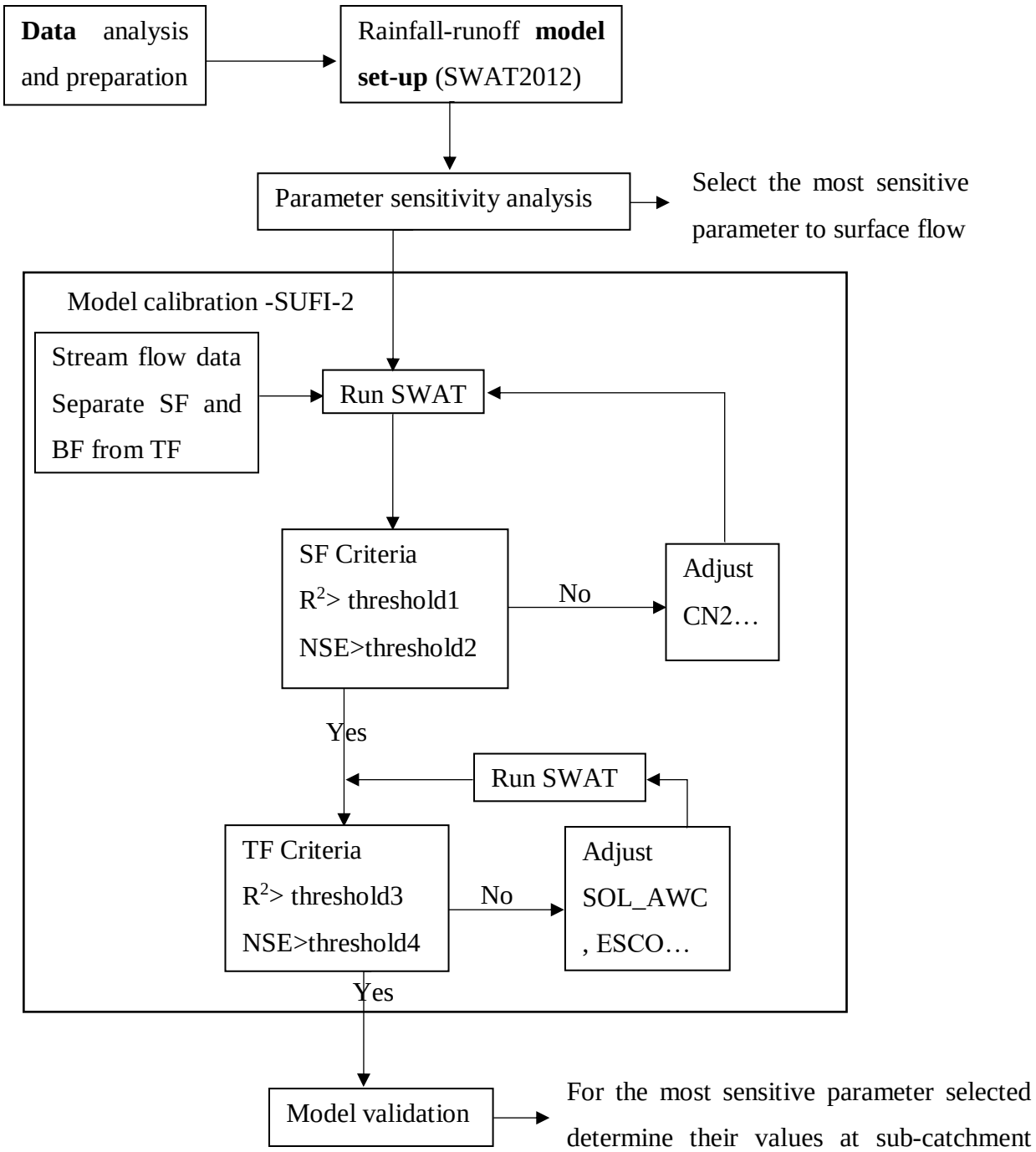


**Figure 3. 9: Model set-up, calibration and validation flowchart**

In SUFI-II therefore, model uncertainty was quantified as a 95PPU band, the p-factor reported the fraction of observed data bracketed in the 95 PPU band and r-factor reported the mean thickness of the 95 PPU band as a ratio of the standard deviation of the observed data. A p-factor = 1 and r- factor = 0 was considered to represent an ideal model (Abbaspour et al., 2015).

### 3.2.7 SWAT Model Validation

Validation involved comparison of simulated stream flow to observed stream flow from a different time frame with the one used in calibration but by using the parameter values obtained during the calibration period (Nkonge, 2017). Therefore, another four-year set (2005-2008) of observed monthly stream flow data was used for the validation process. The performance of the model was checked by the Nash-Sutcliffe (NS), the coefficient of determination ($R^2$), percent bias (PBIAS) and the root mean square error-observations deviation ratio (RSR). This was achieved in SWAT-CUP by running equal number of simulations (1000) as in calibration process. The parameters and their ranges were used as they were in the best iteration of the calibration. In validation process, only time frame input was edited to reflect the validation period (2005-2008).

## 3.4 3.3 Hydro-geomorphological Catchment Characteristics

Primary morphologic characteristics of a catchment such as the drainage network and catchment geometry can be derived from Digital Elevation Model (DEM) in GIS environment. ArcGIS is a key GIS environment for analyzing, visualizing and interactive map analyzing. Geomorphologic characteristics of a catchment are important in exploring morphometry and surface drainage network physiognomies. These in turn can be used to quantify runoff, infiltration, soil erosion, surface water ponding and other hydrological characteristics of a catchment. In this objective a quantitative analysis of geomorphologic characteristics of Amala River catchment using Shuttle Radar Topography Mission (SRTM)-DEM, topographic maps and ArcGIS tools was done and related to its hydrologic characteristics.

### 3.3.1 Data Acquisition and Preprocessing

The data required for quantitative geomorphologic analysis of the catchment included topographic maps and DEM. The Kenya Survey Topographic map sheets (117/4, 118/3, 118/4, 131/2, 132/1, 132/2, 131/4, 132/3 and 132/4) at a scale of 1:50000 were obtained, digitized and georeferenced. SRTM-DEM, 30-m spatial resolution, downloaded and preprocessed in section 3.2.1 in former objective was used.

### 3.3.2 Quantitative Analysis of Geomorphologic Characteristics

To derive geomorphological parameters of the catchment, the morphometry of the catchment was computed from the DEM on GIS environment (ArcMap). In this study, morphometric parameters were derived for the catchment and for the sub-catchments. These parameters were used in mathematical equations to derive geomorphological parameters.

In raster processing environment, the DEM was preprocessed to fill the sinks and a flow accumulation raster was developed. A drainage network map was generated by applying a pixel threshold to the flow accumulation raster using map algebra tool. Figure 3.11 shows a flow chart model in ArcMap used to derive stream network and delineate the catchment for the morphometric analysis. In order to ensure the generated stream was representative of the natural stream, different thresholds were applied in the flow accumulation map algebra. A threshold value of 500 pixels gave a stream network closely overlaying with the topo sheet stream network (Figure 3.10). The stream network map indicates the streams of various orders and was used for determination of morphometric parameters of the catchment and sub-catchments (Figure 3.10). For stream network parameterizing, stream orders were derived from generated stream network in Spatial Analyst Tool interface of ArcGIS based on Strahler model.

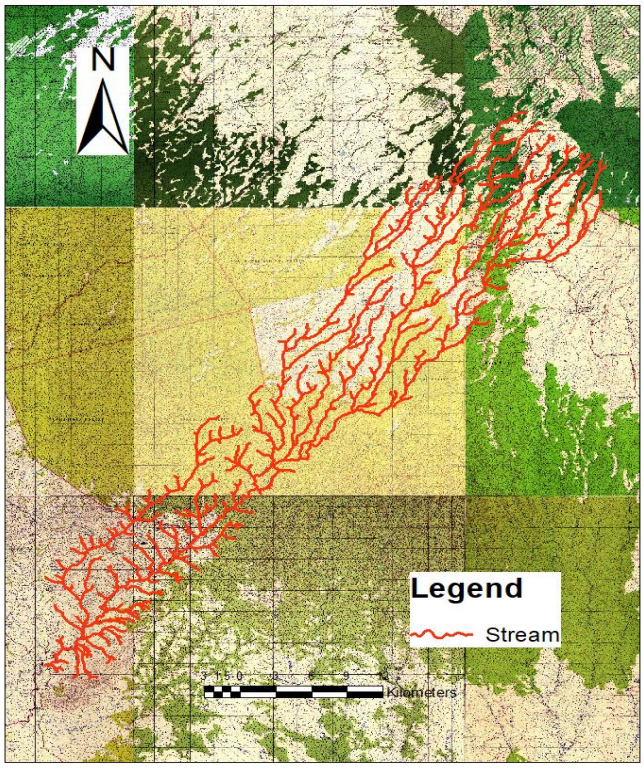


**Figure 3.10: An overlay of generated stream with toposheets**

Values of morphometric parameters were derived from the attribute tables of the vector layers generated using Spatial Analyst tool in Arc Map environment. These parameters included; number of stream segments of order u (Su), sum stream lengths of order u (Lu), length of the catchment (L), perimeter of the catchment (P), area of the catchment (A), maximum elevation (ELEVmax) and minimum elevation (ELEVmin).

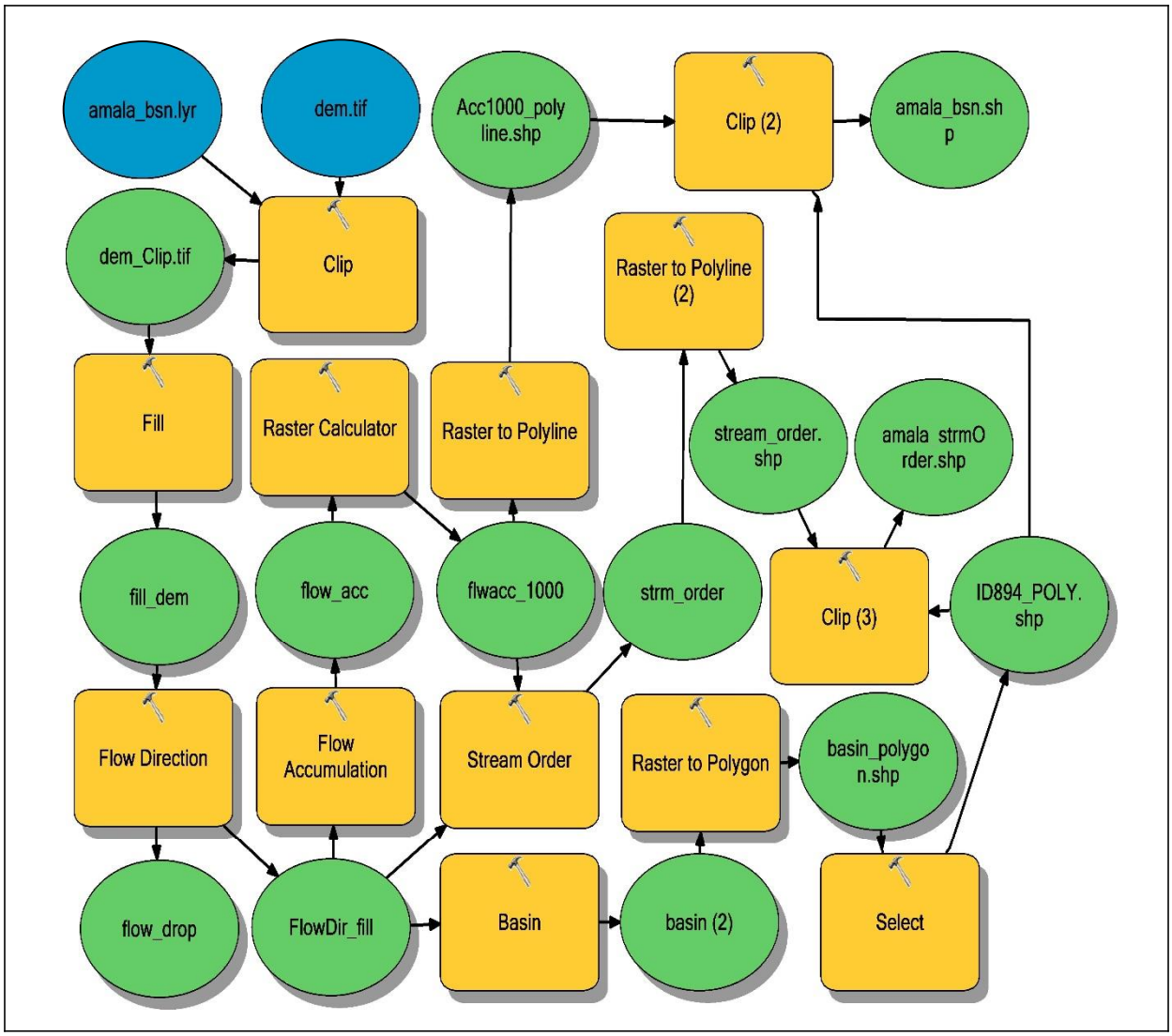


**Figure 3. 11: A flow chart model used to generate stream network map**

In this study thirteen geomorphologic parameters were computed to characterize Amala River catchment and its sub-catchments; stream length ratio, bifurcation ratio, rho coefficient, drainage density, drainage texture, drainage frequency, infiltration number, overland flow length, form factor, elongation ratio, compactness coefficient, relief ratio and ruggedness number. These

parameters were categorized into: stream network characterization, basin geometry, drainage parameters, and relief parameters (Table 3.5).

**Table 3.5a: List of drainage network parameters, their symbols and computation equations**

| S. No. | Parameters | Abbreviation | Formula |
|---|---|---|---|
| 1 | Stream Order | So | Strahler model |
| 2 | Stream Number | Nu | $Nu = N_1 + N_2 + \ldots N_n$ |
| 3 | Stream Length | Lu | $Lu = L_1 + L_2 + \ldots L_n$ |
| 4 | Stream Length Ratio | Lr | $Lr = \frac{mean\_Lu_n}{mean\_Lu_{n-1}}$ |
| 5 | Weighted length ratio | $\widehat{Lr}$ | $\widehat{Lr} = \frac{1}{n}\sum_{i=1}^{n}(w_i * Lr_i)$ |
| 6 | Bifurcation Ratio | $R_b$ | $R_b = \frac{N_n}{N_{n+1}}$ |
| 7 | Weighted bifurcation ratio | $\widehat{R_b}$ | $\widehat{R_b} = \frac{1}{n}\sum_{i=1}^{n}(w_i * R_{bi})$ |
| 8 | Rho coefficient | P | $\rho = \frac{Lr}{R_b}$ |

**Table 3.5b: List of basin geometry parameters, their symbols and computation equations**

| S. No. | Parameters | Abbreviation | Formula |
|---|---|---|---|
| 9 | Length of the basin | Lb | Schumm (1956) |
| 10 | Basin Area | A | Spatial Analyst tool |
| 11 | Basin Perimeter | P | Spatial Analyst tool |
| 12 | Form Factor | $F_f$ | $F_f = \frac{A}{L^2}$ |
| 13 | Elongation Ratio | Re | $Re = (\frac{2}{Lb}) * (\frac{A}{\pi})^{0.5}$ |
| 14 | Texture Ratio | Rt | $Rt = \frac{N1}{P}$ |
| 15 | Circularity Ratio | Rc | $Rc = 12.57 * (A/P\text{^}2)$ |
| 16 | Drainage Texture | Dt | $Dt = \frac{Nu}{P}$ |
| 17 | Compactness Coefficient | $K_c$ | $K_c = \frac{0.2841P}{A^{0.5}}$ |

**Table 3.5 c: List of drainage texture analysis parameters, their symbols and computation equations**

| S. No. | Parameters | Abbreviation | Formula |
|---|---|---|---|
| 18 | Stream Frequency | Fs | $\mathrm{Fs} = \frac{\mathrm{Nu}}{\mathrm{A}}$ |
| 19 | Drainage Density | Dd | $\mathrm{Dd} = \frac{\mathrm{Lu}}{\mathrm{A}}$ |
| 20 | Infiltration number | $I_f$ | $\mathrm{I_f} = \mathrm{Fs} * \mathrm{Dd}$ |
| 21 | Length of overland flow | L | $\mathrm{L} = \frac{1}{2\mathrm{Dd}}$ |
| 22 | Drainage Intensity | Di | $\mathrm{Di} = \frac{\mathrm{Fs}}{\mathrm{Dd}}$ |

**Table 3.5 d: List of relief parameters, their symbols and computation equations**

| S. No. | Parameters | Abbreviation | Formula |
|---|---|---|---|
| 23 | Maximum height of the watershed | Z | DEM processing |
| 24 | Minimum height of the watershed | Z | DEM processing |
| 25 | Total basin relief | H | $\mathrm{H} = \mathrm{Z} - \mathrm{z}$ |
| 26 | Relief Ratio | Rh | $\mathrm{Rh} = \frac{\mathrm{H}}{\mathrm{Lb}}$ |
| 27 | Ruggedness number | Rn | $\mathrm{Rn} = \mathrm{Dd} * \mathrm{H}$ |

### 3.3.3 Regression Analysis Between SWAT Model Parameter and Geomorphological Characteristics

Sub-catchments whose hydrologic response does not depend on others were selected for this analysis that is, those which do not receive surface water flow from an upstream sub-catchment. This was to reduce uncertainties in the regressions developed. Regressions relating the most sensitive model parameters to geomorphological characteristics were derived within each of the selected 12 sub-catchments. The most sensitive model parameter was picked from the sensitivity analysis in section 3.2. To overcome challenges resulting from co-linearity between the geomorphological characteristics, they were assessed for linear correlation using $R^2$ and where $R^2 > 0.50$ only one of them was used in the regression. A linear correlation was tested between each model parameter and individual geomorphologic characteristic, only those with $R^2 > 0.50$ were used in the regression.

The general objective was to minimize the effect of co-linearity by choosing geomorphological characteristics with minimal or no interdependence. Pearson correlation coefficients were the measure of dependence between these characteristics. Where co-linearity was found, only one of the characteristics concerned was included in the regression equation. Initial model parameter and geomorphological characteristics combinations were selected subjectively by linear correlation ($R^2$> 0.50) and based on hydrological and physical meaning. Several combinations of variables were considered starting with a simple regression with the geomorphological characteristic which has greatest influence on the given model parameter (Figure 3.12). For each model parameter, the geomorphological characteristics suggested by correlation analysis and stepwise regression was combined in a multiple regression model enabling the parameters to be described in terms of geomorphological characteristics as below:

$$P(n) = \beta_0(n) + \beta_1 GC_1(n) + \beta_2 GC_2(n) + \ldots\ldots\ldots + \beta_k GC_k(n) + \varepsilon(n) \quad (3.5)$$

Where;

P = model parameter

GC= geomorphologic characteristic

n = 1, 2..., N–rank of model parameter in terms of sensitivity,

k =1, 2…, K –number of GCs

β = regression coefficients

ε = error term

In addition, customized regressions were also considered by introducing quadratic terms and interaction between the characteristics to better the regression (Figure 3.12). For the estimation of each model parameter finally the formulae with lowest standard error of estimate, a higher adjusted $R^2$ and highest $R^2$ was selected. Where relationships obtained were significant, resulting equations were used to compute model parameters for all the other sub-catchments (Table 3.6). Two tools were used in the regression analysis; Ms. Excel- data preparation and linear correlations tests, and MATLAB (Curve fitting tool) for multivariate regression fitting.

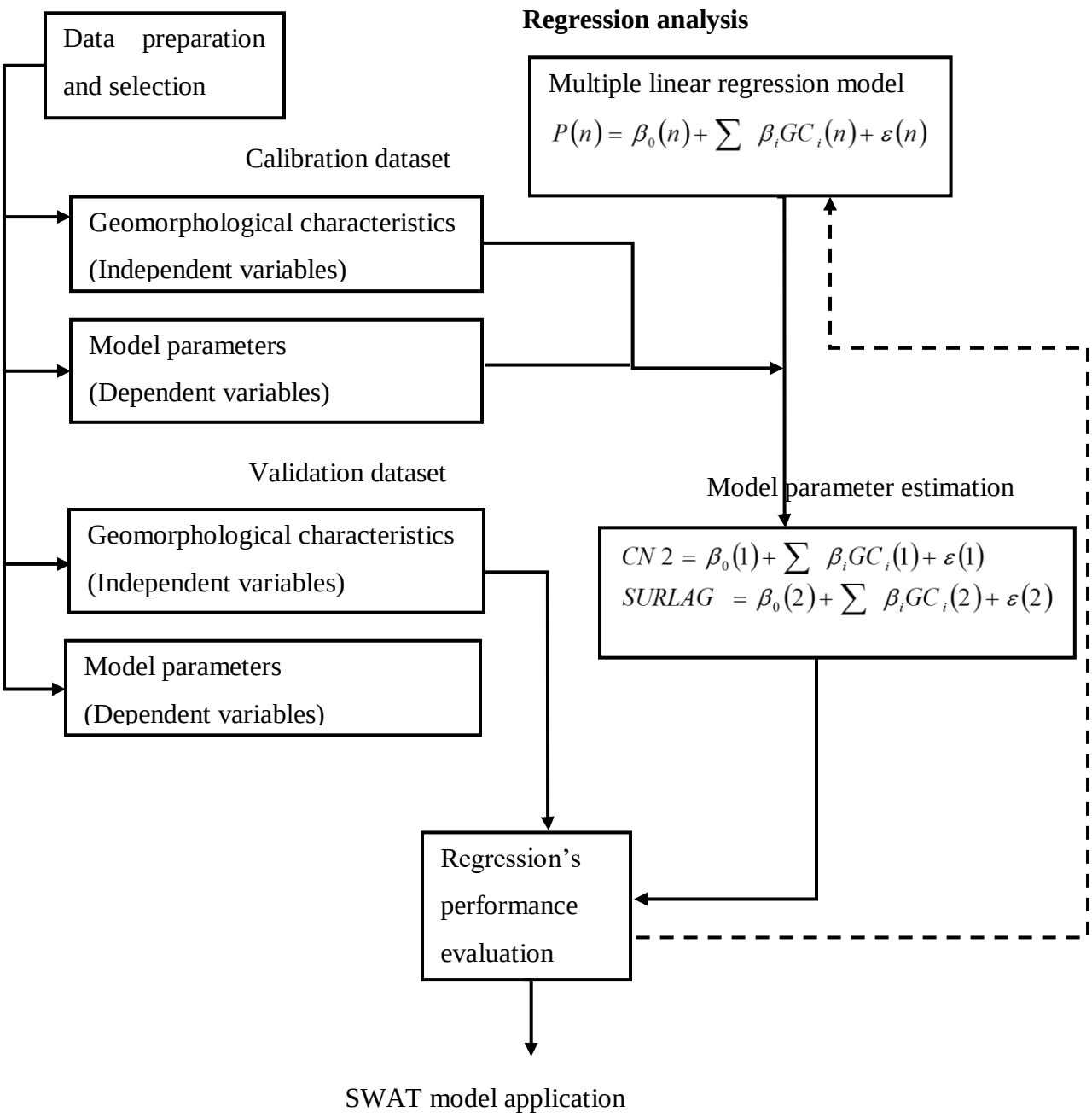


**Figure 3. 12: Determination of model parameter using multivariate regression**

**Table 3.6: Linear regression analysis relating model parameters to geomorphological characteristics**

| Regression equation | Standard error | $R^2$ and Adj. $R^2$ |
|---|---|---|
| $P(1) = \beta_0(1) + \beta_1 GC_1(1) \ldots\ldots\ldots + \beta_k GC_k(1) + \varepsilon(1)$<br>$P(2) = \beta_0(2) + \beta_1 GC_1(2) \ldots\ldots\ldots + \beta_k GC_k(2) + \varepsilon(2)$<br>…<br>$P(N) = \beta_0(N) + \beta_1 GC_1(N) \ldots\ldots\ldots + \beta_k GC_k(N) + \varepsilon(N)$ | Minimized | Maximized |

## 3.5 Spatial Flow Analysis Based on Derived Model Parameters

Model parameters were computed at ungauged pour points within the catchment, for every sub-catchment, based on geomorphological characteristics using regression with the highest $R^2$. These was done for all the sensitive parameters obtained in sub-section 3.2.5. These were then edited into the initially model set up in section 3.2, this was done to ensure the model was giving realistic flow simulation within each sub-catchment. The flow output was compared to observed data and performance evaluated. The Figure 3.13 below shows sample parameterization in a text file used to input derived parameter into the model.

By relating sub-catchments hydrologic behavior to their geomorphological characteristics, the spatial distribution of flow is calibrated. The geomorphological-calibrated model was run to simulate the catchment and a detailed analysis of flows at sub-catchment were done and the following key analysis reported; quantities of flow components at each sub-catchment, the spatial variability of flow components, a surface runoff evaluation case for water harvesting pans and a mapping of suitable development sites.

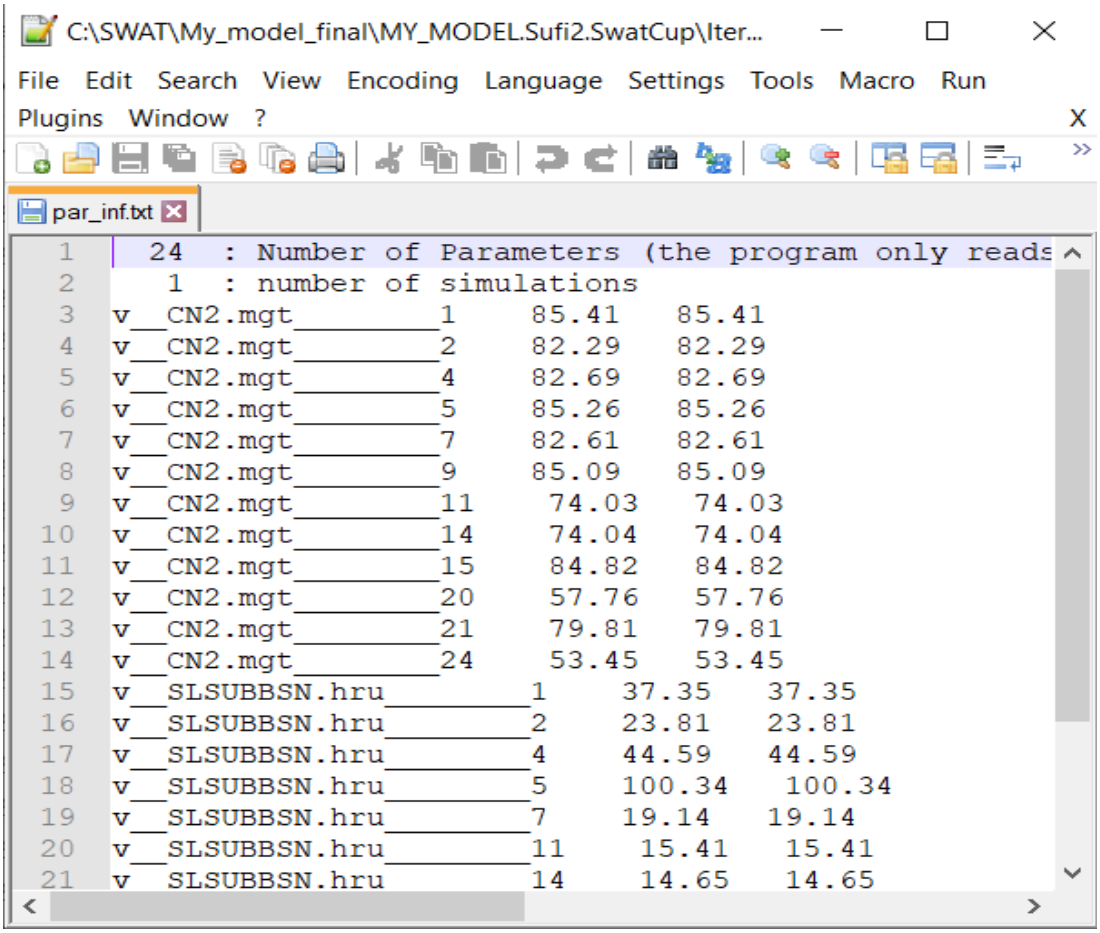


**Figure 3. 13: A screen capture showing model parameterization required to input derived parameters into the model**

# CHAPTER FOUR

# RESULTS AND DISCUSSION

## 3.6 4.1 Calibration and Validation of SWAT Model

SWAT model was successfully setup for Amala River catchment with 25 sub-catchments delineated, parameterized and the model spatial distributed to 253 hydrologic response units (Figure 4.1). Each HRU was a unique combination of land cover class, soil hydrological group and terrain slope.

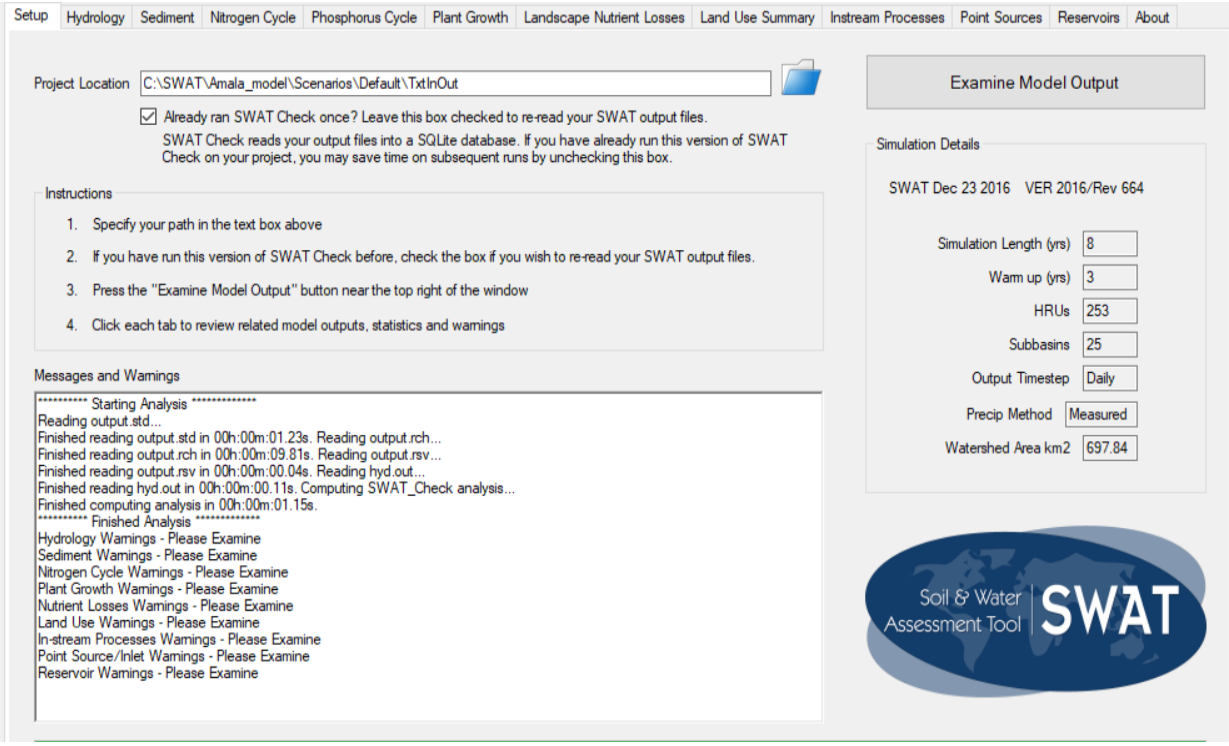


**Figure 4. 1: SWAT model setup report showing the number of HRUs and sub-catchments created**

During the setup, Amala River catchment was characterized in terms of land cover (Figure 3.3 and 4.2), soil distribution and relief. The catchment is predominately covered by rainfed agricultural lands (cropland & farrow) approximately 58.6% of the total area. The catchment has a considerable forest cover at ~33.2% of the total area, with closed evergreen broadleaves type of forest cover being predoniminant. There is minimal irrigated cropland cover thus irrigation had no significant effect on model response.

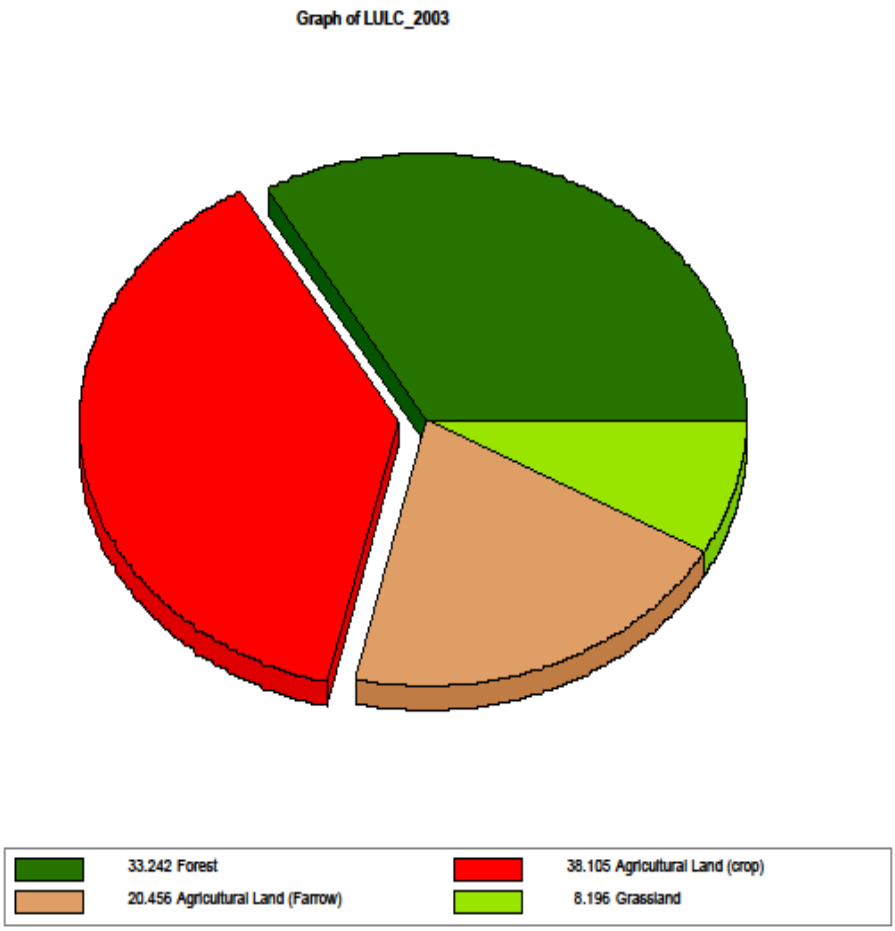


**Figure 4.2: Amala River catchment land cover characteristics for the year 2003 in percentage of total area**

The catchment has a maximum and minimum elevation of 3065 m and 1845 m above mean sea level, respectively. This gives a flow potential head of 1220 m, meaning channel/ overland velocity of flow is relatively high on average for the catchment. This favours high runoff component over infiltration. The upper area of the catchment is covered with Mollic Andosols, which is also the predominant soil class over the catchment (~73.6%) (Figure 3.4). The lower part of the catchment is mainly Pellic Vertisols and Eutric Planosols covering approximately 15.1% and 10.0%, respectively. Humic Nitosols at ~1.2% is the least soil distribution class (Figure 4.3).

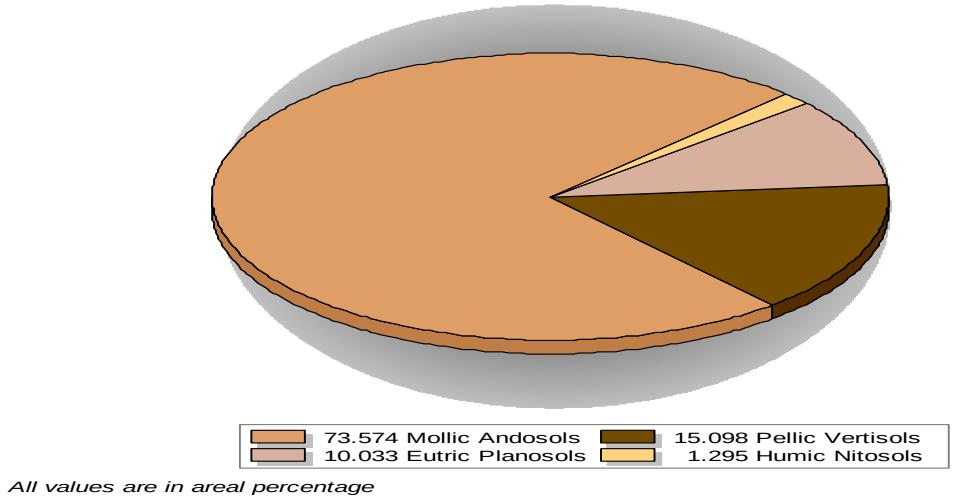


**Figure 4.3: Soil distribution within Amala River catchment**

Loamy texture is the predominant characteristic with relatively high water retention capacity ranging from 0.166 to 0.192 indicated by the soil available moisture content. High values of hydraulic conductivity, as in Mollic Andosols (79.62) indicates high potential for groudwater recharge and soil lateral flows. The soils in the catchment are characterized as summarized in Table 4.1 below.

**Table 4. 1: Soil properties details in Amala River catchment**

| Soil name | Soil properties | | | | |
|---|---|---|---|---|---|
| | FAO code | Hydrological group | Texture | Available moisture content ratio | Hydraulic conductivity (mm/h) |
| Humic Nitosols | Nh2-2c-848 | C | Loam | 0.166 | 79.62 |
| Mollic Andosols | Tm10-2bc-941 | C | Loam | 0.192 | 24.74 |
| Pellic Vertisols | Vp45-2-3a-960 | C | Clay | 0.125 | 8.4 |
| Eutric Planosols | We4-2a-977 | D | Loam | 0.175 | 6.16 |

On weather data, the following statistics were computed to customize the weather generator database to local conditions. The customized database was used to simulate and estimate missing data and fill gaps in weather data.

**Table 4.2: Input statistics used to customize weather generator database to local conditions**

| Variable | Description | Computed statistical value |
|---|---|---|
| WLATITUDE | Latitude of weather station | -0.45 |
| WLONGITUDE | Longitude of the weather station | 35.76 |
| WELEV | Elevation of the weather station | 2980 |
| RAIN_YRS | Number of years of rain data used to compute weather statistics | 10 |
| TMPMX(mon) | Mean daily maximum air temperature ([JF-ND]) | [24.58 23.72 23.33 23.07 23.55 24.43 24.42 23.77 24.54 24.99 26.42 25.51] |
| TMPMN(mon) | Mean daily minimum air temperature ([JF-ND]) | [11.23 11.31 11.44 11.91 11.91 11.39 11.12 11.27 10.94 10.95 11.32 10.95] |
| TMPSTDMX(mon) | Standard deviation of daily maximum air temperature ([JF-ND]) | [1.78 1.49 1.20 1.54 1.55 1.35 1.52 1.43 1.81 1.94 2.28 2.22] |
| TMPSTDMN(mon) | Standard deviation of daily minimum air temperature ([JF-ND]) | [2.22 2.21 2.10 1.66 1.75 1.51 1.40 1.43 1.63 1.64 1.65 1.98] |
| PCPMM(mon) | Mean total precipitation ([JF-ND]) | [165.39 69.15 164.31 252.05 274.56 173.59 145.89 184.05 167.45 175.94 155.22 120.16] |
| PCPSTD(mon) | Standard deviation of precipitation ([JF-ND]) | [13.42 7.44 10.79 11.64 13.28 8.30 7.92 9.48 9.02 9.83 9.63 10.45] |
| PCPSKW(mon) | Skew coefficient of precipitation | [4.38 4.32 3.29 1.83 3.32 2.06 3.63 2.55 2.96 3.51 3.21 5.07] |
| PR_W1_(mon) | Probability of a wet day following a dry day ([JF-ND]) | [0.24 0.14 0.33 0.49 0.46 0.55 0.59 0.56 0.56 0.54 0.40 0.23] |
| PR_W2_(mon) | Probability of a wet day following a wet day ([JF-ND]) | [0.58 0.51 0.67 0.81 0.82 0.72 0.66 0.75 0.73 0.72 0.67 0.58] |
| PCPD(mon) | Average number of days of precipitation ([JF-ND]) | [12.2 7.1 15.9 22.3 23.8 20.8 20.1 22 21.4 21.7 17.7 12] |
| RAINHHMX(mon) | Maximum 0.5 hour rainfall ([JF-ND]) | [15.01 10.77 14.82 14.85 18.34 10.44 10.25 12.76 11.66 13.24 12.11 11.81] |
| SOLARAV(mon) | Average daily solar radiation ([JF-ND]) | [25.35 27.17 24.28 21.57 21.68 20.51 21.03 21.17 22.92 21.25 22.53 25.32] |
| DEWPT(mon) | Average daily dew point temperature ([JF-ND]) | [0.65 0.58 0.66 0.73 0.77 0.77 0.78 0.77 0.71 0.67 0.67 0.63] |
| WNDAV(mon) | Average daily wind speed ([JF-ND]) | [9.20 10.10 9.68 7.41 6.84 6.88 7.14 7.66 7.98 8.56 9.45 9.94] |

Key: ([JF-ND]) means January all through to December.

The initial model simulation before calibration ('flat run'), in daily time step was as shown in hydrograph Figure 4.4. The model was run from 1st January, 1998 to 31st December 2004 with a 2-year warm up (1998 and 1999) period with default parameters. The warm up period was to initialize the model and thus no output was printed for this period. The model overestimated the peak flows as shown in the comparison between simulated and observed daily stream flow values. Such deviations between the observed and simulated shows the importance of model calibration in order to obtain satisfactory prediction accuracy.

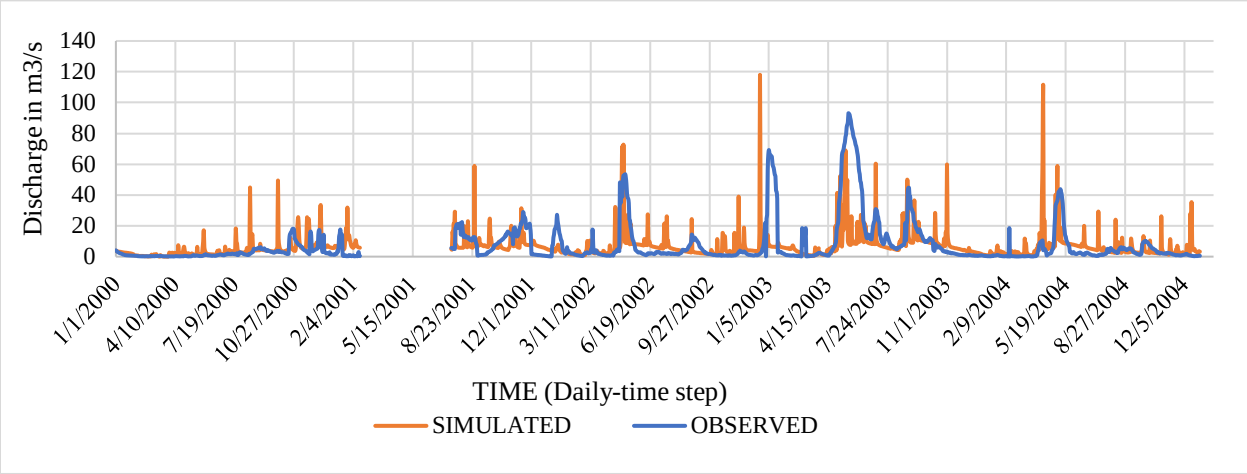


**Figure 4. 4: A daily time step hydrograph of initial model before calibration**

### 4.1.1 Sensitivity Analysis

A global sensitivity analysis carried out in SWAT-CUP with initial 13 sensitive parameters was as shown in Table 4.3. The analysis indicated that the most sensitive parameters in stream flow simulation are those representing surface runoff and groundwater. Stream flow had minimal sensitivity to soil properties. In this study, CN2 was the most sensitive parameter, in water yield estimation, with a very high absolute t-stat of 33.82 and a P-value of zero. This parameter controls the abstraction component of the SWAT model where low values of CN2 indicate low runoff potential and higher values implies increased runoff potential. Other sensitive parameters are ALPHA_BF, GWQMN, RCHRG_DP, HRU_SLP and OV_N in decreasing order of sensitivity. Parameter sensitivity is indicated by a lower P-value and a higher absolute t-stat, the results are depicted below in a descending order of sensitivity (Figure 4.5; Table 4.3). The results are comparable with previous studies in Upper Mara River catchment (Dessu & Melesse, 2012; Mango et al., 2011; Mwangi et al., 2016) who found CN2 to be the most sensitive

parameter affecting discharge simulation. A review of SWAT model application in other catchments in the East Africa region including Mara region shown that CN2 is the most sensitive parameter (W. Mwangi et al., 2017).

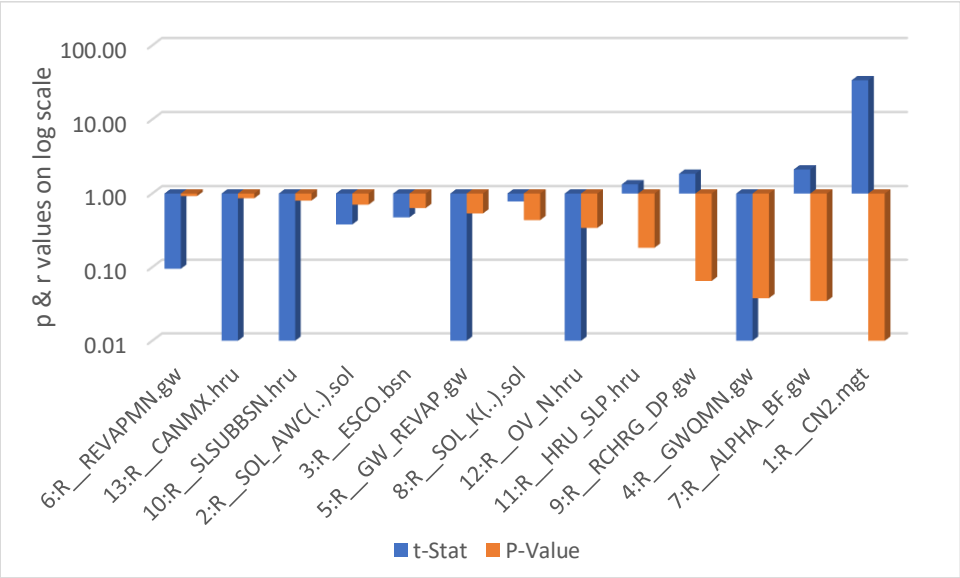


**Figure 4.5: Result of sensitivity analysis of model parameters**

**Table 4.3: Sensitive parameters and their ranking for Amala River catchment**

| Sensitivity rank | Parameter Name | t-Stat | P-Value |
|---|---|---|---|
| 1 | CN2.mgt | 33.82 | 0.00 |
| 2 | ALPHA_BF.gw | 2.12 | 0.03 |
| 3 | GWQMN.gw | -2.08 | 0.04 |
| 4 | RCHRG_DP.gw | 1.85 | 0.06 |
| 5 | HRU_SLP.hru | 1.33 | 0.18 |
| 6 | OV_N.hru | -0.95 | 0.34 |
| 7 | SOL_K(..).sol | 0.78 | 0.44 |
| 8 | GW_REVAP.gw | -0.62 | 0.54 |
| 9 | ESCO.bsn | 0.47 | 0.64 |
| 10 | SOL_AWC(..).sol | 0.38 | 0.70 |
| 11 | SLSUBBSN.hru | -0.25 | 0.80 |
| 12 | CANMX.hru | -0.17 | 0.86 |
| 13 | REVAPMN.gw | 0.10 | 0.92 |

### 4.1.2 SWAT Model Calibration

Monthly flow data was used for calibration, where gauged (observed) discharge data from 1LB02 were used to check the simulated flow. Discharge calibration using SUFI-II in SWAT_CUP resulted in a NS efficiency and a coefficient of determination ($R^2$) of 0.80 and 0.81, respectively (Table 4.4). Figure 4.6 shows the calibration output hydrograph plot for stream flow compared to the observed for time period between 2000-2004. The data fit for simulated discharge against the observed discharge depicted in Figure 4.7 shows $R^2$ of 0.81 for the calibration period.

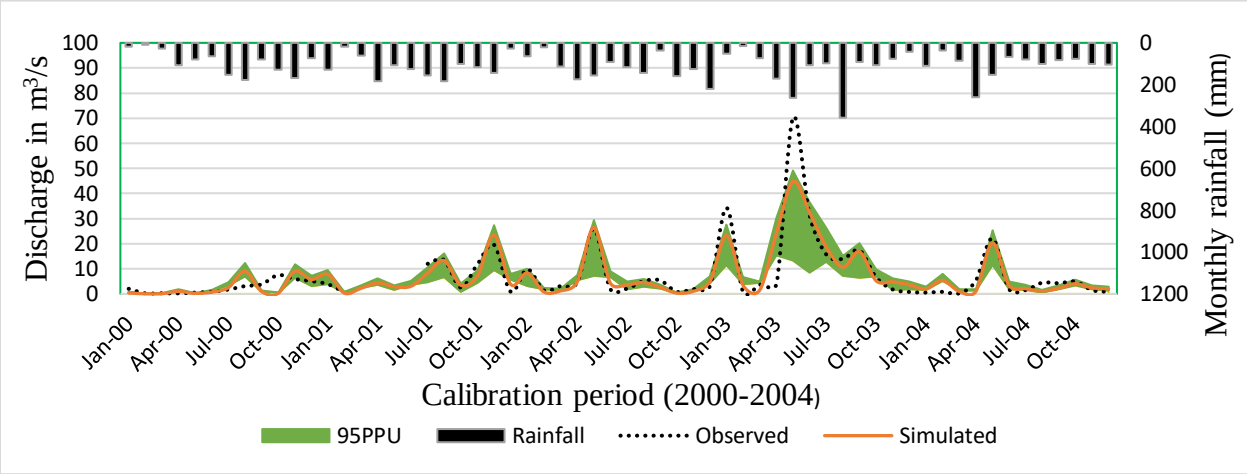


**Figure 4. 6: Model calibration output hydrograph and input rainfall**

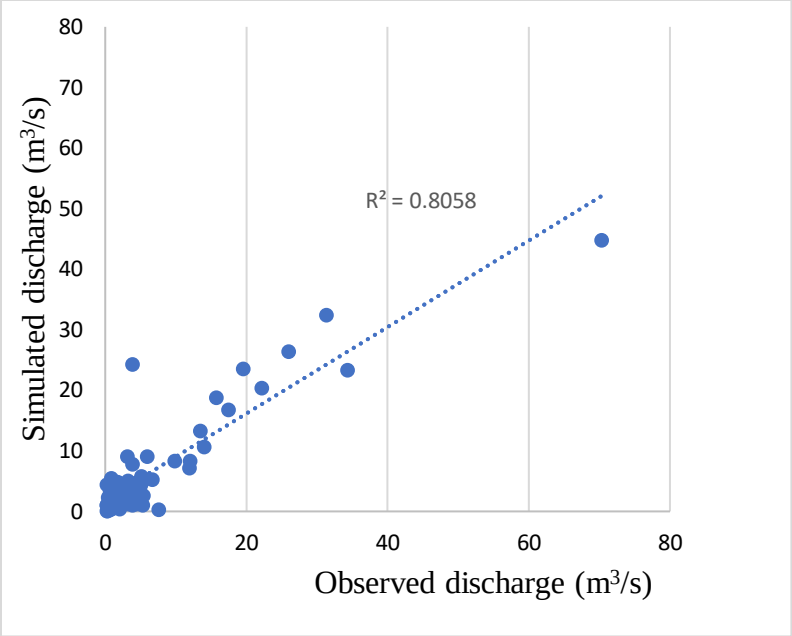


**Figure 4. 7: A plot of simulated against observed discharge for the calibration period (2000-2004)**

Based on Table 4.4, PBIAS indicates 15% overestimation in water discharge simulation. Uncertainty analysis indicates that 55% of the measured data are bracketed by the 95PPU and the p-factor has a reasonable value of 0.55 (Figure 4.6). Values of p-factor obtained is smaller than recommended of > 0.7 however, the model uncertainty quantified by the r-factor is within the recommended value of <1.2 (Abbaspour et al. 2007). The model performance for Amala River catchment is detailed in the Table 4.4.

**Table 4.4: Model performance indices for calibration using SUFI-II in SWAT_CUP**

| Variable | Values |
|---|---|
| p-factor | 0.55 |
| r-factor | 0.35 |
| $R^2$ | 0.81 |
| NS | 0.80 |
| bR2 | 0.5752 |
| MSE | 2.6e+001 |
| SSQR | 1.2e+001 |
| PBIAS | 1.5 |
| KGE | 0. 77 |
| RSR | 0.45 |
| MNS | 0.00 |
| VOL_FR | 1.02 |
| Mean simulated flow (Mean observed flow) | 6.84(6.95) |
| StdDev_simulated flow (StdDev_observed flow) | 8.91(11.20) |

Figure 4.6 shows a monthly hydrograph. It was observed that the model reproduced the observed discharge and therefore simulate the catchment discharge satisfactorily. This is quantified by PBIAS which indicates the average tendency of the simulated discharge deviating from observed stream flow (Gupta et al., 1999). The monthly NSE, KGE, PBIAS and RSR values obtained for calibration are 0.80, 0.77, 15% and 0.45, respectively. Model simulation was judged as satisfactory as the NSE > 0.5, RSR ≤ 0.70 and PBIAS ±25% (Mbungu & Kashaigili, 2017; Moriasi et al., 2007).

### 4.1.3 SWAT Model Validation

An independent dataset of four years 2005-2008 was used for model validation. The values of model evaluation statistics such as NS efficiency, $R^2$, NSE, KGE, PBIAS and RSR during validation period were 0.73, 0.51, 0.74, -23.1 and 0.45 respectively and it indicates that the calibrated model performed satisfactorily on simulating discharge outside the calibration period as shown in Figure 4.8 and 4.9.

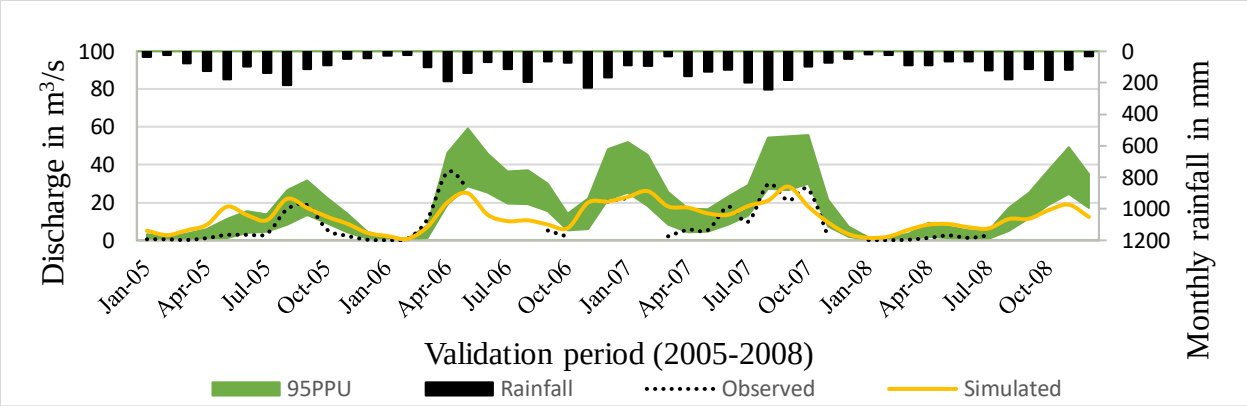


**Figure 4. 8: Model output hydrograph and input rainfall for the validation**

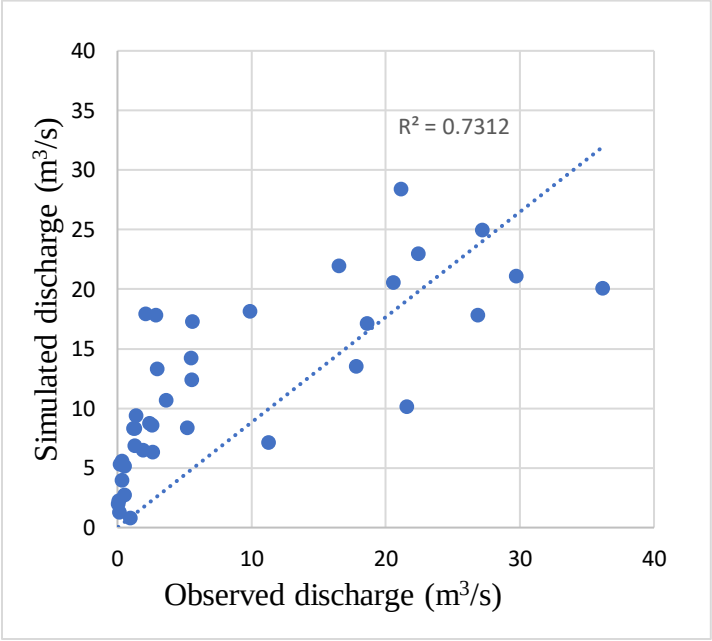


**Figure 4.9: A scatter plot for simulated discharge against observed discharged for the validated model**

The validation performance indices are shown in Table 4.5. Previous studies using SWAT on the catchment reported poor performance; NS ($R^2$) of 0.3 (0.4) (Dessu and Melesse, 2012), and NS ($R^2$) of 0.43 (0.56) (Mango et al., 2011). The two studies cited input data (rainfall and discharge) inconsistency and model uncertainty as the main reason for the poor performance. By ensuring a better representation of tree growth for tropical conditions better performance was reported as NS (KGE) of 0.75 (0.68) (Mwangi et al., 2016). In the present study, SWAT model performed better than the previous studies in the catchment. This is attributed to the use of areal CHIRPS rainfall data in nexus to recording gauge value to improve rainfall spatial distribution

representation. Also, the spatial scale as the model was set up for Amala River catchment and not the entire Mara catchment as done by previous researchers.

The efficiency for the validation period was slightly lower than the calibration indices, this can be attributed partial to gaps in observed dataset and partial to the fact that the land use map (map year 2003) used to set up the model is more representative to the calibration period (2000-2004) than the validation period (2005-2008). In the validation period, p-factor and r-factor were 0.52 and 0.33, respectively, which indicates satisfactory model certainty though only 52% of the observed is bracketed by the 95PPU.

**Table 4.5: Model performance parameters for validation using SUFI-II in SWAT_CUP**

| Variable | Values |
|---|---|
| p-factor | 0.52 |
| r-factor | 0.33 |
| $R^2$ | 0.73 |
| NS | 0.51 |
| bR2 | 0.7584 |
| MSE | 1.9e+001 |
| SSQR | 9.5e+000 |
| PBIAS | -23.1 |
| KGE | 0.74 |
| RSR | 0.45 |
| MNS | 0.00 |
| VOL_FR | 0.81 |
| Mean simulated flow (Mean observed flow) | 12.35 (8.72) |
| Std Dev_simulated flow (Std Dev_observed flow) | 10.7 (9.77) |

## 4.2 Regression Models Based on Geomorphological Characteristics

A quantitative geomorphological characterization of Amala River catchment and its sub-catchment was successfully done. The derived geomorphologic parameters were then related to SWAT model most sensitive parameter in a total of 5 regressions. The five regressions models with $R^2$ >0.8 were used to estimate SWAT model parameter within the sub-catchment to ensure

the model simulated correctly spatial flows at all 25-sub-catchment as presented in the following sub sections.

### 4.2.1 Quantitative Analysis of Geomorphologic Characteristics

Geomorphological characterization results were reported under three categories; stream network, catchment geometry, drainage and relief analysis results. The results were reported for the entire Amala river catchment and for the sub-catchments in sections 4.2.2 through to 4.2.6.

### 4.2.2 Stream Network Analysis

The stream network analysis included parameters which influence the flow of water. The geomorphologic parameters under this category are reported in following paragraphs. Stream ordering is the basic step in stream network analysis. The stream orders derived based on Strahler (1952) model are shown in Figure 4.10. The main stream reaching the outlet of the catchment is shown as a 5th order. The stream order ranged from $1^{st}$ to $5^{th}$ with order count of sum of ranging from 306 to 1 respectively (Table 4.6). The results indicate a total stream count of 396.

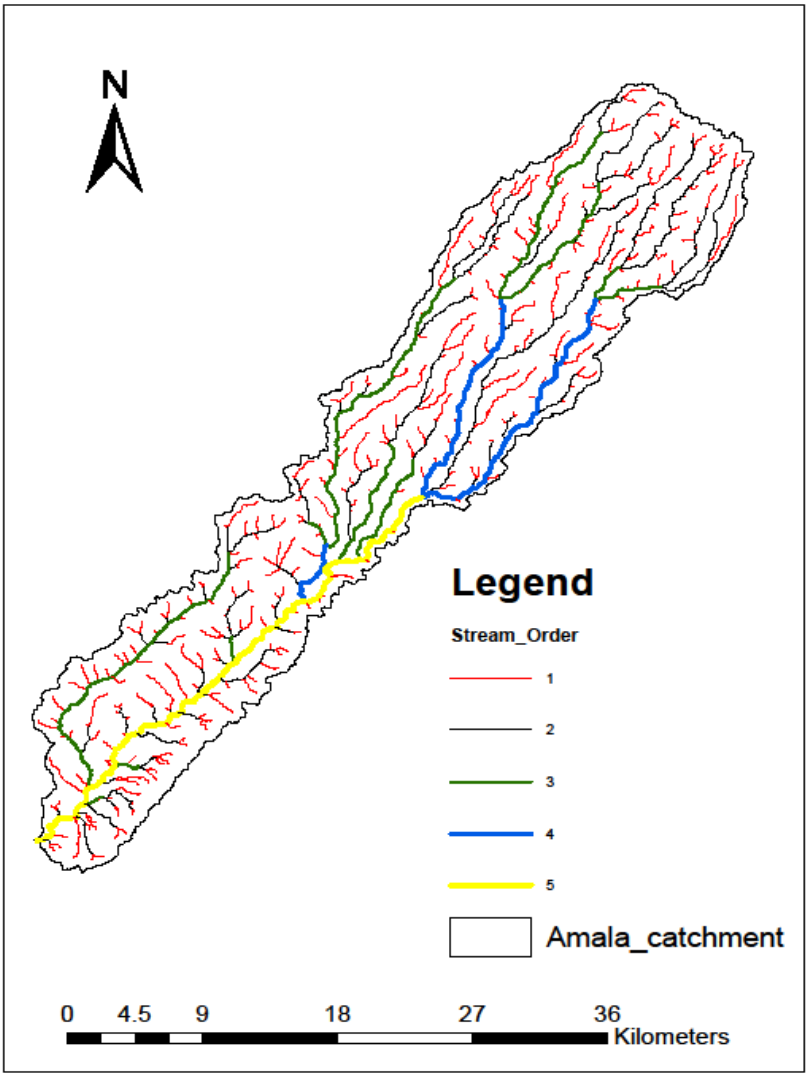


**Figure 4. 10: Stream order based on Strahler model for Amala River catchment**

**Table 4. 6: Stream order, stream number and stream length results**

| So | Nu | Lu (M) |
|---|---|---|
| 1 | 306 | 317506.12 |
| 2 | 71 | 222981.24 |
| 3 | 15 | 111261.15 |
| 4 | 3 | 44225.12 |
| 5 | 1 | 44924.83 |

The results for stream number obeys Horton's law of stream numbers which states that the total number of stream counts decrease as stream order increases. Deviations indicate a high relief with steep slopes terrain. The logarithms of the number of streams of each order were plotted against the order and the points lie on a straight line (Figure 4.11). Thus, a geometric relationship between stream order and stream numbers. Also, a geometric relationship exists between stream order and stream length. These indicate that the catchment is underlain by almost uniform lithology, and geologically there is no likelihood of an uplift (Altaf et al.,2013).

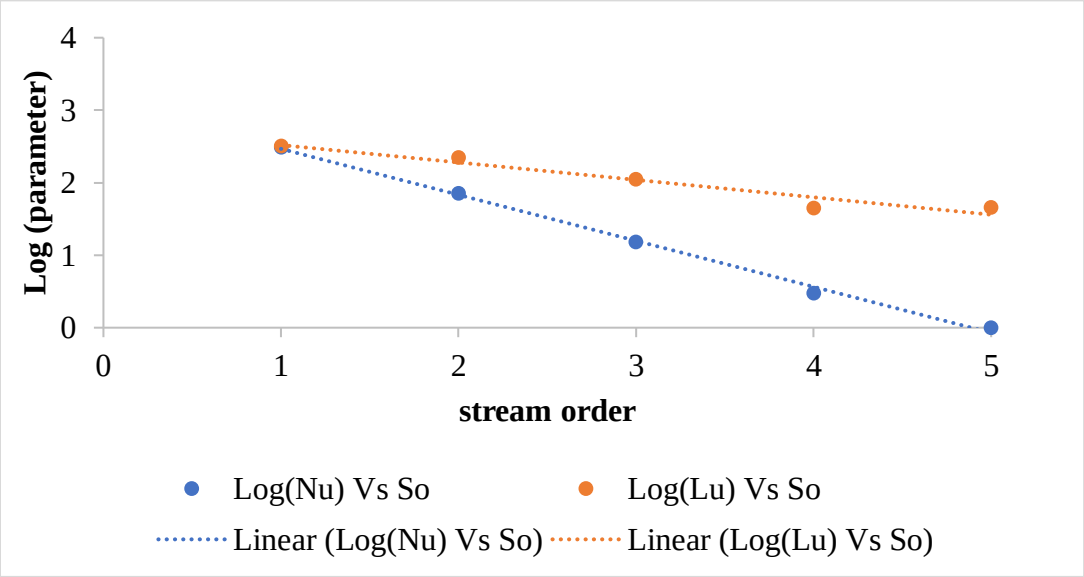


**Figure 4. 11: A plot of log stream number and log stream length against stream order**

The sum of stream lengths of a given order were computed from Amala stream shapefile using Spatial Analyst tool in ArcGIS (Table 4.6). The total stream length for the catchment is 740.9 km. Mean stream length was computed by dividing the sum length of streams of a given order by the total number of streams in that order. The length ratio (Lr) was computed as the ratio of the mean length of streams of a given order to mean length of streams of the previous lower order. On the other hand, the average length ratio for the basin was computed as 2.6 and the weighted average (using number of streams used to compute the ratio) as 2.7 (Figure 4.12).

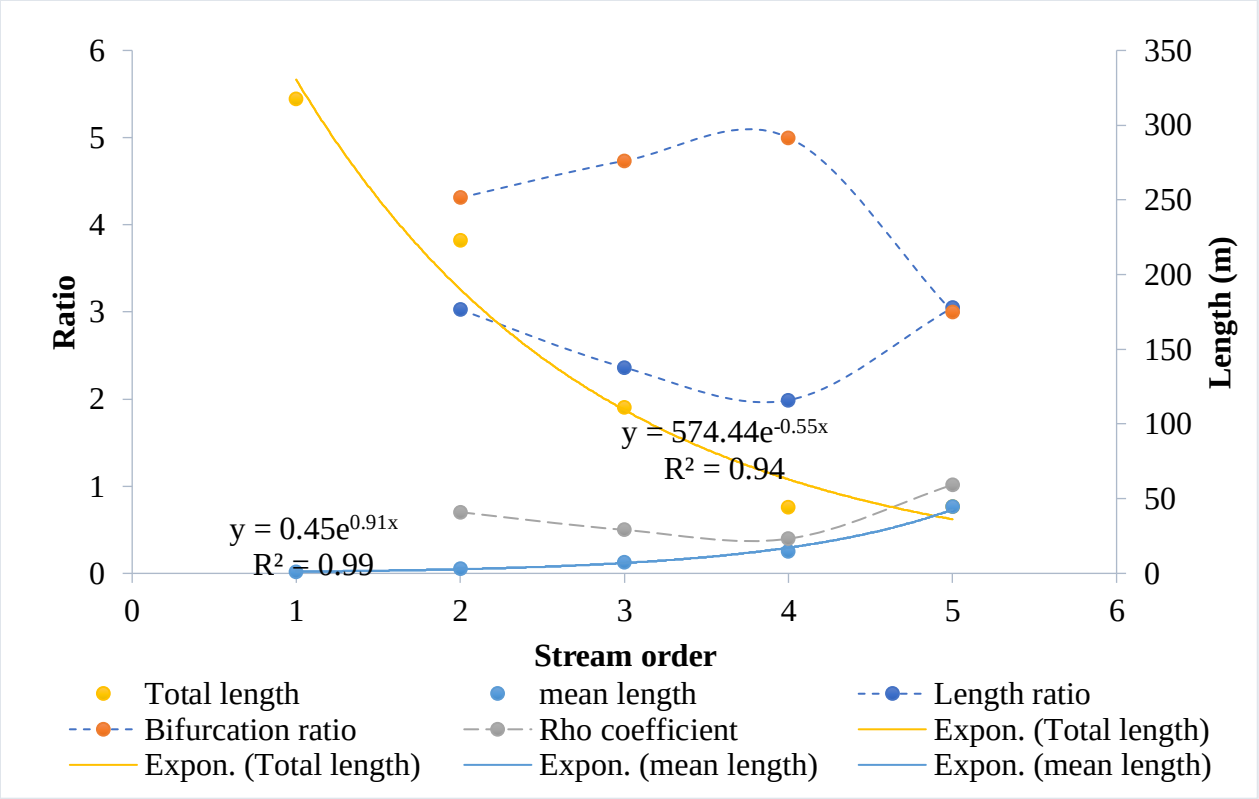


**Figure 4.12: Variation of total stream length, mean stream length, length ratio and bifurcation ratio with stream order**

The total steam length decreases exponentially as the stream order increases while the mean stream length increases exponentially with stream order (Figure 4.12) and Equations 3.1 and 3.2 respectively

$$y = 574.44e^{-0.55x} \quad (3.1)$$

$$y = 0.45e^{-0.91x} \quad (3.2)$$

The exponential relationships were strong and highly reliable given the reported high values of $R^2$ of 0.94 and 0.99 for Equations 3.3 and 3.2 respectively. Such a relationship indicates a dendritic drainage network in Amala River catchment where the movement of water depends only on the drainage characteristics (Altaf et al.,2013).

Weighted average bifurcation ratio was suggested by Strahler (1952) as a more representative bifurcation number (Pareta & Pareta, 2011). It is a dimensionless characteristic generally ranging from 3 to 5. In Figure 4.12, the variation with stream order is shown indicating Amala River catchment has a higher average bifurcation ratio of 4.26 and the computed weighted ratio of 4.40. The high values characterize the catchment as one that has suffered

structural disturbances and the drainage network has been influenced by structural disturbances (Pareta & Pareta, 2011).

The Rho coefficient relates drainage density to physiographic development of catchment which is instrumental to evaluate the storage capacity of drainage network (Pareta & Pareta, 2011). It was computed by dividing the length ratio by bifurcation ratio. Rho coefficient of Amala River catchment was found to be 0.62 (Table 4.7). The variation of this coefficient with stream order is similar to that of length ratio. This indicates a direct relationship between storage capacity of a drainage network and the stream length.

**Table 4.7: Rho coefficient**

| | $L_r$ | $R_b$ | P |
|---|---|---|---|
| Simple average | 2.605 | 4.260 | 0.612 |
| Weighted average | 2.728 | 4.399 | 0.620 |

### 4.2.3 Catchment Geometry Analysis

The main catchment geometric analysis involved the length of the catchment, catchment area, perimeter, form factor, elongation ratio and compactness coefficient which are described in the following respective paragraphs. Schumm (1956) defined the length of the catchment as the longest distance parallel to the principal stream of the catchment. According to this definition, the length of the Amala River catchment was found to be 68.28 km (Table 4.8). The catchment area was computed as 697.77 $km^2$ (Table 4.8). Catchment perimeter is the length of the divide that encloses the catchment area. It is an indicator of watershed size and shape. The catchment perimeter was computed as 207.26 km as shown in Table 4.8.

Form factor describes the shape of the basin and it is defined as the ratio of catchment area to the square of its length. In this case, the catchment form factor was found to be 0.15. The value varies from 0 to 1. This low value indicates that the Amala River catchment is elongated rather than circular (high value). Elongation ratio is the ratio of the diameter of a circle of equal area as the catchment to the length of the catchment. This parameter indicates infiltration characteristics along the flow path and varies from 0.6 to 1.0 over different climatic and geologic types (Charizopoulos & Psilovikos, 2015). A value between 0.9 and 0.8 shows that the catchment is circular, between 0.8 and 0.7 means that it is oval and a value less than 0.7 indicates

an elongated catchment (Appendix A.5). For the present study it was computed as 0.437 (Table 4.8), this characterizes Amala River catchment as elongated. Elongated catchments are less efficient in discharge than the circular ones (Charizopoulos & Psilovikos, 2015). Compactness coefficient was computed as the ratio of the perimeter of the catchment to the perimeter of an imaginary circle whose area is equivalent to the surface of the corresponding catchment. The computed compactness coefficient of Amala River catchment is 2.23.

**Table 4. 8: Catchment geometry analysis result**

| S. No | Geometry parameter | Calculated value |
|---|---|---|
| 1 | Area ($km^2$) | 697.77 |
| 2 | Perimeter (km) | 207.26 |
| 3 | Catchment length (km) | 68.28 |
| 4 | Form factor | 0.15 |
| 5 | Elongation ratio | 0.44 |
| 6 | Compactness coefficient | 2.23 |
| 7 | Drainage density | 1.07 |
| 8 | Drainage texture | 1.91 |
| 9 | Drainage frequency | 0.57 |
| 10 | Infiltration number | 0.61 |
| 11 | Overland flow length | 0.47 |

### 4.2.4 Drainage Analysis

Drainage analysis included main parameters such as drainage texture, drainage density, drainage frequency, infiltration number and length of overland flow as described in the following respective paragraphs. Drainage texture is the relative spacing of drainage lines. It is the ratio of stream number of all orders to the perimeter of that area. In this study, the drainage texture of the catchment is 1.91 (Table 4.8). Drainage density is the sum length of stream per unit catchment area. Spatial distribution of drainage density is shown in Figure 4.13 which was computed using Spatial Analyst Tool. The overall average drainage density of Amala River catchment is 1.073 $km/km^2$ (Table 4.8). This is a low value indicating dense vegetation cover in most part of the catchment while its spatially distribution is controlled by the catchment lithology (Charizopoulos & Psilovikos, 2015).

Drainage frequency indicates that the origin and development of stream in the catchment and that is directly depend on lithological characteristics. The drainage frequency (Fd) is the number of stream segments per unit catchment area. The drainage frequency of the Amala River catchment is 0.58 streams/km$^2$ (Table 4.8). The low value of this parameter shows a coarse drainage texture (Charizopoulos & Psilovikos, 2015). The infiltration number was computed as the product of drainage frequency and drainage density. This parameter gives an indication of the infiltration characteristics of a catchment. The higher value indicates reduced infiltration and more of run-off. The infiltration number was computed as 0.61 (Table 4.8).

Length of overland flow was considered as the length of flow of rainwater on the surface before it joins definite channels. This parameter is taken as half the reciprocal of drainage density. Length of overland flow for Amala River catchment is shown as 0.47 km (Table 4.8). It depends on the physiographic and hydrologic condition of the catchment. It inversely related to slope hence high value of length of overland flow indicates increased surface runoff.

### 4.2.5 Relief Analysis

Relief parameters were computed as three-dimension geomorphological parameters. Relief ratio and ruggedness number were derived and reported as a characterization of the catchment terrain. The relief of a catchment was computed by getting the difference in elevation between the point of maximum elevation and the floor elevation of the outlet point of the catchment. The total relief of the catchment was found to be 1220 m, implying a high potential energy of the drainage network. Relief ratio was computed by dividing relief with the length of a catchment to describe the steepness of relief over the catchment. In this study, the catchment relief ratio was determined as 0.02 (Table 4.9).

**Table 4. 9: Catchment relief analysis parameters**

| Relief parameter | Reported value |
|---|---|
| Elevation at outlet (m) | 1845 |
| Max elevation (m) | 3065 |
| Relief (m) | 1220 |
| Relief ratio | 0.02 |
| Ruggedness number | 1.31 |

Ruggedness number according to Strahler is the product of relief and the drainage density of a catchment. For a given catchment the number combines slope steepness to its length. Depending on slope and drainage density, high value implies high stream flow velocity. Amala River catchment has a ruggedness number of 1.31 (Table 4.9).

### 4.2.6 Sub-Catchment Level Analysis

Amala River catchment was delineated into 25 sub-catchments by defining pour point for each sub-catchment in ArcHydo tool in ArcGIS (Figure 4.13). The ones receiving flows from upstream sub-catchments were ignored, only those with stream starting from first order were used in geomorphologic analysis. A total of 12 sub-catchments were used in the analysis. The geomorphological characterizations of the sub-catchments are as shown in Table 4.10.

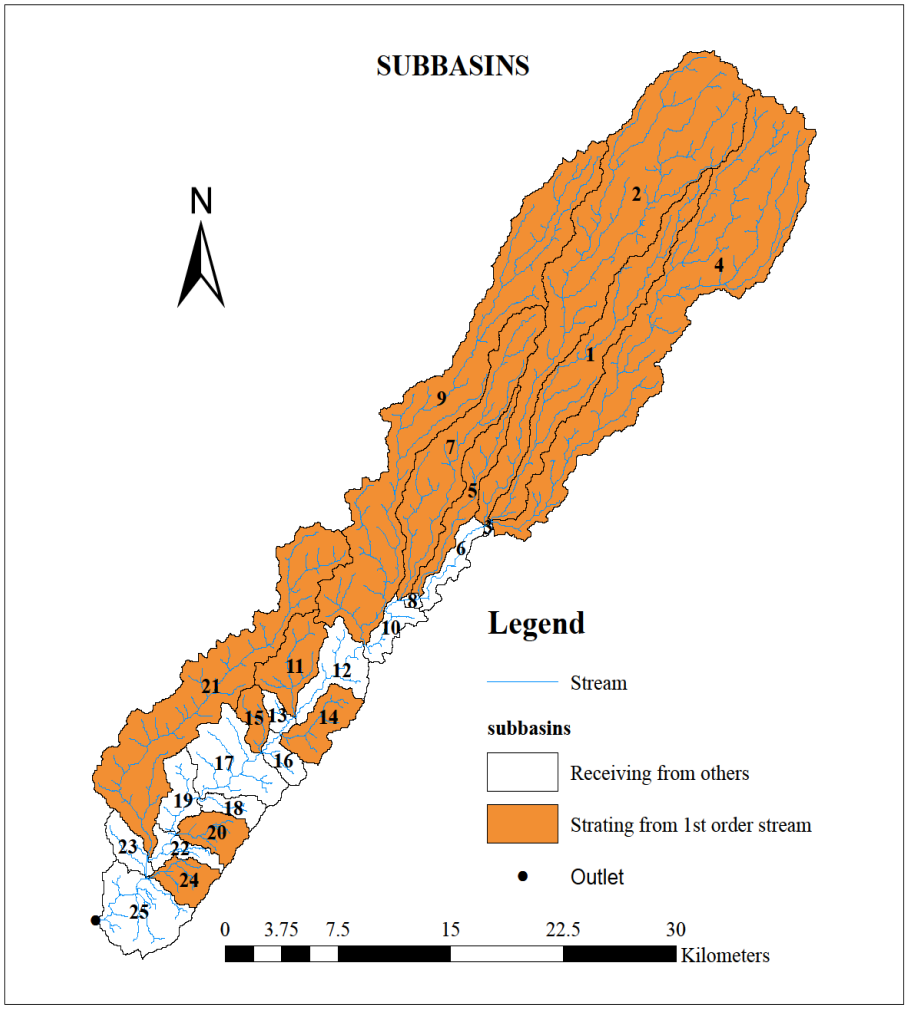


**Figure 4.13: Sub-catchments delineation and selection for geomorphologic analysis**

Analysis at this level studied spatial variability of the geomorphologic characteristics within Amala River catchment. In stream network analysis, sub-catchments 1, 5, 7 and 21 shows higher stream length ratio of 16.41, 11.71, 8.26 and 7.80 respectively. The four sub-catchments have a non-dendritic drainage structure, with one long main stream and thus longer lag time. The others have values lower than 3.5, and thus will likely experience shorter basin lag time. The Bifurcation ratio spatially lies between 2.5 and 14.0 with high values indicating fast hydrograph peak thus a likelihood of flash flooding after a storm (Altaf et al., 2013). The rho coefficient values lie between 0.52-2.34, higher values indicating a stronger relationship between drainage network storage capacity and the stream length.

From geometric analysis, the form factor describes the shape of the basin. Lower values indicate much elongated basin shape as in the case of sub-catchments 1, sub-catchments 5 and sub-catchments 9. As the values increase the shape changes from elongated to circular. The characterization of the shape is given by the elongation ratio where all values below 0.7 characterizes elongated basins and values above 0.7 are circular basins. Compactness coefficient ($K_c$) characterizes the time of concentration of a catchment before peak flow occurs. A $K_c$ value of 1 indicates a catchment whose time of concentration equals that of a circular basin. Values $K_c > 1$ indicates deviation a circular catchment hydrological behavior. The sub-catchments 15 has the minimum $K_c$ value in the series of 1.65 and sub-catchments 9 has maximum $K_c$ value of 3.4). As per this parameter, sub-catchments 9 will has the longest time of concentration ($T_c$) while sub-catchments 15 has the shortest $T_c$.

Low values for drainage density depict regions underlain with highly resistant permeable material with vegetative cover and low relief while as, high values imply weak and impermeable subsurface material and sparse vegetation and mountainous relief (Altaf et al., 2013). The spatial variation of the drainage density is shown in Figure 4.14 and Table 4.10 with values are below 2 $km/km^2$. Variations in other drainage characteristics; drainage texture, infiltration number and length of overland flow are plotted in Figure 4.15.

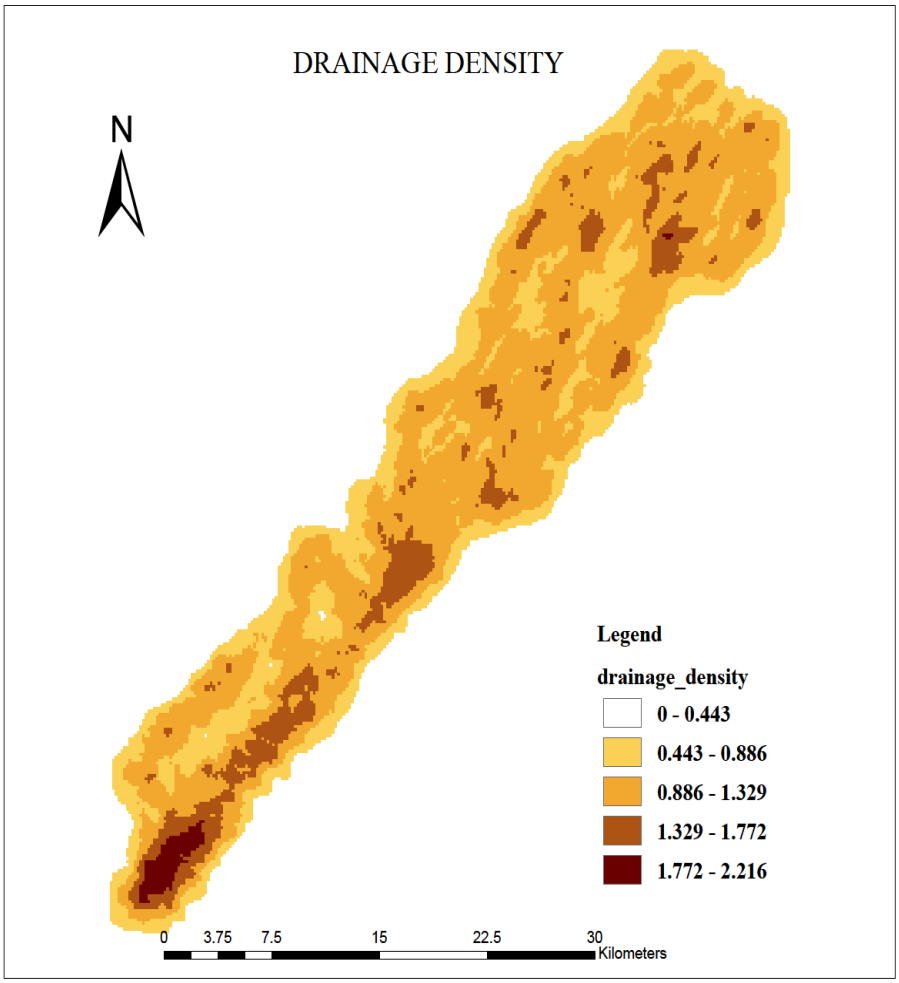


**Figure 4. 14: Drainage density map for Amala River catchment**

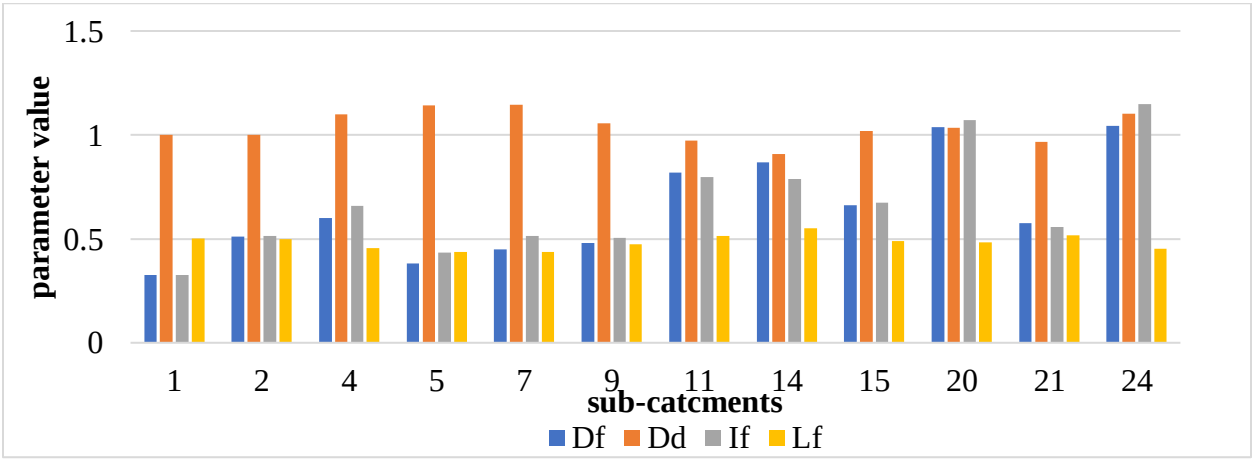


**Figure 4. 15: Variations of drainage network parameters within sub-catchments**

**Table 4.10: Sub-catchment level geomorphologic analysis result**

| Parameter | Sub-basins ID | | | | | | | | | | | |
|---|---|---|---|---|---|---|---|---|---|---|---|---|
| | 1 | 2 | 4 | 5 | 7 | 9 | 11 | 14 | 15 | 20 | 21 | 24 |
| Stream network analysis | | | | | | | | | | | | |
| Total Nu | 15 | 62 | 73 | 6 | 20 | 51 | 13 | 11 | 4 | 10 | 44 | 9 |
| Total Lu (Km) | 45.82 | 121.16 | 133.76 | 17.99 | 51.07 | 112.48 | 15.44 | 11.49 | 6.16 | 9.95 | 73.73 | 9.52 |
| Mean Lu (Km) | 3.05 | 1.95 | 1.83 | 3.00 | 2.55 | 2.21 | 1.19 | 1.04 | 1.54 | 1.00 | 1.68 | 1.06 |
| Lu ratio | 16.41 | 3.29 | 2.91 | 11.71 | 8.26 | 2.29 | 1.57 | 1.91 | 1.61 | 1.52 | 7.80 | 2.43 |
| $R_b$ | 14 | 3.95 | 4.39 | 5 | 5.25 | 3.67 | 3 | 3 | 3 | 2.75 | 6.07 | 2.5 |
| Rho coefficient | 1.17 | 0.83 | 0.66 | 2.34 | 1.57 | 0.62 | 0.52 | 0.64 | 0.54 | 0.55 | 1.29 | 0.97 |
| Catchment geometry analysis | | | | | | | | | | | | |
| Lb(Km) | 26.21 | 32.96 | 32.59 | 14.71 | 20.42 | 35.45 | 6.46 | 5.54 | 4.18 | 4.74 | 23.64 | 4.97 |
| Area ($Km^2$) | 45.86 | 121.01 | 121.68 | 15.78 | 44.57 | 106.47 | 15.86 | 12.66 | 6.04 | 9.63 | 76.33 | 8.63 |
| Perimeter (Km) | 80.58 | 106.98 | 116.20 | 44.22 | 63.38 | 124.43 | 26.78 | 22.91 | 14.31 | 18.55 | 93.17 | 17.69 |
| $F_f$ | 0.07 | 0.11 | 0.11 | 0.07 | 0.11 | 0.08 | 0.38 | 0.41 | 0.35 | 0.43 | 0.14 | 0.35 |
| Elongation ratio | 0.29 | 0.38 | 0.38 | 0.30 | 0.37 | 0.33 | 0.70 | 0.72 | 0.66 | 0.74 | 0.42 | 0.67 |
| $K_c$ | 3.38 | 2.76 | 2.99 | 3.16 | 2.70 | 3.43 | 1.91 | 1.83 | 1.65 | 1.70 | 3.03 | 1.71 |
| Drainage texture analysis | | | | | | | | | | | | |
| Df ($No./Km^2$) | 0.33 | 0.51 | 0.60 | 0.38 | 0.45 | 0.48 | 0.82 | 0.87 | 0.66 | 1.04 | 0.58 | 1.04 |
| Dd($km/Km^2$) | 1.00 | 1.00 | 1.10 | 1.14 | 1.15 | 1.06 | 0.97 | 0.91 | 1.02 | 1.03 | 0.97 | 1.10 |
| Infiltration number | 0.33 | 0.51 | 0.66 | 0.43 | 0.51 | 0.51 | 0.80 | 0.79 | 0.68 | 1.07 | 0.56 | 1.15 |
| Lf (Km) | 0.50 | 0.50 | 0.46 | 0.44 | 0.44 | 0.47 | 0.51 | 0.55 | 0.49 | 0.48 | 0.52 | 0.45 |
| Relief analysis | | | | | | | | | | | | |
| Elevmin(M) | 2340 | 2324 | 2333 | 2250 | 2220 | 2171 | 2064 | 2017 | 1991 | 1886 | 1876 | 1874 |
| Elevmax(M) | 2888 | 3006 | 3065 | 2562 | 2638 | 2792 | 2405 | 2370 | 2333 | 2259 | 2464 | 2230 |
| Relief(M) | 548 | 682 | 732 | 312 | 418 | 621 | 341 | 353 | 342 | 373 | 588 | 356 |
| Relief ratio | 0.02 | 0.02 | 0.02 | 0.02 | 0.02 | 0.02 | 0.05 | 0.06 | 0.08 | 0.08 | 0.02 | 0.07 |
| Ruggedness number | 0.55 | 0.68 | 0.81 | 0.36 | 0.48 | 0.66 | 0.33 | 0.32 | 0.35 | 0.39 | 0.57 | 0.39 |

Nu-stream number, Lu-stream length, Br-bifurcation ratio, Lb-length of the catchment, Ff-form factor, Kc-compactness coefficient, Df-drainage frequency, Dd-drainage density, Lf- Length of overland flow.

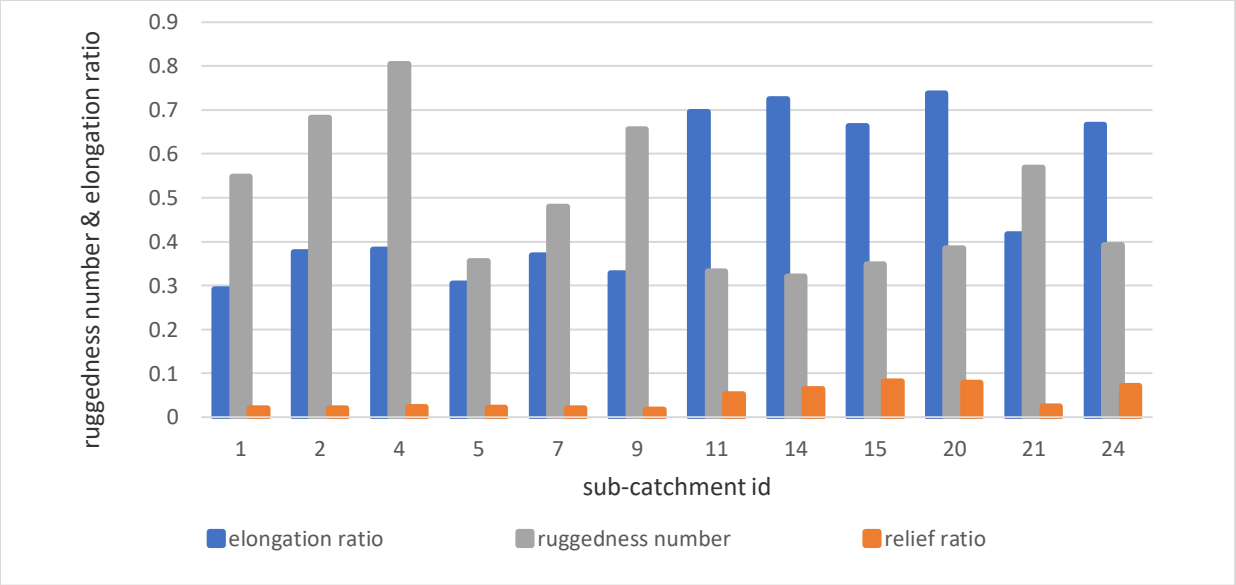


**Figure 4. 16: A comparison of trends between relief parameters and shape of the sub-catchments**

The relief expressed in meters varies between 341 and 732 for the sub-catchments, this parameter shows the maximum potential energy of water flow within the sub-catchments. The steepness of this potential is indicated by the relief ratio. The relief ratio of each sub-catchments has a positive relationship with the shape of the catchment, this is depicted by the similarity between elongation ratio trend and relief ratio as indicated in Figure 4.16. Ruggedness number gives insight on the stream flow velocity, it combines relief and drainage density. High values indicate high stream velocity and vice versa. Sub-catchments 4 has the highest ruggedness number value of 0.81, thus high stream velocity compared to other sub-catchments. This further implies that Sub-catchments 4 is more prone to erosion than all the other analyzed sub-catchments.

### 4.2.7 Regression Analysis

A total number of 12 sub-catchments, which do not receive water from other sub-catchments, were selected for the regression analysis; SUB_1, _2, _4, _7, _9, _11, _14, _15, _20, _21, _24 and _25 (Table 4.11). Five model parameters were weight-averaged for the selected sub-catchments from the output files of the SWAT model calibrated in section 4.1 of this document, the values are shown in Table 4.11.

**Table 4. 11: SWAT model parameter for sub-catchment level**

| Model parameters | Sub-catchment ID | | | | | | | | | | | |
|---|---|---|---|---|---|---|---|---|---|---|---|---|
| | 1 | 2 | 4 | 5 | 7 | 9 | 11 | 14 | 15 | 20 | 21 | 24 |
| HRU_SLP | 0.13 | 0.12 | 0.11 | 0.25 | 0.24 | 0.19 | 0.30 | 0.24 | 0.24 | 0.12 | 0.23 | 0.10 |
| SOL_AWC | 0.19 | 0.19 | 0.19 | 0.19 | 0.19 | 0.19 | 0.19 | 0.19 | 0.13 | 0.18 | 0.13 | 0.18 |
| SLSUBBSN | 38.88 | 41.32 | 44.45 | 14.62 | 15.62 | 29.22 | 13.23 | 14.59 | 14.47 | 44.36 | 18.18 | 53.58 |
| CN2 | 84.53 | 82.19 | 82.52 | 84.28 | 83.70 | 81.41 | 73.81 | 87.90 | 85.06 | 89.05 | 79.80 | 87.34 |
| OV_N | 0.121 | 0.115 | 0.117 | 0.122 | 0.121 | 0.114 | 0.091 | 0.127 | 0.120 | 0.122 | 0.107 | 0.119 |
| CH_L2 | 6.297 | 17.26 | 11.61 | 10.77 | 1.835 | 1.409 | 4.137 | 3.681 | 0.768 | 2.005 | 3.132 | 1.686 |
| CH_S2 | 0.016 | 0.013 | 0.015 | 0.013 | 0.027 | 0.018 | 0.025 | 0.026 | 0.042 | 0.019 | 0.021 | 0.012 |
| GW_REVAP | 0.022 | 0.022 | 0.022 | 0.022 | 0.022 | 0.022 | 0.022 | 0.022 | 0.022 | 0.022 | 0.022 | 0.022 |
| ESCO | 0.95 | 0.95 | 0.95 | 0.95 | 0.95 | 0.95 | 0.95 | 0.95 | 0.95 | 0.95 | 0.95 | 0.95 |
| GWQMN | 1056.5 | 1056.5 | 1056.5 | 1056.5 | 1056.5 | 1056.5 | 1056.5 | 1056.5 | 1056.5 | 1056.5 | 1056.5 | 1056.5 |
| EPCO | 1 | 1 | 1 | 1 | 1 | 1 | 1 | 1 | 1 | 1 | 1 | 1 |
| ALPHA_BF | 0.048 | 0.048 | 0.048 | 0.048 | 0.048 | 0.048 | 0.048 | 0.048 | 0.048 | 0.048 | 0.048 | 0.048 |
| RCHRG_DP | 0.05 | 0.05 | 0.05 | 0.05 | 0.05 | 0.05 | 0.05 | 0.05 | 0.05 | 0.05 | 0.05 | 0.05 |
| CH_N2 | 0.014 | 0.014 | 0.014 | 0.014 | 0.014 | 0.014 | 0.014 | 0.014 | 0.014 | 0.014 | 0.014 | 0.014 |

### 4.2.8 Spatial Variability of SWAT Parameter

The values for HRU_SLP, SLSUBBSN, CN2, OV_N and CH_S2 show spatial variation. These variations highlight a hilly terrain with a varying land cover across the catchment. The soil available water content (SOL_AWC) values did not change for sub-catchments with same soil type as this is a soil parameter, the only variation depended on soil classes combination present in the sub-catchment. All ground water model parameters were constant across all the sub-catchments such as GW_REVAP, GWQMN, ALPHA_BF and RCHRG_DP. This is because of the small spatial scale of the study area thus; ground water characteristics of the catchment were not expected to vary significantly. The soil evaporation compensation factor (ESCO) and the plant evaporation compensation factor (EPCO) were constant over for all the study sub-catchments with values 0.95 and 1 respectively which are the default values of these parameters. ESCO controls the range of the soil depth used to meet the soil evaporative demands. A value of 0.95 means that lower soil layers were not compensating for water deficit in upper layers. EPCO defines the range of soil depth used to meet plant water uptake and therefore during calibration the default values were maintained as soil water from deeper soil profiles was not used significantly by the crop cover only except for the forest cover. The main channel manning's roughness coefficient (CH_N2) was 0.014 across all the sub-catchments.

### 4.2.9 Collinearity Between Geomorphological Characteristics

The collinearity test results between the geomorphological parameters as shown in the Table 4.12 in terms of $R^2$ values and graphically in Figure 4.17. The bond values indicate a collinearity of $R^2$ >50 and the respective characteristics were considered to have a higher collinearity. For instance, the collinearity between length of overland flow(km) and drainage density(km/sq.km) was quite high of almost 100% and therefore they are equivalent in physical meaning. Contrary, collinearity between ruggedness number and stream length ratio was below 1% and therefore they can be used together in a regression because they are not equivalent in physical meaning. In general, all parameters with high collinearity only one was used in the regression in later section.

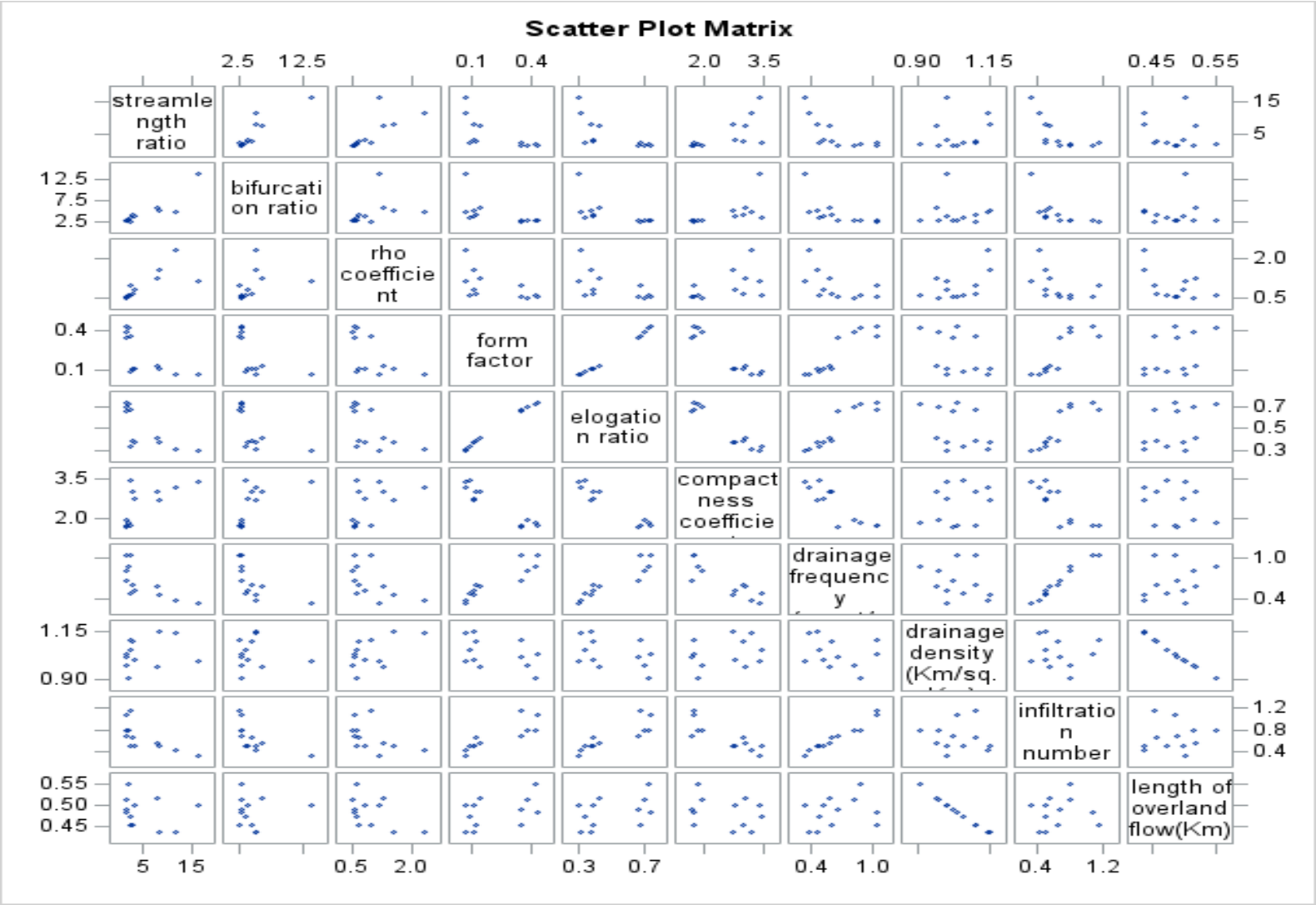


**Figure 4.17: Collinearity matrix between geomorphological parameters**

**Table 4.12: Collinearity matrix between geomorphological parameters (values show the $R^2$)**

| | Lr | $R_b$ | p | $F_f$ | Re | $K_c$ | Df | Dd | $I_f$ | L | Rh | Rn |
|---|---|---|---|---|---|---|---|---|---|---|---|---|
| Lr | 1 | | | | | | | | | | | |
| $R_b$ | 0.68 | 1 | | | | | | | | | | |
| p | 0.96 | 0.52 | 1 | | | | | | | | | |
| $F_f$ | 0.39 | 0.74 | 0.3 | 1 | | | | | | | | |
| Re | 0.41 | 0.74 | 0.32 | 1 | 1 | | | | | | | |
| $K_c$ | 0.29 | 0.6 | 0.2 | 0.9 | 0.92 | 1 | | | | | | |
| Df | 0.42 | 0.75 | 0.29 | 0.81 | 0.81 | 0.71 | 1 | | | | | |
| Dd | 0.45 | 0.39 | 0.45 | 0.38 | 0.38 | 0.24 | 0.18 | 1 | | | | |
| $I_f$ | 0.33 | 0.64 | 0.2 | 0.67 | 0.67 | 0.62 | 0.95 | 0.05 | 1 | | | |
| L | 0.4 | 0.35 | 0.4 | 0.38 | 0.37 | 0.24 | 0.17 | 0.99 | 0.05 | 1 | | |
| Rh | 0.31 | 0.7 | 0.22 | 0.88 | 0.88 | 0.9 | 0.7 | 0.19 | 0.64 | 0.18 | 1 | |
| Rn | 0.01 | 0.16 | 0.02 | 0.46 | 0.44 | 0.46 | 0.2 | 0.07 | 0.16 | 0.08 | 0.45 | 1 |

Key; Lr=Stream length ratio, Rb=Bifurcation ratio, p=rho coefficient, Ff=form factor, Re=elongation ratio, Kc=compactness coefficient, Df=drainage frequency, Dd=drainage density, If=infiltration number, L=length of overland flow, Rh=relief ratio, Rn=ruggedness number

### 4.2.10 Correlation Between Model Parameters and Geomorphologic Characteristics

A one-one test for correlation between the most sensitive model parameters and geomorphological parameters was done and results reported by $R^2$ values (Table 4.13). A threshold was set such that $R^2>0.5$ indicates a correlation. For instance, CH_S2 and compactness coefficient were highly correlated with $R^2$ value of 0.72 while HRU_SLP and stream length ratio were poorly correlated as indicated by a lower $R^2$ value of 0.2043706. Pairs that were considered to have a correlation were picked out as depicted in the bond section of Table 4.13, these were used to develop linear regressions subject to physical meaning.

**Table 4.13: Linear relationship between geomorphologic parameter and model parameter**

| | Lr | Rb | p | Ff | Re | Kc | Df | Dd | If | L | Rh | Rn |
|---|---|---|---|---|---|---|---|---|---|---|---|---|
| HRU_SLP | 0.2 | 0.33 | 0.01 | 0.51 | 0.53 | 0.51 | 0.37 | 0.08 | 0.3 | 0.1 | 0.27 | 0.69 |
| SLSUBBSN | 0.15 | 0.29 | 0 | 0.4 | 0.43 | 0.49 | 0.23 | 0.04 | 0.18 | 0.05 | 0.29 | 0.7 |
| CN2 | 0.16 | 0.14 | 0.1 | 0.26 | 0.26 | 0.08 | 0.51 | 0.23 | 0.39 | 0.25 | 0.01 | 0.08 |
| OV_N | 0.19 | 0.16 | 0.16 | 0.35 | 0.35 | 0.13 | 0.58 | 0.33 | 0.42 | 0.35 | 0.04 | 0.13 |
| CH_S2 | 0.23 | 0.28 | 0.07 | 0.47 | 0.49 | 0.72 | 0.14 | 0 | 0.15 | 0 | 0.74 | 0.56 |

Key; Lr=Stream length ratio, Rb=Bifurcation ratio, p=rho coefficient, Ff=form factor, Re=elongation ratio, Kc=compactness coefficient, Df=drainage frequency, Dd=drainage density, If=infiltration number, L=length of overland flow, Rh=relief ratio, Rn=ruggedness number

### 4.2.11 Regression for SWAT Model Parameter Estimation at Sub-Catchment Level

The regression models developed for each model parameter contained a unique combination of geomorphological characteristic based on collinearity threshold, correlation $R^2$ and physical meaning. Two regression models were developed for each model parameter; multiple linear regression and customized regression. Of the two customized regressions performed the best for all the model parameters within the selected sub-catchments. Customized regressions for all the five-model parameter had $R^2$ values > 0.9 and an adjusted $R^2$ > 0.75. Also, for multiple linear regression models some had very high $R^2$ and adjusted $R^2$ values but generally the values ranges were 0.51-0.92 for $R^2$ and 0.38 - 0.62 for adjusted $R^2$ (Table 4.14). For linear regressions, the $R^2$ for the HRU_SLP and CH_S2 regressions were 0.92 and 0.78 respectively implying very high efficiencies but CN2 and OV_N regressions had a relatively low efficiency - $R^2$ were 0.51 and 0.58 respectively. However, by customizing regressions subject to physical meaning and to include interaction between independent variables the $R^2$ values improved for all cases especially in CN2 and OV_N which improved to 0.97 and 0.93 respectively.

**Table 4.14: Developed linear regression, showing the $R^2$ and adjusted $R^2$**

| Model parameter | Regression model | Transform | $R^2$ | Adjusted $R^2$ |
|---|---|---|---|---|
| CN2 | $CN2 = 91.69 - 17.69Dd$ | Linear | 0.51 | 0.385 |
| | $CN2 = 64.57(Df)^2 + 808.1(F_f)^2 - 555.7(Df \times F_f) + 87.03$ | Customized | 0.97 | 0.94 |
| SLSUBBSN | $SLSUBBSN = 66.32R_N - 9.9$ | Linear | 0.69 | 0.62 |
| | $SLSUBBSN = 946.1(R_N)^2 + 41.38(Kc)^2 - 393.9(R_N \times Kc) + 9.934$ | Customized | 0.96 | 0.91 |
| HRU_SLP | $HRU_{SLP} = 2.99EL_r + 0.072Kc - 0.4473R_N - 3.41F_f - 0.5$ | Linear | 0.92 | 0.60 |
| | $HRU_{SLP} = 0.29 + 0.05(R_N \times B_r) - 0.48(R_N)^2$ | Customized | 0.94 | 0.85 |
| OV_N | $OV_N = 0.1434 - 0.053Df$ | Linear | 0.58 | 0.47 |
| | $OV_N = 0.2799(Dd)^2 + 0.0325(Kc)^2 - 0.1573(Dd \times Kc) + 0.0025$ | Customized | 0.93 | 0.83 |
| CH_S2 | $CH_{S2} = 0.0326 - 0.00315Kc + 0.1898R_r - 0.014R_N$ | Linear | 0.78 | 0.47 |
| | $CH\_S2 = 7.725(R_r)^2 - 0.4414(R_r \times Kc) + 0.05112$ | Customized | 0.91 | 0.77 |

Br-bifurcation ratio, Ff-form factor, Kc-compactness coefficient, Df-drainage frequency, Dd-drainage density, RN-ruggedness number, Rr-relief ratio.

### 4.2.12 Regression Models

The best regression model for predicting CN2 was the customized regression with an $R^2$ (adj. $R^2$) of 0.97 (0.94). This regression model included drainage frequency and form factor as the independent variables with an interaction component. Since drainage frequency is a factor of drainage streams per unit area and form factor is a factor of the shape of the catchment affecting time of concentration relating these two factors has a physical meaning. Both customized and linear regression performed well for the estimation of HRU_SLP at $R^2$ (adj. $R^2$) of 0.94 (0.85) and 0.92 (0.6) respectively. The customized regression was based on a combination of ruggedness number, bifurcation ratio including an interaction component. The linear regression

was a combination of elongation ratio, compactness coefficient, ruggedness number and form factor. For OV_N, a customized combination of drainage density, compactness coefficient and the interaction between the two, gave the best efficiency ($R^2$ = 0.93, adj. $R^2$ = 0.83). SLSUBBSN was best estimated by a customized polynomial relationship between ruggedness number and compactness coefficient. A combination of relief ratio and compactness coefficient related best to the main channel slope parameter (CH_S2) under a customized polynomial. The geomorphological parameters selected in the regressions were drainage density, drainage frequency, form factor, ruggedness number, compactness coefficient, bifurcation ratio and relief ratio. Ruggedness number and drainage frequency were found to be dominant parameters.

### 4.3 Simulated Spatial Surface Flows

Table 4.15 presents estimated model parameters for all the order one sub-catchments derived from the five regressions with highest $R^2$ and adj. $R^2$ in the former section 4.2 based on geomorphological characteristics.

**Table 4.15: Estimated values for model parameters based on geomorphological characteristics**

| Sub-catchment ID | Estimated values for model parameters at sub-catchment level | | | | |
|---|---|---|---|---|---|
| | CN2 | SLSUBBSN | CH_S2 | OV_N | HRU_SLP |
| 1 | 85.41 | 37.35 | 0.02 | 0.12 | 0.53 |
| 2 | 82.29 | 23.81 | 0.03 | 0.10 | 0.20 |
| 4 | 82.69 | 44.59 | 0.03 | 0.11 | 0.16 |
| 5 | 85.26 | 100.34 | 0.02 | 0.12 | 0.32 |
| 7 | 82.61 | 19.14 | 0.03 | 0.12 | 0.31 |
| 9 | 85.09 | 17.49 | 0.03 | 0.13 | 0.20 |
| 11 | 74.03 | 15.41 | 0.03 | 0.09 | 0.29 |
| 14 | 74.04 | 14.65 | 0.03 | 0.08 | 0.29 |
| 15 | 84.82 | 11.00 | 0.04 | 0.12 | 0.28 |
| 20 | 57.76 | 11.99 | 0.04 | 0.12 | 0.27 |
| 21 | 79.81 | 17.15 | 0.02 | 0.10 | 0.31 |
| 24 | 53.45 | 12.31 | 0.04 | 0.14 | 0.27 |

The derived model parameters were used in SWAT model to calibrate at sub-catchments level. The spatially calibrated model was used to analyze the hydrological characteristics of the catchment. Spatial variation in precipitation was the major factor that induced variation in catchment flow components. In the following sub sections, we discuss the spatial variability of the anomaly (were averaged over 5 years period) values of catchment water flow components on the sub-catchment scale.

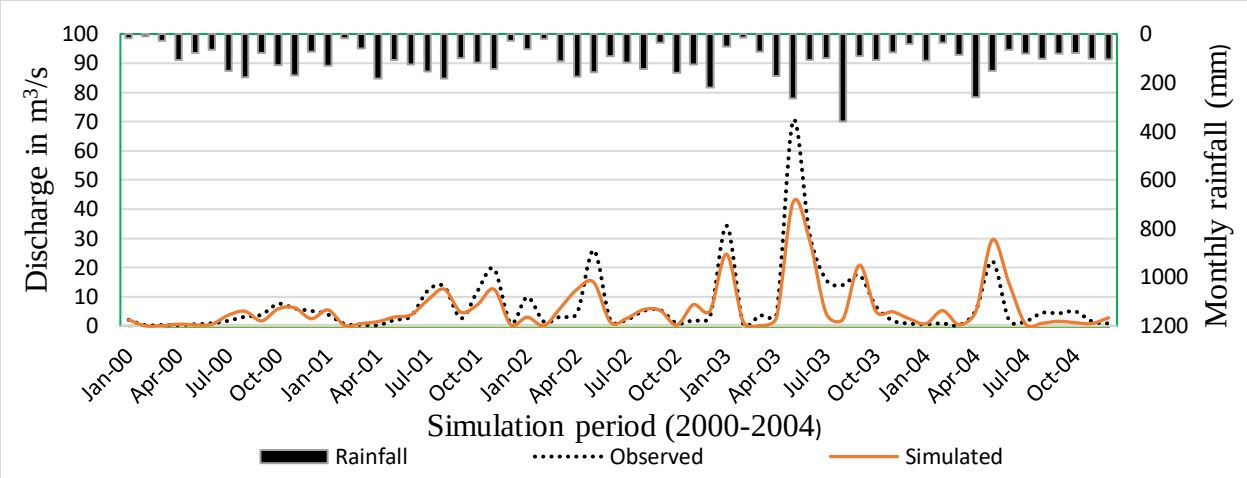


**Figure 4.18: Model output hydrograph based on geomorphological derived SWAT parameters**

Model run based on geomorphological derived parameters resulted in a NS efficiency and a coefficient of determination ($R^2$) of 0.77 and 0.78, respectively. Figure 4.18 shows the simulated output hydrograph plot for stream flow compared to the observed values for time period between 2000-2004. The data fit for simulated discharge against the observed discharge depicted in Figure 4.19 shows $R^2$ of 0.78 for the calibration period. This is a confirmation that based on geomorphological characteristics SWAT model can be used where there is not gauged data for calibration. However, this method had a lower $R^2$ value (0.78) compared to model calibrated using observed data ($R^2$=0.81) on SUFI- II algorithm. Calibration using observed data gives a better model but where such data is not available or unreliable geomorphological characteristics were to estimate model parameters and give a satisfactory model.

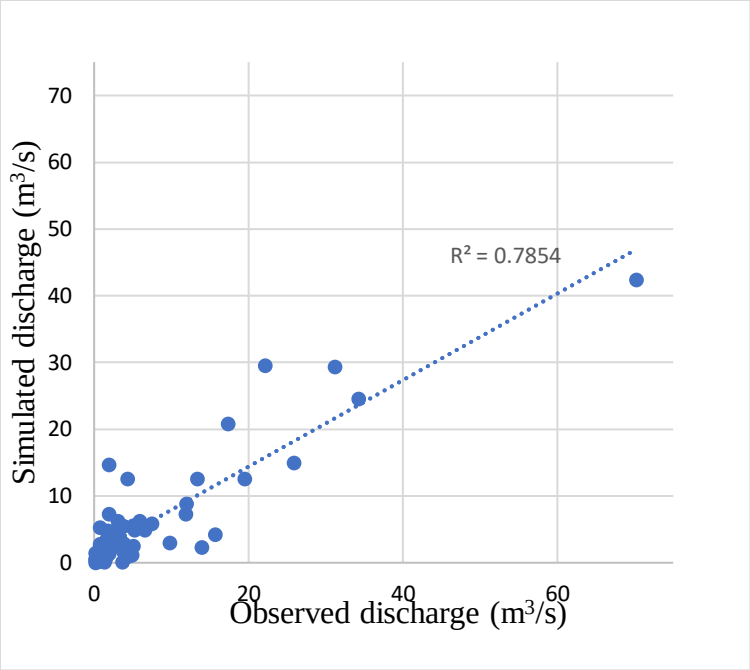


**Figure 4.19: A data fit for simulated discharge against observed discharges for the geomorphologic based model**

### 4.3.1 Anomaly Rainfall Distribution at Sub-Catchment Scale

The anomaly precipitation over the entire catchment ranges from 1450 mm to 1505 mm with higher values on the North-West upper side of the catchment and decrease Southwards towards the outlet. High rainfall depth between 1492 mm to 1501 mm per year was reported at upper sub-catchments (_1, _2, _5, _7 & _8) and on lower sub-catchments (_11, _13, _15 & _19). Average rainfall ranging from 1485 mm to 1492 mm per year was distributed in some parts of the upper catchments and also middle area of the catchment. Low amount of rainfall of values below 1451 mm per year was received mostly in the lower catchment and also some parts at the middle of the catchment as depicted in Figure 4.20.

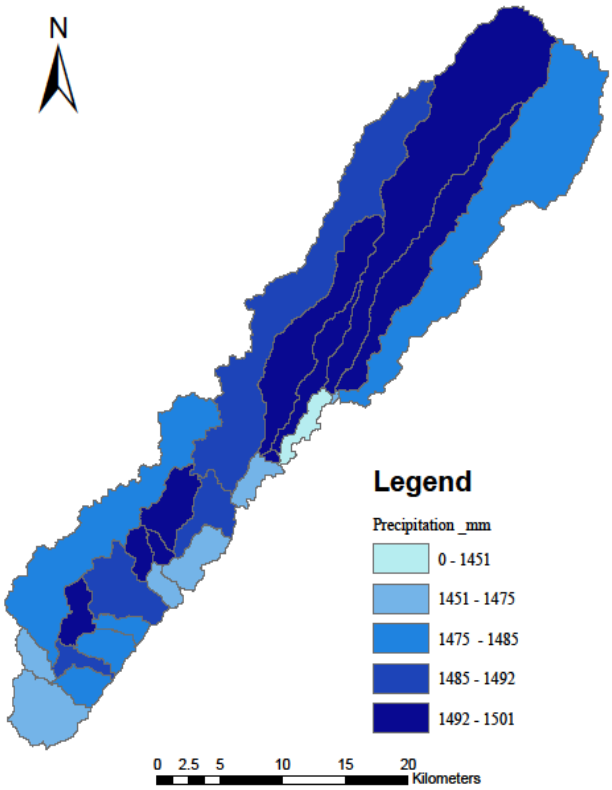


**Figure 4.20: A map showing anomaly rainfall distribution at sub-catchment scale**

### 4.3.2 Anomaly Actual Evapotranspiration Distribution

Actual evapotranspiration (ET) ranged between 785 mm and 910 mm, and the mean value for the entire catchment is 840 mm. The ET distribution at sub-catchment level is depicted in Figure 4.21. High ET depths were observed to be distributed on the North-East upper parts of the catchment with values ranging from 882 mm to 907 mm per year. At the Southern parts of the catchment, lower evapotranspiration was reported with values ranging from 785 mm to 801 mm per year. Some parts of the middle and lower catchment had an evapotranspiration of values ranging between 801 mm to 827 mm per year. Average evapotranspiration was highly distributed at the middle parts of the catchment and some parts of the lower catchment of values ranging from 801 mm to 827 mm annually. ET distribution related highly with the soil distribution, with higher rates corresponding with Mollic Andosols soil type and lower rates corresponding to Eutric Planosols.

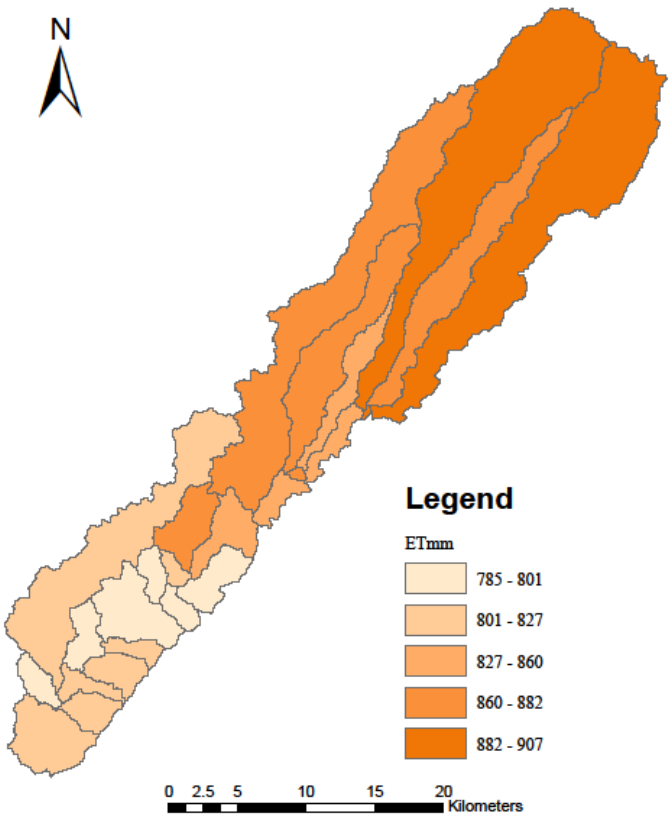


**Figure 4. 21: Anomaly actual evapotranspiration distribution map at sub-catchment scale**

### 4.3.3 Anomaly Groundwater Contribution to Surface Water Flow

Surface water flow received much water from the groundwater at the lower parts of the catchment of values ranging from 177 mm to 233 mm per year. The south-west part of the catchment which was characterized by clayey soil with low hydraulic conductivity recorded the high values of groundwater contribution to surface water flows, this is due to the presence of a natural forest cover with a thick peat layer above the soil surface. An average contribution to the surface water flow from the underground was observed at some parts of middle catchment and more at the upper northern part of the catchment ranging from 84 mm to 130 mm per year. Very low amount of water from the groundwater to the surface water flow was distributed at a very small area at the middle of the catchment falling between 27 mm to 39 mm per year (Figure 4. 22).

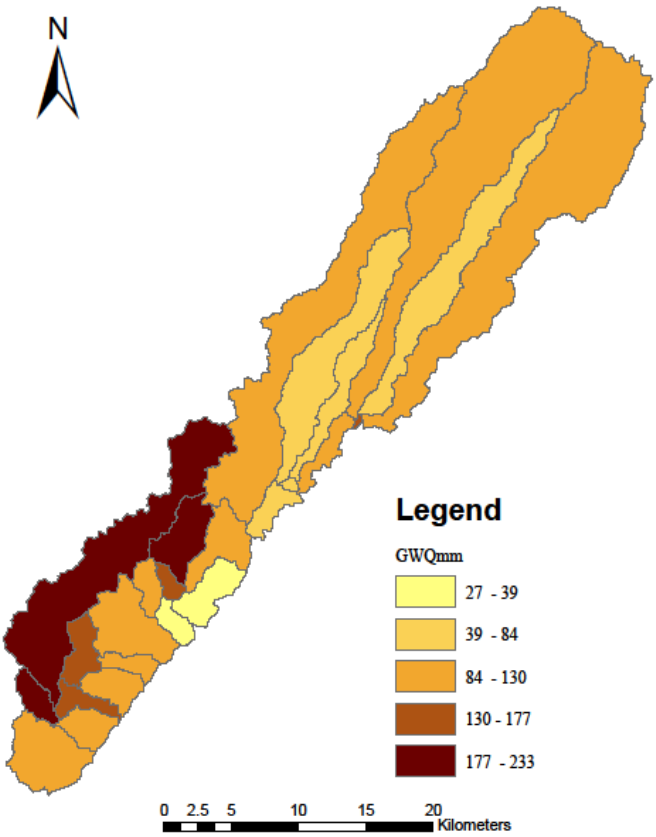


**Figure 4.22: A map of anomaly groundwater contribution to water flow at sub-catchment scale**

### 4.3.4 Anomaly Percolation Out of Root Zone Distribution

The high depth of water that percolated out of root zone was observed at the southwest part of the catchment ranging from 244 mm to 300 mm per year. On the northern part of the catchment and some parts of the middle catchment, there was an average percolation of values ranging from 199 mm to 244 mm per year. Very low amount of water percolated to the ground in the catchment was distributed at some few parts of the middle and southeast parts falling between 105 mm to 128 mm per year (Figure 4.23).

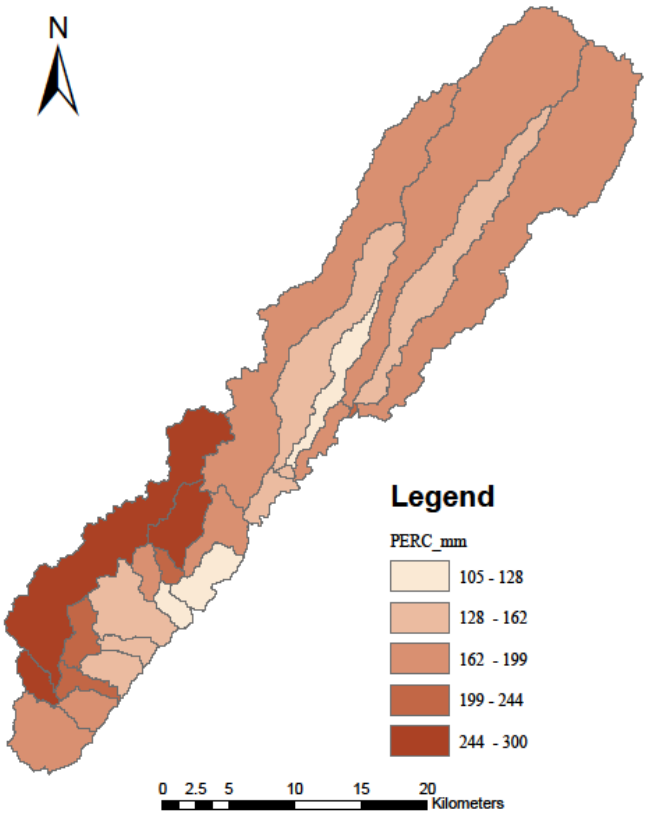


**Figure 4.23: Anomaly percolation out of root zone distribution map**

### 4.3.5 Anomaly Potential Evapotranspiration Distribution

The high potential evapotranspiration was distributed in the northeast part of the catchment of values ranging from 2017 mm to 2083 mm per year. Average potential was distributed in northwest and more at the middle part of the catchment with values ranging from 1975 mm to 2017 mm per year. Low values were distributed at some parts of the middle catchment and at the southern side of the catchment with values falling between 1856 mm to 1888 mm per year (Figure 4.24).

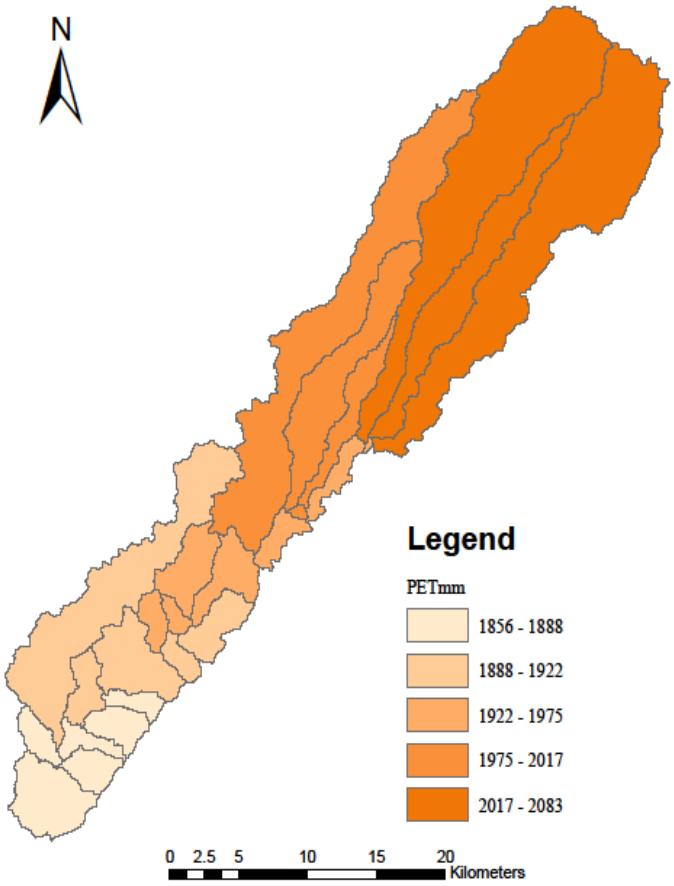


**Figure 4.24: Anomaly potential evapotranspiration distribution map**

### 4.3.6 Anomaly Soil Water Content Distribution

The soil water content was higher in a small part at the middle of the catchment of values ranging between 156 mm to 161 mm per year as shown in Figure 4.25. At the upper part (northern side) of the catchment and some parts of the middle catchment, there was an average soil water content of values ranging from 148 mm to 156 mm per year. At the lower catchment, the soil water content was very lover falling between 102 mm to 116 mm per year with southwest region having the lowest values (Figure 4.25).

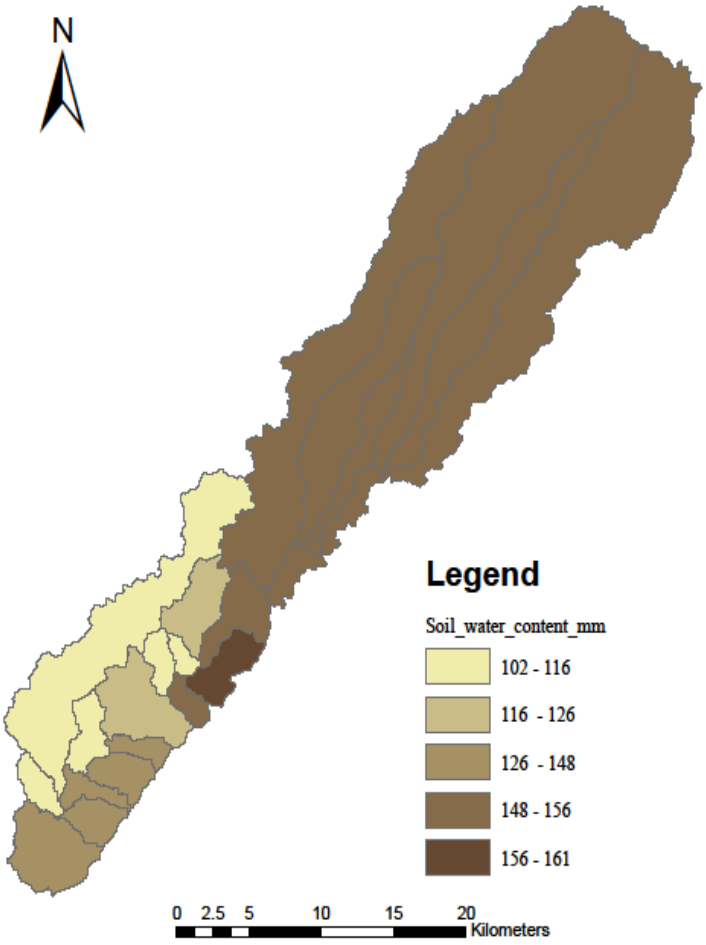


**Figure 4.25: Anomaly soil water content distribution map**

### 4.3.7 Anomaly Surface Water Flow Distribution

The high depths of surface water flow were distributed at the southeast part of catchment with the values of the available water ranging between 447 mm to 497 mm per year. Sub-catchments 14, 16, 17, 18, 20 and 24 have a higher surface water flow of greater than 447 mm (Table 4.16). Some parts of the middle catchment and the northern part catchment had values of surface runoff ranging from 384 mm to 447 mm per year. An average surface runoff of 285 mm to 384 mm per year was distributed over the most northern parts of the catchment and some parts of in the middle part of the catchment. Lower surface runoff of values ranging between 152 mm to 164 mm per year was distributed on a very small area at the middle of the catchment as shown in Figure 4.26.

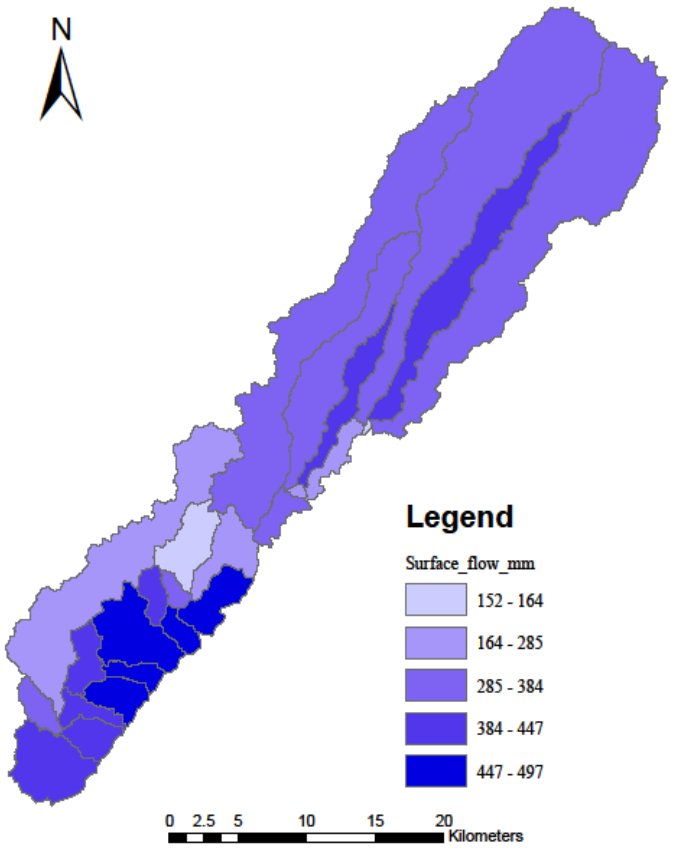


**Figure 4.26: A map depicting anomaly surface water flow distribution at sub-catchment scale**

Table 4.16 presents how, given the potential evapotranspiration, the precipitation received in each sub catchment was partitioned in to different flow components. The results of the analysis showed that; surface water flows are the overall predominant component spatially with an average of 372.3 mm annually. Also, groundwater processes and lateral soil flows were both significant in the catchment, for example in sub-catchment 3, 6, 11, 21 and 23 they had higher proportions of 150.1(184.2), 111.8 (159.5), 225.1 (153.3), 214.2 (99.3) and 233.3 (7.5) respectively (Table 4.16). Thus, this study estimates the annual surface water flow depth available over the catchment for harvesting as 372.3 mm.

**Table 4.16: SWAT anomaly flow output a sub-catchment level**

| Sub-catchment | PRECIP (mm) | PET (mm) | ET (mm) | SW (mm) | PERC (mm) | SURQ (mm) | GWQ (mm) | LATQ (mm) |
|---|---|---|---|---|---|---|---|---|
| 1 | 1501.9 | 2062.4 | 881.5 | 155.4 | 151.0 | 415.5 | 69.7 | 39.2 |
| 2 | 1498.0 | 2083.6 | 907.8 | 153.9 | 186.9 | 357.1 | 109.1 | 33.4 |
| 3 | 1475.1 | 1975.7 | 901.5 | 150.6 | 220.0 | 164.1 | 150.1 | 184.2 |
| 4 | 1485.6 | 2076.8 | 904.4 | 154.0 | 177.2 | 363.4 | 98.2 | 32.9 |
| 5 | 1500.0 | 2012.2 | 860.2 | 155.6 | 128.0 | 398.8 | 55.5 | 97.3 |
| 6 | 1451.7 | 1935.4 | 852.4 | 153.3 | 180.3 | 263.5 | 111.8 | 159.5 |
| 7 | 1500.2 | 2017.3 | 868.8 | 155.2 | 138.7 | 384.7 | 63.3 | 92.9 |
| 8 | 1499.0 | 1986.9 | 880.5 | 154.0 | 160.8 | 250.3 | 84.9 | 191.8 |
| 9 | 1488.5 | 2007.5 | 879.5 | 153.9 | 174.3 | 342.9 | 94.4 | 82.3 |
| 10 | 1469.5 | 1942.4 | 838.2 | 156.0 | 142.9 | 325.7 | 69.4 | 159.3 |
| 11 | 1498.2 | 1966.8 | 882.9 | 126.1 | 298.6 | 152.6 | 225.1 | 153.3 |
| 12 | 1488.2 | 1951.9 | 858.3 | 154.9 | 178.7 | 285.7 | 105.3 | 154.5 |
| 13 | 1497.4 | 1944.1 | 807.9 | 111.4 | 225.7 | 355.0 | 153.8 | 101.3 |
| 14 | 1474.9 | 1922.7 | 787.6 | 161.3 | 109.3 | 489.2 | 27.2 | 83.8 |
| 15 | 1497.4 | 1945.4 | 798.6 | 116.1 | 199.6 | 415.3 | 130.5 | 76.1 |
| 16 | 1473.1 | 1903.7 | 801.3 | 151.6 | 105.8 | 497.1 | 39.1 | 67.2 |
| 17 | 1491.9 | 1917.4 | 798.2 | 126.5 | 162.4 | 476.0 | 98.8 | 48.1 |
| 18 | 1480.3 | 1888.5 | 814.5 | 148.3 | 153.8 | 485.5 | 93.3 | 23.9 |
| 19 | 1495.8 | 1902.9 | 789.1 | 102.3 | 244.7 | 418.0 | 177.3 | 37.2 |
| 20 | 1483.5 | 1883.6 | 814.5 | 148.6 | 161.3 | 482.9 | 101.3 | 20.8 |
| 21 | 1479.1 | 1922.3 | 820.9 | 110.3 | 286.8 | 272.9 | 214.2 | 99.3 |
| 22 | 1492.0 | 1877.2 | 822.7 | 138.4 | 219.2 | 435.9 | 154.4 | 8.0 |
| 23 | 1474.4 | 1856.7 | 785.7 | 108.6 | 300.8 | 383.9 | 233.3 | 7.5 |
| 24 | 1482.1 | 1874.7 | 827.4 | 146.4 | 184.5 | 447.1 | 118.8 | 20.9 |
| 25 | 1469.7 | 1859.2 | 817.4 | 146.0 | 183.8 | 444.6 | 116.4 | 27.5 |

# CHAPTER FIVE

# CONCLUSIONS AND RECOMMEDATIONS

## 5.1 Conclusions

Based on the findings from the three specific objectives, the following conclusions are drawn;

The SWAT model was successfully parameterized, calibrated and validated on Amala River catchment and therefore with reliable rainfall data available, SWAT model can be used in Amala River catchment and the region. On a small catchment such as Amala, SWAT model had a higher $R^2$ of 0.81 as compared to larger catchment as reported in previous literature for the entire Mara River catchment. Its calibration on SWAT- CUP was more efficient as higher number of iteration and simulation could be done in a few minutes as compared to manual calibration. Therefore, it's an efficient tool for handling SWAT model calibration, validation, sensitivity analysis and uncertainty analysis. Finally, CN2 was found to be the most sensitive parameter in the catchment and thus a better establishment of this parameter will yield to a better model set up.

Digital Elevation Model was used successfully to geomorphologically characterize Amala River catchment on ArcMap. The catchment has a dendritic drainage network, it is elongated thus less efficient in runoff discharge and has a total relief of 1220 m, implying a high potential energy of the drainage network thus high stream velocity. The catchment has hilly and mountainous relief characterized by high infiltration as compared to surface water flow, this varies spatially, with sub-catchments far North of the outlet having high infiltration than those near the outlet. The spatial variability of geomorphological parameters analyzed is significant and thus the catchment hydrological behavior will vary across different sub-catchments.

Geomorphological based regression was used to estimate SWAT model parameter which performed satisfactorily with an $R^2$ of 0.77 compared to $R^2 = 0.81$ for a model calibrated using observed data and the recommend $R^2 > 0.75$ for a good model (Abbaspour et al., 2017). Therefore, geomorphological characteristics can be used where gauged data is unavailable or not reliable, and for better flow spatial distribution. This study estimates the annual surface water flow depth available over the catchment for harvesting as 372.3 mm. The spatial distribution and water balance components across different scales can further inform surface water harvesting structure designs in data-scarce catchments.

## 5.2 Recommendations

Based on the results of the study nexus the conclusions thereof, the following recommendations are made. Further research on the following aspects should be pursued;

i. The performance of SWAT model under satellite derived areal rainfall and surface temperature as an alternative to ground recorded weather data which may not be available or could be unreliable.

ii. The use of other type of regressions other than linear and polynomial, should be investigated to better the model parameter estimation from geomorphological characteristics. This should also consider encompassing other physiographic characteristics such a land use land cover factor, soil factor etc. in model parameter estimation.

iii. Geomorphological based SWAT model set up should be evaluated on other catchment and to check its performance in comparison to this study.

## REFERENCES


Abbaspour, K. C., Rouholahnejad, E., Vaghefi, S. R., Srinivasan, R., Yang, H., & Kløve, B. (2015). A continental-scale hydrology and water quality model for Europe: Calibration and uncertainty of a high-resolution large-scale SWAT model. *Journal of Hydrology, 524*, 733-752.

Abbaspour, K. C., Vaghefi, S. A., & Srinivasan, R. (2018). A guideline for successful calibration and uncertainty analysis for soil and water assessment: a review of papers from the 2016 international SWAT conference.

Abbaspour, K. C., Yang, J., Maximov, I., Siber, R., Bogner, K., Mieleitner, J., & Srinivasan, R. (2007). Modelling hydrology and water quality in the pre-alpine/alpine Thur watershed using SWAT. *Journal of Hydrology, 333*(2-4), 413-430.

Abebe, N. A., Ogden, F. L., & Pradhan, N. R. (2010). Sensitivity and uncertainty analysis of the conceptual HBV rainfall–runoff model: Implications for parameter estimation. *Journal of Hydrology, 389*(3-4), 301-310.

Altaf, F., Meraj, G., & Romshoo, S. A. (2013). Morphometric analysis to infer hydrological behaviour of Lidder watershed, Western Himalaya, India. *Geography Journal, 2013*.

Aparicio, F. (1996). *Fundamentos de Hidrología de Superficie (Fundamentals of Surface Hydrology)*. (4th. Ed.). Editorial Limusa S.A.

Arnold, J. G., Morias, D. N., Gasman, P. M., Abbaspour, K. C., White, M. J., Srinivasan, R., Santhi, C., Harmel, R. D., Griensven, A., Liew, M. W., Kannan, N. and Jha, M. K. (2012). SWAT: Model Use, Calibration and Validation. *Journal of American Society of Agricultural and Biological Engineers, 55*(4), 1491-1508.

Bansod, R. D., & Ajabe, G. S. (2018). Determination of geomorphological characteristics of Karpri-Kalu watershed using GIS techniques. *Journal of Pharmacognosy and Phytochemistry, 7*(1), 1940-1944.

Bao, Z., Zhang, J., Liu, J., Fu, G., Wang, G., He, R., ... & Liu, H. (2012). Comparison of regionalization approaches based on regression and similarity for predictions in ungauged catchments under multiple hydro-climatic conditions. *Journal of Hydrology, 466*, 37-46.

Bergström, S., Carlsson, B., Gardelin, M., Lindström, G., Pettersson, A., & Rummukainen, M. (2001). Climate change impacts on runoff in Sweden assessments by global climate

models, dynamical downscaling and hydrological modelling. *Climate Research, 16*(2), 101-112.

Bertoldi, G., Rigon, R., & Over, T. M. (2006). Impact of watershed geomorphic characteristics on the energy and water budgets. *Journal of Hydrometeorology, 7*(3), 389-403.

Bicknell, B. R., Imhoff, J. C., Kittle Jr, J. L., Donigian Jr, A. S., & Johanson, R. C. (1996). Hydrological simulation program-FORTRAN. user's manual for release 11. *US EPA*.

Bingwa, F. (2013). *A quantitative analysis of the impact of land use changes on floods in the Manafwa River Basin* (Doctoral dissertation, Massachusetts Institute of Technology).

Charizopoulos, N., & Psilovikos, A. (2015). Geomorphological analysis of Scopia catchment (Central Greece), using DEM data and GIS. *Fresenius Environmental Bulletin, 24*(11), 3973-3983.

Chethan, B. J., & Vishnu, B. (2018). Determination of the geomorphologic parameters of the Thutha puzha River Basin in Central Kerala, India, Using GIS and Remote Sensing. *International Journal of Current Microbiology and Applied Sciences, 7*(09), 1245-1260.

Chow, V. T., Maidment, D. R., & Mays, L. W. (1988). *Applied hydrology*. McGraw-Hill International editions.

Dessu, S. B., & Melesse, A. M. (2012). Modelling the rainfall–runoff process of the Mara River basin using the Soil and Water Assessment Tool. *Hydrological Processes, 26*(26), 4038-4049.

Dhakal, N., Fang, X., Cleveland, T. G., Thompson, D. B., Asquith, W. H., & Marzen, L. J. (2012). Estimation of volumetric runoff coefficients for Texas watersheds using land-use and rainfall-runoff data. *Journal of Irrigation and Drainage Engineering, 138*(1), 43-54.

Donigian, A. S. Jr. (2000). *HSPF Training Workshop Handbook. Calibration and Verification Issues*. Office of Water, Office of Science and Technology, U.S. Environmental Protection Agency.

Dutton, C. L., Subalusky, A. L., Anisfeld, S. C., Njoroge, L., Rosi, E. J., & Post, D. M. (2018). The influence of a semi-arid sub-catchment on suspended sediments in the Mara River, Kenya. *PLoS One, 13*(2), e0192828.

Dwarakish, G. S., & Ganasri, B. P. (2015). Impact of land use change on hydrological systems: A review of current modeling approaches. *Cogent Geoscience, 1*(1), 1115691.

Fadil, A., Rhinane, H., Kaoukaya, A., Kharchaf, Y., & Bachir, O. A. (2011). Hydrologic modeling of the Bouregreg watershed (Morocco) using GIS and SWAT model. *Journal of Geographic Information System, 3*(04), 279.

Gassman, P. W., Reyes, M. R., Green, C. H., & Arnold, J. G. (2007). The soil and water assessment tool: historical development, applications, and future research directions. *Transactions of the ASABE, 50*(4), 1211-1250.

Devia, G. K., Ganasri, B. P., & Dwarakish, G. S. (2015). A review on hydrological models. *Aquatic procedia, 4*, 1001-1007.

Grillakis, M. G., Koutroulis, A. G., & Tsanis, I. K. (2011). Climate change impact on the hydrology of Spencer Creek watershed in Southern Ontario, Canada. *Journal of Hydrology, 409*(1-2), 1-19.

Günal, A. Y., & Güven, A. (2015). Determination of geomorphological parameters of Damlıca basin using GIS. *Acta Physica Polonica A, 128*(2), 221-223.

Gupta, H. V., Sorooshian, S., & Yapo, P. O. (1999). Status of automatic calibration for hydrologic models: Comparison with multilevel expert calibration. *Journal of Hydrologic engineering, 4*(2), 135-143.

Ismael, O., Sang Joseph, K., & Home Patrick, G. (2017). HEC-HMS model for runoff simulation in Ruiru reservoir watershed. *American Journal of Engineering Research, 6*(4), 1-7.

Nongthombam, J., Choudhury, P., Ullah, N., & Singh, K. V. (2011). A Geomorphological based rainfallrunoff model for ungauged watersheds. *International Journal of Geomatics and Geosciences, 2*(2), 676-687.

Kambombe, O. C. (2018). *Impact of climate variability and land use change on stream flow in Lake Chilwa basin, Malawi* (Master dissertation, Egerton University).

Kipampi, O. S., Kitheka, J., & Mwangi, M. (2017). The Study of the Effects of Mau Catchment Degradation on the Flow of the Mara River, Kenya. *Journal of Environment and Earth Science, 7*(2), 79-91.

Lee, W. H., Lee, J. H., Park, J. H., & Choi, H. S. (2016). The relationship between parameters of the SWAT model and the geomorphological characteristics of a watershed. *Ecology and Resilient Infrastructure, 3*(1), 35-45.

Liu, Z., & Tong, S. T. Y. (2011). Using HSPF to Model the Hydrologic and Water Quality Impacts of Riparian Land-Use Change in a Small Watershed. *Journal of Environmental Informatics, 17*(1).

Mo, X., Liu, S., Lin, Z., Wang, S., & Hu, S. (2015). Trends in land surface evapotranspiration across China with remotely sensed NDVI and climatological data for 1981–2010. *Hydrological Sciences Journal, 60*(12), 2163-2177.

Mango, L. M., Melesse, A. M., McClain, M. E., Gann, D., & Setegn, S. (2011). Land use and climate change impacts on the hydrology of the upper Mara River Basin, Kenya: results of a modeling study to support better resource management. *Hydrology and Earth System Sciences, 15*(7), 2245-2258.

Mark, D. M. (1975). Geomorphometric parameters: a review and evaluation. *Geografiska Annaler: Series A, Physical Geography, 57*(3-4), 165-177.

Martz, L. (2002). *Background Material for SLURP–TOPAZ MAGS Model* (Cross-Training Workshop, York University).

Mbungu, W. M., & Kashaigili, J. J. (2017). Assessing the hydrology of a data-scarce tropical watershed using the soil and water assessment tool: case of the Little Ruaha River Watershed in Iringa, Tanzania. *Open Journal of Modern Hydrology, 7*, 65-89.

Moriasi, D. N., Arnold, J. G., Van Liew, M. W., Bingner, R. L., Harmel, R. D., & Veith, T. L. (2009). Model evaluation guidelines for systematic quantification of accuracy in watershed simulations. *Transactions of the ASABE, 50*(3), 885-900.

Mulwa, F., Li, Z., & Fangninou, F. F. (2021). Water Scarcity in Kenya: Current Status, Challenges and Future Solutions. *Open Access Library Journal, 8*(1), 1-15.

Mutie, S. M., Mati, B., Home, P., Gadain, H. and Gathenya, J. (2006). *Evaluating Land Use Change Effects on River Flow Using USGS Geospatial Stream Flow Model in Mara River Basin, Kenya*. Center for Remote Sensing of Land Surfaces. Bonn.

Mwangi, H. M., Julich, S., Patil, S. D., McDonald, M. A., & Feger, K. H. (2016). Modelling the impact of agroforestry on hydrology of Mara River Basin in East Africa. *Hydrological Processes, 30*(18), 3139-3155.

Mwangi, W., Nyandega, I., & Kıthiia, S. (2017). Application Of Hydrological Models in Poorly Gauged Watersheds: A Review of The Usage of The Soil and Water Assessment Tool

(SWAT) in Kenya. *International Journal of Scientific & Technology Research, 06*(08), 132–141.

Mwania, J. M. (2014). *Runoff modeling of the mara river using satellite soil moisture and rainfall* (Master Thesis, University of Twente).

Nash, J. E., & Sutcliffe, J. V. (1970). River flow forecasting through conceptual models' part I—A discussion of principles. *Journal of hydrology, 10*(3), 282-290.

Nayak, T., Verma, M. K., & Bindu, S. H. (2012). SCS curve number method in Narmada basin. *International Journal of Geomatics and Geosciences, 3*(1), 219-228.

Nazir, M. H. M., Sulaiman, W. N. A., & Juahir, H. (2015). Hydrologic response characteristics of a tropical catchment to land use changes: a case study of The Nerus catchment. *Environmental Earth Sciences, 73*(11), 7533-7545.

Neitsch, S. L., Arnold, J. G., Kiniry, J. R., & Williams, J. R. (2011). *Soil and water assessment tool theoretical documentation version 2009*. Texas Water Resources Institute.

Nkonge, L. K. (2017). *Assessment of the Transferability of SWAT Model Parameters from Gauged to Ungauged Sub-Watersheds for Streamflow Simulation in the Upper Tana Watershed, Kenya* (Doctoral dissertation, SEMATEC-JKUAT).

Nyadawa, M. O., & Mwangi, J. K. (2017). Geomorphologic characteritics of Nzoia river basin. *Journal of Agriculture, Science, and Technology, 12*(2), 145-161.

Onyando, J. O., Chemelil, M. C., Awer, M., & Kisoyan, P. (2004). Development of frequency models for predicting design storms in Lake Baringo drainage basin in Kenya. *Botswana Journal of Technology, 13*(1), 1-6.

Onyando, J. O., & Sharma, T. C. (1995). Simulation of direct runoff volumes and peak rates for rural catchments in Kenya, East Africa. *Hydrological sciences journal, 40*(3), 367-380.

Osoro, G. M., Mourad, K. A., & Ribbe, L. (2018). Water demand simulation using WEAP 21: a case study of the Mara River Basin, Kenya.

Ouédraogo, W. A. A., Raude, J. M., & Gathenya, J. M. (2018). Continuous modeling of the Mkurumudzi River catchment in Kenya using the HEC-HMS conceptual model: Calibration, validation, model performance evaluation and sensitivity analysis. *Hydrology, 5*(3), 44-60.

Pareta, K., & Pareta, U. (2011). Quantitative morphometric analysis of a watershed of Yamuna basin, India using ASTER (DEM) data and GIS. *International journal of Geomatics and Geosciences, 2*(1), 248-269.

Raude, J. M. (2006). *Determination of surface runoff and soil loss under varying rainfall intensity in selected land use practices in River Njoro catchment of Kenya* (Master Thesis, Egerton University, Kenya).

Schmalz, B., Zhang, Q., Kuemmerlen, M., Cai, Q., Jähnig, S. C., & Fohrer, N. (2015). Modelling spatial distribution of surface runoff and sediment yield in a Chinese river basin without continuous sediment monitoring. *Hydrological Sciences Journal, 60*(5), 801-824.

Schumm, S. A. (1956). Evolution of drainage systems and slopes in badlands at Perth Amboy, New Jersey. *Geological society of America bulletin, 67*(5), 597-646.

Sellami, H., La Jeunesse, I., Benabdallah, S., Baghdadi, N., & Vanclooster, M. (2014). Uncertainty analysis in model parameters regionalization: a case study involving the SWAT model in Mediterranean catchments (Southern France). *Hydrology and Earth System Sciences, 18*(6), 2393-2413.

Shaw, E. (1994). *Hydrology in practice*. CRC press.

Sophocleous, M. (1997). Managing water resources systems: Why" safe yield" is not sustainable. *Ground water, 35*(4), 561.

Strahler, A. N. (1952). Hypsometric (area-altitude) analysis of erosional topography. *Geological Society of America Bulletin, 63*(11), 1117-1142.

Krysanova, V., & White, M. (2015). Advances in water resources assessment with SWAT—an overview. *Hydrological Sciences Journal, 60*(5), 771-783.

Williams, J. R., Arnold, J. G., Kiniry, J. R., Gassman, P. W., & Green, C. H. (2008). History of model development at Temple, Texas. *Hydrological Sciences Journal, 53*(5), 948-960.

Williams, J. R., Kannan, N., Wang, X., Santhi, C., & Arnold, J. G. (2012). Evolution of the SCS runoff curve number method and its application to continuous runoff simulation. *Journal of Hydrologic Engineering, 17*(11), 1221-1229.

Gustard, A., & Demuth, S. (2009). *Manual on low-flow estimation and prediction, Operational Hydrology Report No. 50*. WMO-No. 1029.

Winchell, M., Srinivasan, R., Di Luzio, M., & Arnold, J. (2013). *ArcSWAT interface for SWAT2012: user's guide*. Blackland Research and Extension Center, Texas Agrilife

Research. Grassland. Soil and Water Research Laboratory, USDA Agricultural Research Service, Texas.

Zelelew, M. B., & Alfredsen, K. (2014). Transferability of hydrological model parameter spaces in the estimation of runoff in ungauged catchments. *Hydrological Sciences Journal, 59*(8), 1470-1490.

Zvolenský, M., Hlavčová, K., Kohnová, S., & Szolgay, J. (2007). Prediction of rainfall-runoff model parameters in ungauged catchments. *Quantification and Reduction of Predictive Uncertainty for Sustainable Water Resources Management,* 357-364.

## APPENDICES

**Appendix A. 1: A screen capture of P-stat program used to compute weather statistics**

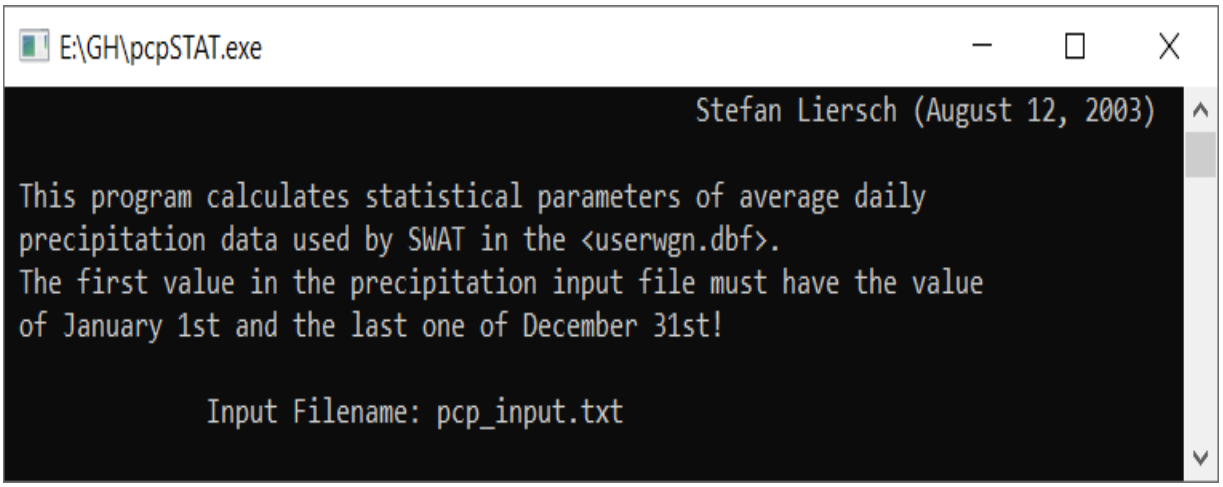


**Appendix A. 2: SWAT Weather data definition graphical user interface**

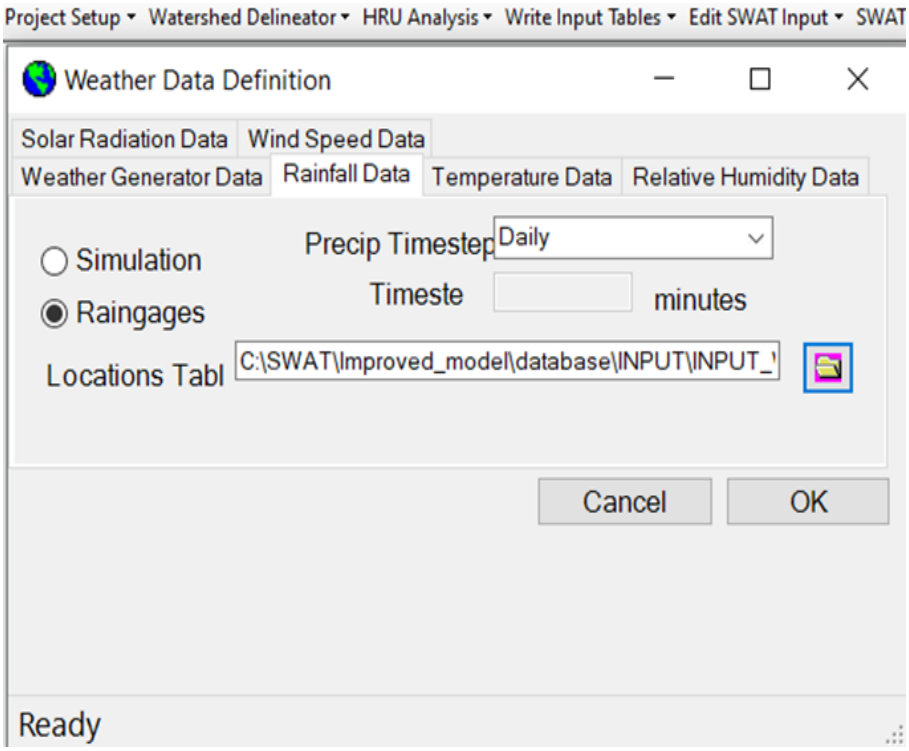

**Appendix A. 3:SWAT variables/symbols definition.**

| tblSubDef | |
|---|---|
| **Variable name** | **Definition** |
| SUB | Sub-catchment number. |
| GIS | GIS code reprinted from watershed configuration file (.fig). See explanation of sub-catchment command. |
| MON | Daily time step: the julian date, Monthly time step: the month (1-12), Annual time step: 4-digit year, Average annual summary lines: number of years averaged together |
| AREA | Area of the sub-catchment (km2). |
| PRECIP | Total amount of precipitation falling on the sub-catchment during time step (mm H2O). |
| SNOMELT | Amount of snow or ice melting during time step (water-equivalent mm H2O). |
| PET | Potential evapotranspiration from the sub-catchment during the time step (mm H2O). |
| ET | Actual evapotranspiration from the sub-catchment during the time step (mm). |
| SW | Soil water content (mm). Amount of water in the soil profile at the end of the time period. |
| PERC | Water that percolates past the root zone during the time step (mm). There is potentially a lag between the time the water leaves the bottom of the root zone and reaches the shallow aquifer. Over a long period of time, this variable should equal groundwater percolation. |
| SURQ | Surface runoff contribution to stream flow during time step (mm H2O). |
| GW_Q | Groundwater contribution to stream flow (mm). Water from the shallow aquifer that returns to the reach during the time step. |
| WYLD | Water yield (mm H2O). The net amount of water that leaves the sub-catchment and contributes to stream flow in the reach during the time step. (WYLD = SURQ + LATQ + GWQ – TLOSS – pond abstractions) |
| SYLD | Sediment yield (metric tons/ha). Sediment from the sub-catchment that is transported into the reach during the time step. |
| ORGN | Organic N yield (kg N/ha). Organic nitrogen transported out of the sub-catchment and into the reach during the time step. |

| tblSubDef | |
|---|---|
| **Variable name** | **Definition** |
| ORGP | Organic P yield (kg P/ha). Organic phosphorus transported with sediment into the reach during the time step. |
| NSURQ | NO3 in surface runoff (kg N/ha). Nitrate transported by the surface runoff into the reach during the time step. |
| SOLP | Soluble P yield (kg P/ha). Phosphorus that is transported by surface runoff into the reach during the time step. |
| SEDP | Mineral P yield (kg P/ha). Mineral phosphorus attached to sediment that is transported by surface runoff into the reach during the time step. |
| LATQ | Lateral flow contribution to stream flow during timestep (mm H2O) |
| LAT_Q_NO3 | Lateral flow nitrate contributions to stream flow (kg/ha) |
| GWMO3 | Groundwater nitrate contributions to stream flow (kg/ha) |
| HRU | Hydrologic response unit number |
| GIS | GIS code reprinted from watershed configuration file (.fig). See explanation of sub-catchment command (Chapter 2). |
| SUB | Topographically-defined sub-catchment to which the HRU belongs. |
| MGT | Management number. This is pulled from the management (.mgt) file. Used by the SWAT/GRASS interface to allow development of output maps by land use/management type. |
| MON | Daily time step: the julian date, Monthly time step: the month (1-12), Annual time step: 4-digit year, Average annual summary lines: number of years averaged together |
| PERC | Water that percolates past the root zone during the time step (mm H2O). There is usually a lag between the time the water leaves the bottom of the root zone and reaches the shallow aquifer. Over a long period of time, this variable should equal groundwater recharge (PERC = GW_RCHG as time → ∞). |
| GW_RCHG | Recharge entering aquifers during time step (total amount of water entering shallow and deep aquifers during time step) (mm H2O). |

| tblSubDef | |
|---|---|
| **Variable name** | **Definition** |
| DA_RCHG | Deep aquifer recharge (mm H2O). The amount of water from the root zone that recharges the deep aquifer during the time step. (Shallow aquifer recharge = GW_RCHG - DA_RCHG) |
| REVAP | Water in the shallow aquifer returning to the root zone in response to a moisture deficit during the time step (mm H2O). The variable also includes water uptake directly from the shallow aquifer by deep tree and shrub roots. |
| TMP_AV | Average daily air temperature (°C). Average of mean daily air temperature for time period. |
| TMP_MX | Average maximum air temperature (°C). Average of maximum daily air temperatures for time period. |
| TMP_MN | Average minimum air temperature (°C). Average of minimum daily air temperatures for time period. |
| SOL_TMP | Soil temperature (°C). Average soil temperature of first soil layer for time period. |
| SOLAR | Average daily solar radiation (MJ/m2). Average of daily solar radiation values for time period. |
| SYLD | Sediment yield (metric tons/ha). Sediment from the HRU that is transported into the main channel during the time step. |
| USLE | Soil loss during the time step calculated with the USLE equation (metric tons/ha). This value is reported for comparison purposes only. |

## Appendix A. 4: Statistical Analysis of Daily Precipitation Data (2001 - 2017) on Pstat program

Statistical Analysis of Daily Precipitation Data (2001 - 2017)

Input Filename = pcp_input.txt

Number of Years = 17

Number of Leap Years = 4

Number of Records = 6209

Number of NoData values = 0

| Month | PCP_MM | PCPSTD | PCPSKW | PR_W1 | PR_W2 | PCPD |
|---|---|---|---|---|---|---|
| Jan. | 75.16 | 4.6598 | 4.0381 | 0.4061 | 0.7873 | 21.29 |
| Feb. | 60.01 | 4.1244 | 3.1625 | 0.4321 | 0.7484 | 18.71 |
| Mar. | 94.83 | 4.7040 | 2.9723 | 0.5345 | 0.8200 | 24.18 |
| Apr. | 153.11 | 6.1375 | 1.8253 | 0.5949 | 0.8608 | 25.35 |
| May. | 117.65 | 5.0546 | 1.9917 | 0.6154 | 0.8109 | 24.88 |
| Jun. | 67.80 | 3.1842 | 2.0948 | 0.4745 | 0.7882 | 21.94 |
| Jul. | 51.08 | 2.7196 | 3.2104 | 0.4774 | 0.7634 | 21.88 |
| Aug. | 77.66 | 3.7448 | 2.6084 | 0.6061 | 0.7747 | 23.24 |
| Sep. | 80.91 | 3.6213 | 2.4344 | 0.5854 | 0.8528 | 25.18 |
| Oct. | 80.64 | 3.9352 | 2.7316 | 0.5862 | 0.7981 | 24.18 |
| Nov. | 97.29 | 4.6429 | 2.4948 | 0.6129 | 0.7668 | 22.71 |
| Dec. | 80.57 | 4.2729 | 2.5034 | 0.4755 | 0.7865 | 22.59 |

PCP_MM = average monthly precipitation [mm]

PCPSTD = standard deviation

PCPSKW = skew coefficient

PR_W1 = probability of a wet day following a dry day

PR_W2 = probability of a wet day following a wet day

PCPD = average number of days of precipitation in month

(written by Stefan Liersch, Berlin, August 2003)

**Appendix A. 5: Shape characteristics of a catchment based on elongation ratio (Pareta & Pareta, 2011)**

| S. No | Elongation ratio value | Shape of the catchment |
|---|---|---|
| 1 | 0.8 - 0.9 | Circular |
| 2 | 0.7 – 0.8 | Oval |
| 3 | Less than 0.7 | Elongated |

## Appendix A. 6: Details of downloaded Landsat Imageries

LE07_L1TP_169061_20030204_20200916_02_T1_GCP.txt - Notepad

File Edit Format View Help

```
Wed. Sep. 16, 2020              LANDSAT 7                    Time: 05:11
                          Image Assessment System
                            GCP Residual Report
--------------------------------------------------------------------------------
WOID: L2            Path/Row: 169 / 061

L0R Reference Image: L71SGS1203035130100_HDF.201960059
Acquisition Date: Feb 04, 2003

Band Number:  5
```

LE07_L1TP_169060_20030204_20200916_02_T1_GCP.txt - Notepad

File Edit Format View Help

```
Wed. Sep. 16, 2020              LANDSAT 7                    Time: 06:43
                          Image Assessment System
                            GCP Residual Report
--------------------------------------------------------------------------------
WOID: L2            Path/Row: 169 / 060

L0R Reference Image: L71SGS1203035130100_HDF.201960101
Acquisition Date: Feb 04, 2003

Band Number:  5
```

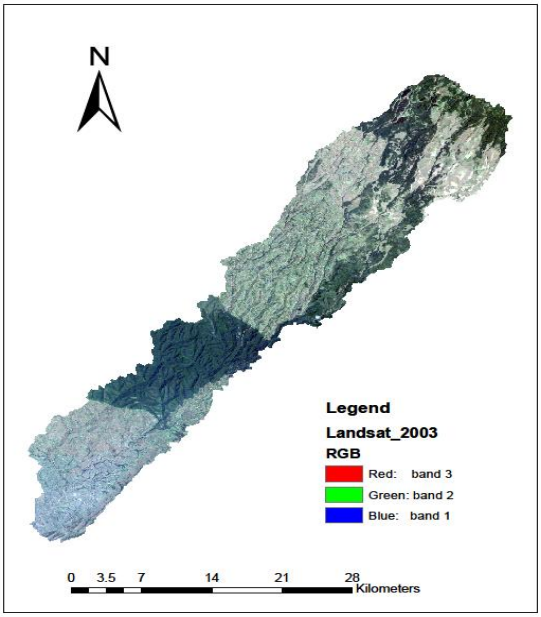


**Appendix A. 6: An RGB map of Landsat imagery used for land use classification**

**Appendix A. 7: Published article based on this research work**

*Journal of Engineering Research and Reports*

*20(2): 91-106, 2021; Article no.JERR.64836*
*ISSN: 2582-2926*

# Quantitative Analysis of Geomorphologic Characteristics for Surface Runoff Determination in Amala River Catchment in Kenya

**Samuel M. Kinyanjui[1*], Japheth O. Onyando[1] and Raphael M. Wambua[1]**

*[1]Department of Agricultural Engineering, Egerton University, P.O.Box 536-20115, Egerton, Kenya.*

*Authors' contributions*

*This work was carried out in collaboration among all authors. Author SMK designed the study, performed the statistical analysis, wrote the protocol and wrote the first draft of the manuscript. Authors JOO and RMW managed the analyses of the study and the literature searches. All authors read and approved the final manuscript.*

*Article Information*

DOI: 10.9734/JERR/2021/v20i217268
Editor(s):
(1) Dr. Tian-Quan Yun, South China University of Technology, China.
Reviewers:
(1) M. C. Manjunatha, Maharaja Institute of Technology Thandavapura, India.
(2) R. K. Dubey, Indian Institute of Technology, India.
Complete Peer review History: http://www.sdiarticle4.com/review-history/64836

*Original Research Article*

*Received 10 November 2020*
*Accepted 20 January 2021*
*Published 17 February 2021*

## ABSTRACT

Hydrological response of a catchment is a function of rainfall as influenced by catchment characteristics comprising geomorphology, land cover, and management practices. In this study, the analysis mainly focused on how geomorphological characteristics influence the catchment hydrological response. Geomorphological analyses of catchment geometry, stream patterns, relief, and slope can be used to characterize the catchment features that affect the drainage network. These characteristics are catchment specific and therefore unique to provide an insight into its hydrologic response. The objective of this research was to quantitatively analyze geomorphologic characteristics; linear, areal, drainage pattern, and relief aspect, of Amala River catchment, using ArcGIS tools and infer its hydrological behavior. The morphometry of the catchment was derived from the DEM within the ArcMap environment. These parameters as well as mathematical map equations were used to derive geomorphological characteristics such as bifurcation ratio, rho coefficient, drainage density, infiltration number, form factor among others. The results show that the Amala River catchment is elongated with uniform lithology and a higher probability of delayed peak hydrographs due to longer lag time and time of concentration. The catchment exhibits a

**Corresponding author: Email: samuelmuhoro76@gmail.com;*

dendritic drainage pattern with an average bifurcation ratio of 4.26 which is closer to the upper bound value of 5. This indicates a reduction in peak flows and a delayed time to peak. The surface runoff yield efficiency was low and non-uniform with an average drainage density of 1.073 km/km2. The catchment was characterized by higher infiltration characteristics as compared to surface flows, this varied spatially, with sub-basins far North of the outlet having high infiltration than those near the outlet. The catchment relief was characterized as steep and therefore high stream velocity was inferred. The investigation and findings of this study on catchment geomorphology and inferred hydrologic behavior will be of great importance in catchment management, water resource planning within the catchment, and water harvesting at a spatial scale. Thus, the outcomes provide a baseline for informed water pan and water harvesting structures site.

*Keywords: Drainage density; geomorphologic characteristics; infiltration number; bifurcation ratio; dendritic drainage.*

## Appendix A. 8: Research permit obtained from NACOSTI

REPUBLIC OF KENYA

NATIONAL COMMISSION FOR SCIENCE,TECHNOLOGY & INNOVATION

Ref No: **926065**

Date of Issue: **11/February/2020**

### RESEARCH LICENSE

**This is to Certify that Mr.. SAMUEL MUHORO KINYANJUI of Egerton University, has been licensed to conduct research in Bomet, Kericho, Narok on the topic: MODELLING SURFACE WATER FLOWS FOR UNGAUGED SITES WITHIN THE UPPER MARA RIVER CATCHMENT USING GEOMORPHOLOGIC CHARACTERISTICS for the period ending : 11/February/2021.**

License No: **NACOSTI/P/20/3850**

**926065**

Applicant Identification Number

Director General
NATIONAL COMMISSION FOR SCIENCE,TECHNOLOGY & INNOVATION

Verification QR Code

NOTE: This is a computer generated License. To verify the authenticity of this document, Scan the QR Code using QR scanner application.